Exploring the cosmological dynamics of a viable theory for $f(R)$-gravity

Sulona Kandhai

December 2013

A dissertation submitted in partial fulfilment of the requirements for the degree M.Sc. in the Department of Mathematics and Applied Mathematics, as part of the National Astrophysics and Space Science Programme
UNIVERSITY OF CAPE TOWN

Supervisor: Prof. Peter. K. S. Dunsby

Abstract

A viable theory for $f(R)$ gravity, the Hu-Sawicki (HS) model, is considered from a dynamical systems perspective. The case for which $n = 1, c_1 = 1$ is treated, and qualitative information regarding the phase space of this model is extracted. Several stable de Sitter equilibrium points are identified, as well as an unstable "matter-like" point, and solution orbits which resemble the ΛCDM evolution are presented. The expansion history produced by integration of the dynamical system of the HS model is compared with that of ΛCDM. It is found that while the HS model *can* produce the desired behaviour in the appropriate regime, this occurs at the expense of ΛCDM values of the observational parameters.

Acknowledgements

I thank my supervisor, Prof. Peter Dunsby, for giving me the opportunity to carry out my Masters studies under his careful guidance; for his kindness, support and immeasurable patience, and for highlighting the significance of the initial value of the correction! Without his invaluable counsel and direction, this work would not have been possible.

I am indebted to Dr. Mohamed Abdelwahab for his assistance with the dynamical systems part of the project, for the many hours and long emails he spent illuminating the Center Manifold Theorem, and for his patience with my relentless silliness.

Many, many thanks to Nicky Walker for her kindness, guidance and for making life, in general, a *lot* easier - I am terrified of facing the bureaucracy without her!

I would like to thank the Children of the Milky Way for the cups and the cakes, and all the right amounts of nonsense during our time together in NASSP.

I am sincerely grateful to Byron, for being there for me during all of the most difficult times of the past two years, as well as being instrumental in the construction of all the best times, for always offering his support, and for the food, drinks and housing!

My deepest thanks to Preeti, Noddy and Shéla, for their unwavering support and encouragement throughout my studies (and my life), for long, motivational conversations and for the virtual hugs and tissues, as well as all the undocumented funds they provided! I am truly grateful to my grandparents, Ved and Deviani Jugessur, for their wise words and wonderful stories, and for their illimitable love and support over the years.

Finally, I acknowledge the National Astrophysics and Space Science Programme (NASSP) in association with the National Research Foundation (NRF), for funding my degree.

Plagiarism Declaration

I, Sulona Kandhai, know the meaning of plagiarism and declare that all of the work in the document, save for that which is properly acknowledged, is my own. The following results presented in this thesis are new:

- The dynamical systems analysis of a Hu-Sawicki model ($n = 1, c_1 = 1$)
  - The dynamical systems equations for the Hu-Sawicki model ($n = 1, c_1 = 1$) are determined.
  - Two stable de Sitter states, an unstable matter-like state, and several unstable radiation-like states were identified. Several demonstrative example orbits are presented.
- The expansion history of a Hu-Sawicki model ($n = 1, c_1 = 1$) determined by the dynamical systems analysis was obtained.
  - Integration of this model was performed separately from two sets of initial conditions; the first set at the present epoch and at $z = 20$.
  - It was found that the initial value of the correction, being critical in the success of the model in matching ΛCDM, at $z = 0$ was not large enough to assume its plateau value.
  - It was found that the initial value of the correction at $z = 20$ was sufficiently large to produce an expansion history promisingly similar to ΛCDM.
  - It was concluded that this Hu-Sawicki model ($n = 1, c_1 = 1$) was only able to simulate ΛCDM at the expense of the present day values of h_0 and q_0.

These results are used in the following publication:

1. de la Cruz-Dombriz, A. *et al.* (2013) arXiv: 1312.2022 [gr-qc]

The results contained in sections 4.2.3, 4.2.4, 4.3 and 4.4 are currently being prepared for publication.

Contents

Introduction and outline of thesis

In recent years, the field of cosmology has taken to considering the effects of a more *generalised* theory of the gravitational interaction. This is toward addressing several troubling issues with the standard model of cosmology, such as the need for exotic forms of energy to facilitate the observed late-time accelerated expansion, as well as severe fine tuning issues associated with Big Bang Cosmology.

Generalising the gravitational theory amounts to picking a more general Lagrangian for the gravitational action. As it stands, the Lagrangian which constitutes the Einstein-Hilbert action (which when varied produces the Einstein's Field Equations) is *linear* in the four-curvature, R. However, in principle, there is no reason (other than its simplicity) to restrict the Lagrangian to linearity in R. In fact, it is quite possible that the addition of higher powers of R and corresponding invariants may improve the characterisation of gravitational fields near singularities [4]. Further impetus to explore results of nonlinear gravitational Lagrangians is the fact that every theory attempting to unify the fundamental interactions require either, that there are non-minimal couplings to the geometry, or, that higher order curvature invariants appear [6],[4]. The gravitation theories which result from investigations of such a nature (modifying the Einsten-Hilbert action), are called modified theories of gravity. At this time, there exist several branches of modified gravity, each approaching the problem from different angles. Hopefully, from this endeavour, a deeper understanding of the gravitational interaction and its consequences will emerge.

In particular, this thesis is concerned with fourth order theories of gravity, that is, theories which stem from Lagrangians involving some of the four possible curvature invariants of the Ricci scalar, Ricci and Riemann tensors; $R^2, R_{ab}R^{ab}, R_{abcd}R^{abcd}$ and $\varepsilon^{iklm}R_{ikst}R^{st}_{lm}$.

The research sphere of $f(R)-$gravity has grown substantially over the past couple of decades, and much work has gone into trying to find ways to combat the extreme complications which arise when considering higher order curvature invariants in the gravitational action. In this thesis, we consider one such way, known as the dynamical systems approach to fourth order cosmology, which has proven to be quite successful in deriving insights into the theory considered.

The dynamical systems approach makes use of the theory of dynamical systems to analyse the form of gravity which is produced when picking a specific function, $f(R)$, and enables the study of the cosmology such a form of gravity would allow.

The particular $f(R)$ theory considered in this thesis is one that has gained popularity over the past few years for its design, the so-called Hu-Sawicki model. In the low curvature limit, the Hu-Sawicki model reduces to standard GR, which is well tested at the solar system level. In the high curvature limit, it is designed to mimic ΛCDM by a corrective term assuming a constant value, simulating the effects of a cosmological constant, *without* a true cosmological term. Thus, this theory manages to overcome several issues faced by other theories and is, therefore, an interesting candidate to describe the gravitational interaction.

In this work, the cosmological equations generated by this theory of gravity are studied in terms of a specific set of dynamic coordinates, and its phase space is constructed in order to analyse global, qualitative features of the resulting cosmology.

Part I - Preliminary Concepts is concerned with covering the key ideas in modern cosmology, modified gravity and dynamical systems: I give a brief review of the basic concepts in cosmology and a background of the best and widely accepted model of the universe - The Big Bang Theory. I outline the major pieces of observational

evidence which support this theory and summarise the details of the main problems and difficulties with which it is faced. Modified gravity is reviewed, with particular emphasis placed on the area of $f(R)-$gravity; I discuss the motivation for modifying gravity and outline a model rubric for a good theory of gravity. For completeness, I include a discussion of the important concepts in the theory of dynamical systems which have been used to aid the research included here.

Part II - The Dynamics of the Hu & Sawicki model for $f(R)-$gravity includes a detailed account of the method and results of the analysis. A dynamical systems analysis is performed, using a compact and non-compact phase space, to identify its equilibrium points, these are then classified in terms of stability and the exact scale factor solutions are determined. The expansion history produced by the dynamical systems equations is presented and compared with the ΛCDM model.

Part I

Preliminary Concepts

Chapter 1

Standard Cosmology

1.1 Basic principles of modern cosmology

1.1.1 General Relativity

The timeline of gravitational physics can undoubtedly be divided into two eras; Before Einstein and After Einstein. Upon the discovery and formalisation of the theory of General Relativity, cosmology was catapulted from the confines of speculation and empirical deduction into the discipline of a formal mathematical science; this marked a watershed in the history of modern physics. We gained a beautiful geometric description of the gravitational interaction and a capacity to predict phenomena in the solar system and beyond with stunning accuracy. One of the pivotal concepts in general relativity is the equivalence principle, which equates the gravitational force or acceleration due to gravitational force, to free fall motion in a curved space-time.

Einstein's Field Equations

The most important consequence of general relativity is its geometric description of the universe and the gravitational interaction; it describes how matter interacts with the geometry of a given space time [30], This description is compactly contained in Einstein's famous field equations which, as Hilbert discovered in 1915, can be derived using the variational principle if the action is given by [30], [65]:

$$S = \int \left[R + \mathcal{L}_M\right] \sqrt{-g} d^4x \ . \tag{1.1}$$

Here, R is the Ricci scalar, $\mathcal{L}_M$ represents the Lagrangian of any matter fields which may be present and g is the determinant of the metric tensor, $g_{\mu\nu}$. The above action is known as the Einstein-Hilbert action, and, when varied, yields the following set of equations:

$$G_{\mu\nu} = \kappa T_{\mu\nu} \ , \tag{1.2}$$

where $\kappa = 8\pi G$ and $G_{\mu\nu}$ is the Einstein tensor of the metric $g_{\mu\nu}$ (Greek letters run from 0 to 3) and is defined as follows:

$$G_{\mu\nu} \equiv R_{\mu\nu} - \frac{1}{2} g_{\mu\nu} R \ . \tag{1.3}$$

$R_{\mu\nu}$ is the Ricci tensor derived by the contraction of the Riemann tensor, which describes the space-time curvature and is defined as:

$$R_{\alpha\ \nu\beta}^{\ \mu} = \Gamma^{\mu}_{\ \nu\delta,\beta} - \Gamma^{\mu}_{\ \beta\delta,\nu} + \Gamma^{\epsilon}_{\ \nu\delta}\Gamma^{\mu}_{\ \beta\epsilon} - \Gamma^{\epsilon}_{\ \beta\delta}\Gamma^{\mu}_{\ \nu\epsilon} \ , \tag{1.4}$$

and the connection, $\Gamma^{\sigma}{}_{\mu\nu}$, in terms of the metric, is

$$\Gamma^{\sigma}{}_{\mu\nu} = \frac{1}{2} g^{\sigma\delta} \left[g_{\delta\mu,\nu} + g_{\delta\nu,\mu} - g_{\mu\nu,\delta} \right] \ . \tag{1.5}$$

The symmetries of the Riemann tensor (skew in the last pair of indices, skew in the first pair of indices, symmetric under pair interchange and considering the cyclic identity) result in only two, equivalent, non-trivial contractions of the Riemann tensor [30]:

$$R^{\alpha}{}_{\mu\alpha\nu} = R_{\mu\nu} \ , \tag{1.6}$$

which is the so-called Ricci tensor. The Ricci scalar, or the *curvature* scalar, is defined by the contraction of the Ricci tensor:

$$R = R^{\mu}{}_{\mu} = g^{\mu\nu} R_{\mu\nu} \ . \tag{1.7}$$

The two quantities above appear explicitly in (1.3).

$T_{\mu\nu}$ in (1.2) is the standard stress energy tensor of a time-like observer with velocity $\mathbf{u}$.

$$T_{\mu\nu} = \rho u_{\mu} u_{\nu} + q_{(\mu} u_{\nu)} + q_{(\nu} u_{\mu)} + P h_{\mu\nu} + \pi_{\mu\nu} \ , \tag{1.8}$$

where $h_{\mu\nu}$ is the projection tensor, ρ is the density, p is the pressure, q is the heat flux and $\pi_{\mu\nu}$ denotes the anisotropic stress. Here,

$$q_{\mu} u^{\mu} = 0, \quad \pi_{\mu\nu} u^{\nu} = 0, \quad \pi_{\mu}{}^{\mu} = 0, \quad \pi_{\mu\nu} = \pi_{\nu\mu}.$$

In general, the contents of the universe will comprise a variety of components. However, for simplicity, and because in reality different components at various times in the history of the universe become negligible relative to another, we consider a fluid with only one form of energy density. To simplify the problem even further, we assume this fluid behaves as a *perfect* fluid, with energy density ρ, pressure P, and barotropic equation of state, $P = P(\rho)$. For such a perfect fluid the stress energy tensor becomes:

$$T_{\mu\nu} = (P + \rho) u_{\mu} u_{\nu} + P g_{\mu\nu} \ , \tag{1.9}$$

owing to the fact that, for a time-like observer, $u^{\mu} u_{\mu} = -1$. The equation of state of this fluid is taken to have the form

$$P = w\rho \ , \tag{1.10}$$

where the constant w is called the equation of state parameter, and determines the form of energy density being considered. Practically, within cosmology, the most significant values for w are $w = 0$ - corresponding to pressure-free, non-relativistic matter, which we refer to as *"dust"* - , $w = \frac{1}{3}$ - corresponding to relativistic matter, or radiation having a pressure given by $P = \rho c^2/3$, and recently due to the overwhelming evidence for change in the dominant form of energy density in the universe [47], $w = -1$, which represents a negative pressure resulting from "Dark Energy" which is detailed in later sections. From now onwards, I assume units such that $c = \kappa = 1$.

It is clear that equation (1.2) describes how the energy density contained in the universe determines the curvature of the space-time. It turns out that the solutions to equation (1.2) imply that the universe should be expanding, an idea that Einstein did not agree with. In order to preserve the static nature of the universe, as he believed it was, Einstein proposed an additional term : $\Lambda g_{\mu\nu}$. This term, which effectively represents the energy of the vacuum, couples gravitationally to matter and serves to collapse the universe to an extent depending on its value, resulting in the stagnation of the size of the universe.

When it was discovered that distant galaxies are hurtling away from us and each other, with velocities proportional to their distance from the observer, it was interpreted that the observable universe *is* undergoing a volume expansion, and the cosmological constant term was dropped from the Einstein equations. New interest in the function of the cosmological constant in (1.2) has been generated by the recent discovery that

the expansion of the universe is accelerating.

1.1.2 Equations of Cosmology

FLRW metric

The Cosmological Principle serves as the bedrock for modern cosmology and much of the progress which has been made stems from this principle. The Cosmological Principle is a statement describing our observing perspective of the *large scale* universe as typical in all directions. This amounts to assuming that the way we view the universe, from our particular spot in this particular galaxy, in this particular cluster etc., is not at all different from what an observer would see had he been placed at *every other* point in the universe. More precisely: at large scales, the universe is both isotropic and homogeneous. Homogeneity implies *where ever you are* the universe appears the same (invariance under translations), and isotropy implies *where ever you look* the universe appears the same (invariance under rotations). This, of course, is only possible on cosmological scales.

There is observational support of the cosmological principle such as [13], [38], [21]:

- the apparently random distribution of radio sources exhibits isotropy across the sky [21],
- there exists an isotropic distribution of diffuse X-ray radiation which gives information about the distribution of unresolved AGNs [13],[21],
- we observe the large scale complexes and structures of galaxy clusters and voids to have a random spatial distribution,
- the cosmological redshift of distant galaxies exhibit isotropic behaviour, this indicates a *uniform* expansion of space [57] [38],
- relic radiation originating early in the history of the universe at the time of decoupling[1], known as the Cosmic Microwave Background (CMB) is an isotropic source of radiation, which is the same in all directions with tiny variations on the order of one part in 100 000. [13]

The only metric, which can be defined on a given space-time, that enables the properties discussed above (isotropy and homogeneity) is now known as the Friedmann-Lemaitre-Robertson-Walker (FLRW) metric, and is an exact solution of the Einstein field equations given by (1.2). This metric can be deduced by purely geometric argument, by allowing temporal dependence of the spatial coordinates [30]:

$$ds^2 = -dt^2 + a(t)^2 \left[\frac{dr^2}{1-kr^2} + r^2 d\theta + r^2 sin^2\theta d\phi \right] . \tag{1.11}$$

The spatial components of the metric contained in the square brackets, correspond to the metric of a maximally symmetric 3-space, of which the basis vectors are $(\hat{r}, \hat{\theta}, \hat{\phi})$. The geometric properties of such a space are characterised by only the constant curvature k. This constant, k, is independent of the coordinates, and can take on the values $1, 0, -1$, depending on whether the spatial section has positive, zero or negative curvature, respectively. The results for each of these cases are outlined, briefly, below [30].

Positive Curvature **-** $k = 1$

When $k = 1$, it seems that at $r = 1$ there exists a singularity, but it can be shown that this is just a result of the coordinates used. In fact, making the following change of coordinates eliminates that issue:

$$r = \sin\chi$$
$$\text{therefore} \quad dr = \cos\chi d\chi = \sqrt{1-r^2}d\chi$$

[1] see section 1.2

The metric becomes:

$$ds^2 = -dt^2 + a(t)^2 \left[d\chi^2 + \sin^2\chi(d\theta^2 + \sin^2\theta d\phi^2)\right] \ . \tag{1.12}$$

Clearly, this corresponds to a spherical, or *closed* geometry; two particles with initially parallel velocity vectors eventually converge.

Negative Curvature **-** $k = -1$

Similarly in the case when $k = -1$, setting $r = \sinh\chi$ in (1.11), then

$$dr = \cosh\chi d\chi = \sqrt{1 + r^2} d\chi \ ,$$

and the metric becomes:

$$ds^2 = -dt^2 + a(t)^2 \left[d\chi^2 + \sinh^2\chi(d\theta^2 + \sin^2\theta d\phi^2)\right] \ ,$$
$$0 \leq \chi < \infty, \quad 0 \leq \theta \leq \pi, \quad 0 \leq \phi \leq 2\pi \ .$$

This corresponds to hyperbolic, or *open*, geometry; two particles with initially parallel velocity vectors eventually diverge.

Zero Curvature **-** $k = 0$

The case $k = 0$, is called flat spatial geometry and is identical to Euclidean 3 space, for which the FLRW metric can be written simply in terms of the above coordinates as:

$$ds^2 = -dt^2 + a(t) \left[d\chi^2 + \chi^2(d\theta^2 + \sin^2\theta d\phi^2)\right] \ . \tag{1.13}$$

Two particles with initially parallel velocity vectors in a spatially flat geometry will remain so forever. There exists a very special density that the universe is required to have in order to be geometrically flat, known as the *critical density*[2]. If the actual density of the universe is greater or smaller than this critical density, then its geometry is spherical or hyperbolic respectively.

Throughout this thesis we assume a flat space-time, for the benefits of simplicity of the field equations corresponding to this case. This choice, however, does not necessarily sacrifice generality. Measurements of Ω_k, the curvature density parameter[3], determined from current observations show that it is very close to zero at the present epoch. We can therefore accept the choice $k = 0$ as an *approximation* of the curvature, as opposed to setting it as an initial condition [59].

Clearly, the only parameters which represent degrees of freedom in the FLRW metric is the curvature constant, k and the function $a(t)$ [21], [38].

Hubble's law and the cosmological redshift

The time dependence of the spatial coordinates in (1.11) is completely contained in the function $a(t)$, which is known as the *scale factor*. This function describes how the comoving distance (which remains constant as the universe expands) between two points in the universe is related to the proper distance between them as a function of time:

$$D(t) = a(t)\chi \ . \tag{1.14}$$

$D(t)$ is the physical distance which, in our expanding universe, increases as a function of time, and χ is the comoving distance - the distance between two points in the universe, measured in *comoving coordinates*. The

[2] See section 1.1.3

[3] This density parameter is defined in Section 1.1.3 at equation (1.50)

comoving distance of an object at scale factor a is given by:

$$\chi(a) = \int_{t(a)}^{t_0} \frac{dt'}{a(t')} \ . \tag{1.15}$$

In an interval dt , unimpeded, light can travel a comoving distance of $d\chi = dt/a$, therefore the total distance a light ray can travel since $t = 0$ is:

$$\eta = \int_0^t \frac{dt'}{a(t')} \ . \tag{1.16}$$

This distance is of critical importance: if two points are separated initially by a distance greater than η then no information can pass between between them; they are not *causally connected*. η is called the *comoving horizon* [21], [43].

The formula at (1.14) can be derived by direct integration of (1.13), if we consider that all information about distant galaxies is bought to us by *photons* travelling with a *radial* component only (photons follow null geodesics):

$$ds^2 = -dt^2 + a(t)^2 d\chi^2 \ .$$

Integrating the above equation, within a constant portion of time (holding $dt = 0$), we obtain exactly (1.14). The differentiation of (1.14) with respect to time, keeping in mind that both scale factor, a, and the comoving distance, χ, are functions of time relative to an observer external to the comoving reference frame, we obtain an expression for the *total* velocity of a distant observable object, such as a galaxy, $\dot{D} = v_{total}$:

$$\begin{aligned} v_{\text{total}} &= \dot{D} = \dot{a}\chi + a\dot{\chi} \\ \rightarrow v_{\text{total}} &= v_{\text{recession}} + v_{\text{peculiar}} \ . \end{aligned} \tag{1.17}$$

The total velocity of a distant galaxy consists of two distinct components, one which involves the derivative of the *scale factor*, and one which involves the derivative of the *comoving distance*. The latter is fairly easy to interpret intuitively, it is clearly the proper velocity of the object - its change in comoving distance with respect to time, known as its *peculiar velocity* of the object. The former component, known as the *recession* velocity, is the rate of change of scale factor with respect to time, and is interpreted as a direct measure of the expansion of the universe. So, the total velocity of a photon traveling toward us from a distant galaxy is not constant, in fact it depends on its distance away from us :

$$v_{total} = v_{recession} - c \ ,$$

the negative sign associated with the speed of light indicates its direction toward us.

The existence of this recession velocity, its interpretation being a smooth expansion of the observable universe, was investigated independently by Friedmann and Lemaitre in 1922 and 1927 respectively [13]. Observational confirmation of this expansion was given by Edwin Hubble in 1929, who measured distances to external galaxies by using Cepheid variable stars (whose periods have direct relationships with their brightness) as standard candles. Upon investigation of the data, Hubble discovered that a correlation existed between the spectral redshift of the galaxies and their distances: the velocity associated with the galaxy calculated from its spectral redshift is directly proportional to the its distance from *any* observer [13], [38]. Of course, the effect is only noticeable at distances large enough that any peculiar velocity components are small relative to the recession velocity. Thus, Hubble discovered empirical evidence to suggest that the universe is undergoing an effective volume expansion around every point contained in it. This evidence is one of the milestones in modern cosmology as it shattered, once and for all, any inhibitions regarding the concept of the expanding universe. The relationship between the cosmological redshift velocity and the distance of a distant object is given by

Hubble's Law:

$$v = HD \ . \tag{1.18}$$

It is the *recession velocity* from equations at (1.17) which features in this formula. H is called the Hubble parameter, which is constant throughout space, but varies temporally. This parameter is defined by the derivative of the scale factor as follows (I drop the independent variable specification for neatness):

$$H = \frac{\dot{a}}{a} \ . \tag{1.19}$$

The cosmological redshift, which is the redshift due solely to the velocity determined by Hubble's law, arises due to the stretching of space itself, and is a general relativistic effect, unlike the *Doppler* shifting of the frequency of light due to motion along the line of sight. However, it is related to the wavelength of the light in the same way, and therefore, is also directly related to the scale factor which scales the wavelengths. The cosmological redshift, z, as a function of scale factor is:

$$z + 1 = \frac{a_0}{a} \ , \tag{1.20}$$

where a_0 denotes the value of the scale factor at the present epoch. By convention, this is set to 1, such that the redshift at the present epoch is appropriately equal to zero.

Cosmological equations for the FLRW metric

Substituting the FLRW metric into the Einstein equations results in a set of equations that describe a homogeneous and isotropic universe. Of the sixteen components of the metric, only the four diagonal elements are non-vanishing; $g_{tt} = -1, g_{rr} = a(t)^2/(1 - kr^2), g_{\theta\theta} = a(t)^2 r^2$ and $g_{\phi\phi} = a(t)^2 r^2 sin^2\theta$, and these involve only one unknown function; $a(t)$ [30].

We can write the Einstein Field Equations as

$$R_{\mu\nu} = -\kappa(T_{\mu\nu} - \frac{1}{2} T g_{\mu\nu}) \tag{1.21}$$

The left hand side of equation 1.21 is determined by calculating the Ricci tensor from the connection. The only non zero values of the Ricci tensor are:

$$\begin{aligned} R_{00} &= 3\frac{\ddot{a}}{a}, \\ R_{11} &= -\frac{(a\ddot{a} + 2\dot{a}^2 + 2k)}{1 - kr^2}, \\ R_{22} &= -(a\ddot{a} + 2\dot{a}^2 + 2k)r^2, \\ R_{33} &= -(a\ddot{a} + 2\dot{a}^2 + 2k)r^2 sin^2\theta. \end{aligned} \tag{1.22}$$

Addressing the energy part of the Einstein field equations; the energy momentum tensor is given by equation 1.9, and its contraction gives:

$$T = T^{\mu}{}_{\mu} = \rho - 3P. \tag{1.23}$$

thus, the components of the left hand side of equation 1.21 read as

$$T_{\mu\nu} - \frac{1}{2} T g_{\mu\nu} = (\rho + P)\delta^0_\mu \delta^0_\nu - \frac{1}{2}(\rho - P) g_{\mu\nu}, \tag{1.24}$$

which is non-zero only for $\mu = \nu$:

$$\begin{aligned} -\kappa(T_{00} - \frac{1}{2}Tg_{00}) &= -\frac{1}{2}(\rho + 3P) \\ -\kappa(T_{11} - \frac{1}{2}Tg_{11}) &= \frac{-\frac{1}{2}(\rho - P)a^2}{1 - kr^2} \\ -\kappa(T_{22} - \frac{1}{2}Tg_{22}) &= -\frac{1}{2}(\rho - P)r^2a^2 \\ -\kappa(T_{33} - \frac{1}{2}Tg_{33}) &= -\frac{1}{2}(\rho - P)a^2r^2sin^2\theta \end{aligned} \tag{1.25}$$

The substitution of the above elements and those of the Ricci tensor into equation 1.21 results in only two independent field equations:

From the 00− component, one obtains:

$$-3\frac{\ddot{a}}{a} = \frac{\kappa}{2}(\rho + 3P) \ , \tag{1.26}$$

and from the 11− component:

$$-\frac{2\dot{a} + a\ddot{a} + 2k}{a^2} = \frac{\kappa}{2}(P - \rho) \ . \tag{1.27}$$

Clearly, the other two space-space components are not independent of (1.27), and off diagonal components reduce to zero. Eliminating $\ddot{a}$ and solving for the first derivative of the scale factor yields the following equation which, when solved, gives the evolution of the scale factor and its relation to the density in the universe:

$$\left(\frac{\dot{a}}{a}\right)^2 = \frac{8\pi G}{3}\rho - \frac{k}{a^2} \ , \tag{1.28}$$

$$\rightarrow H^2 = \frac{8\pi G}{3}\rho - \frac{k}{a^2} \ . \tag{1.29}$$

This equation is known as the *Friedmann equation*.

Eliminating $\dot{a}$ from (1.21) and (1.22), results in the following equation describing the evolution of the second derivative of the scale factor, called the *Raychaudhuri equation*:

$$\frac{\ddot{a}}{a} = -\frac{4\pi G}{3}\rho(1 + 3w) \ . \tag{1.30}$$

Together, (1.29) and (1.30) are the *cosmological field equations* specific to the FLRW metric. The Friedmann equation gives information about the evolution of the scale factor with time, and the Raychaudhuri equation describes how the rate of expansion changes. These equations are essential to any investigation of a cosmological model. The parameters which determine the evolution are w and k which specify the dominant form of matter and the shape of the universe, respectively.

The continuity equation for the specific form of matter can be derived from the Raychaudhuri equation and the Friedmann equation, and is given by:

$$\dot{\rho} = -3H\rho(1 + w), \tag{1.31}$$

which is a statement of conservation of energy density. The solution to the continuity equation will provide a function to describe the way the energy density evolves with *scale factor* if the equation of state parameter, w, is specified.

For $w = 0$, representing any energy density that exerts insignificant pressure, which usually means any non-relativistic matter, we find that $\rho_m \propto a^{-3}$. It is simple and intuitive that the density of ordinary matter would scale as the inverse cube of a distance quantity. Considering (1.30), a dust dominated universe (a universe filled predominantly with dust-like matter) would have its expansion retarded; $\ddot{a}$ is negative which implies deceleration. We can fix the proportionality constant by considering the one known boundary condition to

be the present epoch, for which the scale factor is set equal to one. By convention, present values of various quantities are denoted with a subscript "0", therefore: $\rho_m = \rho_0 a^{-3}$. The cosmic time dependence of the scale factor for a matter dominated universe can be found by direct integration of the Friedmann equation at (1.29). For example for a flat, matter dominated universe we would have:

$$\dot{a}^2 = \frac{8\pi G}{3}\frac{\rho_0}{a} \ . \tag{1.32}$$

Solving the above differential equation gives:

$$a(t) = \left(\frac{t}{t_0}\right)^{2/3} \ , \tag{1.33}$$

therefore we have :

$$\rho(t) = \frac{\rho_0}{a^3} = \frac{\rho_0 t_0^2}{t^2} \ . \tag{1.34}$$

Although this universe expands forever, its expansion slows down with time:

$$H \equiv \frac{\dot{a}}{a} = \frac{2}{3t} \tag{1.35}$$

For $w = \frac{1}{3}$, representing any matter that has relativistic motion; radiation, we find that $\rho_r = \rho_0 a^{-4}$. The extra factor of a^{-1} is obtained due to the fact that the energy of radiation is inversely proportional to its wavelength, and the wavelength is proportional to the scale factor. A radiation dominated universe also has $\ddot{a}$ negative, implying a decelerating expansion. We can find the time evolution of the scale factor for a flat, radiation-dominated FLRW universe in the same way as above:

$$a(t) = \left(\frac{t}{t_0}\right)^{1/2} \quad \Rightarrow H = \frac{1}{2t} \tag{1.36}$$

and

$$\rho(t) = \frac{\rho_0}{a^4} = \frac{\rho_0 t_0^2}{t^2} \ . \tag{1.37}$$

The above two cases are important in standard cosmology and are often referred to as classic cosmological solutions of the Friedmann model.

For $w = -1$, representing a non-negligible constant vacuum energy density that has negative pressure, we find that $\rho_{VE} = Constant$. In this case, $\ddot{a}$ is positive, and thus a universe dominated by the vacuum energy will have an accelerated expansion. We can see this by integrating (1.29) for this case, as we have done for the matter and radiation cases above:

$$\left(\frac{\dot{a}}{a}\right)^2 = \frac{8\pi G}{3}\rho_0 \tag{1.38}$$

$$\Rightarrow \frac{da}{a} = \sqrt{\frac{8\pi G}{3}\rho_0}\,dt \tag{1.39}$$

$$\Rightarrow a(t) = a_0 e^{\sqrt{\frac{8\pi G}{3}\rho_0}(t-t_0)}. \tag{1.40}$$

The scale factor grows exponentially with time. This type of universe, dominated by the vacuum energy, is known as de Sitter-Einstein universes.

In fact, looking at equation (1.30), it is clear that if the dominant form of energy density in the universe has an equation of state parameter, $w < -\frac{1}{3}$, then $\ddot{a} > 0$, resulting in an accelerated expansion phase of the universe. Recent evidence has come to light suggesting that our universe is currently being dominated by such a fluid, which is causing the previously matter dominated deceleration phase to be surpassed by a mysterious energy density whose exact nature and origin is unknown. This new energy density has been dubbed Dark

Energy, and seems to be driving an accelerated phase of expansion in our universe.

1.1.3 Observational cosmological parameters

Expansion rate, H_0

The present value for the Hubble rate defined at (1.19) is called the Hubble constant, denoted H_0, as usual. The task of obtaining an extremely precise measurement of H_0 is troublesome, to say the least. While the linear relationship between recession velocity and distance of an object is excellently established observationally, extracting the exact value of H_0 depends on a number of factors, which lie out of our control as a consequence of the fact that the sky is a difficult laboratory. Every galaxy, while having a recession velocity which depends on position, also has a peculiar velocity which does not. The peculiar velocities should, in principle, be randomly distributed, therefore, at large enough distances, they should be negligible compared to the recession velocity. However, such large distance measurements suffer large uncertainties, therefore, the Hubble constant is given by a second constant parameter, h:

$$H_0 = 100\ h\ \text{km}\ s^{-1}\ \text{Mpc}^{-1}\ , \tag{1.41}$$

where h is left to be determined by observations. The latest value of h was obtained using data from the Planck Mission cosmology probe [48] and was found to be:

$$h = 0.6780 \pm 0.0077\ . \tag{1.42}$$

Because H is such a fundamental parameter in cosmology, its associated uncertainty bleeds through to many other measurable quantities. Thus it is common for these quantities to be expressed in terms of h.

The density parameter, Ω_0

As mentioned previously, the $k = 0$, flat geometry, case is a very special one, and there are several pieces of evidence which support our universe being flat. The density required for a flat universe is called the *critical density*. An expression describing this density may be found by setting $k = 0$ in (1.29):

$$\rho_{crit}(t) = \frac{3H^2}{8\pi G}\ . \tag{1.43}$$

Because H is dynamic and evolves with time, so does the value of the critical density. In terms of the Hubble parameter, h, and $G = 6.67 \times 10^{-11}\text{m}^3\text{kg}^{-1}\text{sec}^{-2}$, the critical density corresponding to the present epoch is [38]:

$$\rho_{crit}(t_0) = 1.88h^2 \times 10^{-26}\text{kg m}^{-3}\ , \tag{1.44}$$

or more transparently

$$\rho_{crit}(t_0) = 2.78h^{-1} \times 10^{11} M_\odot/(h^{-1}\text{Mpc})^3\ . \tag{1.45}$$

It is useful to compare the actual density of the universe to this critical density, and this comparison is the ratio:

$$\Omega \equiv \frac{\rho}{\rho_{crit}} = \frac{8\pi G}{3H^2}\rho\ . \tag{1.46}$$

Ω is called the *density paramater*, and is a function of time. Using this ratio in (1.29), the Friedmann equation can be expressed as:

$$H^2 = H^2\Omega - \frac{k}{a^2}\ , \tag{1.47}$$

or

$$\Omega - 1 = \frac{k}{a^2H^2}\ . \tag{1.48}$$

This is a convenient way to write the Friedmann equation. From this, we can see immediately that $\Omega = 1$ corresponds to a flat universe.

The diversity in the actual composition of the energy density in the universe can be shown in defining separate density parameters for each form of energy, by making its fraction with the critical density:

$$\Omega_i = \frac{\rho_i}{\rho_{crit}} \ , \tag{1.49}$$

where i represents matter or radiation. We define the curvature density parameter from the right hand side of (1.48):

$$\Omega_k \equiv -\frac{k}{a^2 H^2} \ . \tag{1.50}$$

Non-zero values for Ω_k would be indicative of departure from spatial flatness[4] .

The deceleration parameter, q_0

It is convenient to define a parameter which quantifies the rate at which the universe is expanding:

$$q \equiv -\frac{\ddot{a}a}{\dot{a}^2} \ . \tag{1.51}$$

It is called the *deceleration* parameter. If $\ddot{a} > 0$, then $q < 0$ and the expansion of the universe is accelerating. On the other hand, if $\ddot{a} < 0$, as would be in a matter dominated Friedmann universe, then $q > 0$ and the expansion would be decelerating.

1.2 Big Bang Cosmology

The expansion of the universe leads quite naturally to the idea that the universe was once much smaller. If one continues backward in time, it would seem that all the points of the universe would have had to have been very close together. This idea drove the development of what is now known as the Big Bang Theory. The key postulate of the Big Bang Theory is that the universe began with a violent, rapid expansion of all of space from an infinitely hot, dense singularity [13]. Physical laws, as we know them to be, do not apply near this initial singularity, and the mechanisms, forces and natural fields within the first moments of the universe are not understood. However, what happens in the fractions of a second after the Big Bang right up to the present epoch does have a theoretical description, which has gained wide consensus in the field of cosmology and astrophysics, and does very well to describe the current observations. It is important to understand that this theory does not give information about the origin of the universe, such as why and how it came into existence. It *does* succeed in describing and explaining the evolution of the universe just moments *after* it came into existence, in a comprehensive and justifiable manner.

In this section, I will briefly outline the, now widely accepted, Big Bang Theory and give the major observational support pillars upon which it is founded. I will also discuss various problems it faces, one of these problems being the basis for my thesis.

1.2.1 Core ideas of the Big Bang Theory

The theory is founded upon the assumptions that the physical laws are correct throughout the universe, specifically that Einstein's theory of General Relativity is the correct description of gravity, and that the metric defined upon our space-time is given by the FLRW metric at (1.11).

[4]The Hubble rate, H is calculated from the sum of all the forms of energy density in the universe, therefore there exists a degeneracy between the values of components which can result in the same expansion rate. Thus, Ω_k is constrained together with the dark energy density parameter, Ω_Λ [58].

The physics involved at the earliest moments of the universe are extremely speculative. There are no verifiable theories at this stage which outline exactly what took place. It is postulated that the universe was a homogeneous and isotropic distribution of some energy density under extreme conditions, which was very rapidly expanding, which lead to its cooling. It is thought, for reasons discussed later, that a phase transition triggered an exponential expansion era known as cosmic inflation which facilitated the super-cooling of the energy content of the universe [36]. At some time later, the potential energy of the field giving rise to inflation decayed into relativistic particles, such as quarks, gluons, electrons etc. This period is known as reheating, and caused the temperature of the universe to rise to its pre-inflation temperature. This high temperature supported the continuous production and annihilation of particle-antiparticle pairs [13], [21], [37], [36].

Some time during the existence of this plasma, a reaction took place, called baryongenesis, which violated the baryon number conservation. This resulted in a small overproduction of particles relative to anti-particles, which is supposed to explain the obvious over density of matter relative to antimatter in the universe today. The theory behind this reaction is still not understood [13].

As the universe continued to expand, the number density, temperature, pressure and particle energy decreased, in order to allow the interaction, combination and formation of sub-atomic particles. At approximately 10^{-6} seconds after the big bang, protons and neutrons formed from quarks and gluons, and particle-antiparticle pair production was no longer supported by the temperature. Thus, the over density in particles relative to antiparticles was frozen into the universe. Hereafter, the electrons, protons and neutrons had lost sufficient energy such that they were no longer relativistic, and the dominant energy density in the universe was that of photons. During this time the high energy photons prevented the formation of atoms or nuclei [13], [21].

After about three minutes, when the universe was cool enough, such that the energies of the particles in the plasma were well below the binding energy of a typical atomic nucleus, a process called big bang nucleosynthesis began. This is the production of light atomic nuclei, deuterium and helium, from the interaction of some of the protons with neutrons [13].

The universe continued to lose energy due to work done in the expansion, and the temperature decreased, enough so that the energy of the photons was comparable to the rest mass energy density of the baryonic matter, and later, enough so that the energy density of matter *dominated* the energy density of photon radiation. Thereafter, about 379 000 years later, the formation of atoms occurred, this reduced the opacity of the plasma and allowed the radiation to become decoupled from the matter. This radiation is known as cosmic microwave background radiation, and it has since travelled freely through space [13], [38], [57].

Although the assumption is that the universe was initially homogenous, the fact that there exists structure of any sort in the universe today suggests that there must have been fluctuations or over densities in the consistency of the primordial plasma, to which seeded the growth of structure observed [21], [43], [13]. It is thought that gradual gravitational collapse of over dense regions in the almost homogeneous matter density resulted in the formation of gas clouds, which resulted (by much a similar mechanism) in star formation, galaxy formation and even the large scale structure in the universe. The nature and evolution of this era of structure formation depends on how the model is parametrized by the form, and quantity of the various types of matter at that time [21], [6].

One parametrisation of the Big Bang Theory is known as the ΛCDM model, where the Λ represents a cosmological constant for the vacuum energy, and CDM stands for cold dark matter. I will discuss this model in detail in section 1.2.3.

1.2.2 Observational support

There are three major pieces of observational evidence which favour the Big Bang Theory: The Hubble diagram which demonstrates a spatial expansion, the observed abundance of light elements require big bang nucleosynthesis, and the cosmic microwave background radiation.

The Hubble Diagram

In the early 1900s, the nature of external galaxies, then known as "spiral nebulae", was a controversial issue: astronomers could not agree on whether they were part of our galaxy, or island structures. In 1914, astronomer V. M. Slipher obtained information about the radial velocities of some galaxies by measuring their Doppler shifted spectral lines. The aim was to confirm that the motion of the objects is random, to obtain a relationship between the Sun's motion around the Milky Way and the vector sum of the radial velocities of the nebulae. However, surprisingly, he found that most of the galaxies which he observed were receding from us, as well as each other very rapidly, save Andromeda, which revealed a blueshift in its spectral lines. Over the next decade, Slipher, having studied the spectra of forty galaxies, found that nearly every one exhibited redshifted spectral lines as opposed to blue-shifted lines. This was discussed in the context of an expansion [13].

Enter Hubble. In 1925, Hubble discovered Cepheid variable stars in M31, and discovered that the spiral nebulae known as Andromeda is actually a galaxy outside of the Milky Way. Using Cepheid variables, he managed to obtain distances to 18 external galaxies. Consolidating his own results with that of Slipher's redshift data, he discovered that the recession velocity is proportional to its distance.

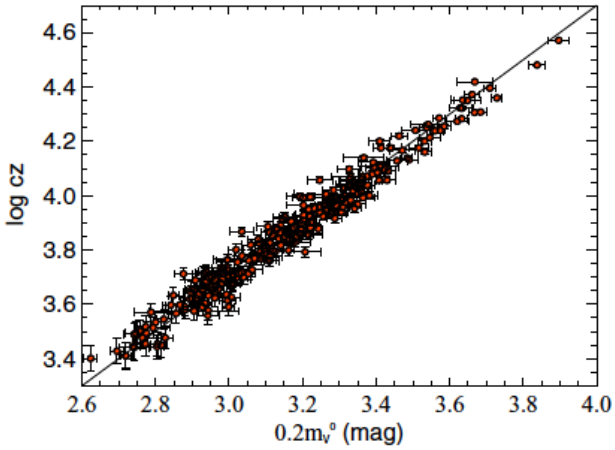

Figure 1.1: Above is a Hubble diagram constructed from 240 nearby ($z < 0.1$) SN Ia, from Hicken et al (2009), showing a magnitude-redshift relation. (A. G. Riess *et al.* 2009 *ApJ* **699** 539)

Together with his assistant, Humason, Hubble obtained distances and velocities of 32 galaxies, and the empirical relationship matured into a law of our universe[5] [13]. This relationship is one of the best pieces of evidence which indicate the expansion of the universe, which is key to the Big Bang Theory.

Light chemical abundances

About one quarter of the baryonic mass contained in the universe is helium. Considering the relative cosmic abundance of heavier elements, it seems impossible that stellar nucleosynthesis can account for the large amount of helium. While conditions within the stellar core are sufficient to create light elements (such as hydrogen, deuterium, helium-3, helium-4, and some isotopes of Lithium), such conditions over the life time of a star would result in these elements eventually being fused into heavier and heavier elements. The creation of these light elements can only have occurred during a fusion epoch much shorter than the typical stellar lifespan [13].

According to the Big Bang model, the era of nucleosynthesis began a few minutes after the initial expansion and ended about 17 minutes later. It supposedly occurred throughout the space of the universe for that period of time, resulting in the several element species which make up large percentages of the baryonic matter content of the universe today.

The model predicts mass abundances as follows: 75% ^{1}H, 25% ^{4}He, 0.01% ^{2}He, with trace amounts of Lithium and Beryllium, and no heavy elements. The fact that these predictions are consistent with the observed

[5] Details are in section 1.1.2

abundances is regarded as strong evidence for the Big Bang theory [13].

Cosmic Microwave Background

The critical idea in the Big Bang Theory is that the early universe was extremely hot and dense, so much so that the mean free paths of the photons were short enough to preserve a state of thermodynamic equilibrium[6], during which the radiation field would have a blackbody spectrum. The peak of this blackbody radiation would have been shifted far into lower energies as the universe expanded and cooled over time.

It was in 1948 that Herman and Alpher predicted that the universe should now be filled with an isotropic blackbody radiation, at a temperature of 5K, after considering the hot, dense radiation that filled the early universe according to the Big Bang Theory [13].

In 1964, Arno Penzias and Robert Wilson, working with a horn reflector antenna, discovered a continuous signal from all directions of the sky, for which they could find no source. They calculated that the radiation comes from a blackbody at 3K, from everywhere. For a year they struggled to get rid of this interference, which they assumed was due to a systematic or physical issue with the antenna itself, unaware of the theoretical predictions of such radiation. It was only in 1965, when Penzias discovered the publications of P. J. E Peebles, that he realised there may have been a connection between their 3K radiation and the black body radiation predicted by theorists' Big Bang model. The radiation peaked in the microwave region of the electromagnetic spectrum, with $\lambda_{max} = 1.06$mm. This radiation is called the Cosmic Microwave Background, and is definitely aggressive supporting evidence for the Big Bang theory. Planck data sets the value for the average temperature of the CMB today to be $2.7255 \pm 0.0006K$ [48], [51].

1.2.3 The ΛCDM Model

The ΛCDM model is a cosmological model which uses the Big Bang Theory as a basis, and fills the universe with 3 parts constant non-zero vacuum energy, where the constant is called "Λ", and 1 part cold dark matter. It has been theoretically constructed to explain several strange observations which suggest that 1.) baryonic matter constitutes only a small percent of the actual matter density of the universe, 2) that the universe is nearly flat and 3) that the expansion of the universe is not constant, but accelerating [21], [30], [38]

Dark Matter

Dark matter is a form of matter energy density which does not interact electromagnetically. Thus, so far, the only means by which we can detect it is through the effects of its gravitational interaction with luminous objects [13], [38], [21].

Its existence was first considered in 1932 by Jan Oort, who, through the study of stellar motions, found that the mass contained in the galactic plane must be larger than what is observed. In 1933, Fritz Zwicky, using the virial theorem to study the Coma galaxy cluster, realised that if the physics were assumed to be correct, there must be 400 times more mass than is observable. The motions of galaxies observed were too fast to maintain the size of the cluster, which he used to conclude that there must exist some form of non-radiating matter which could interact gravitationally that held the cluster together [13]. Further evidence for non-luminous matter is the strange observed galactic rotation curves, which indicate that their gravitational masses extend much farther than the radius of their luminous mass content [57]. While the velocities of the luminous matter contained in the galaxy near the center obeyed Keplerian orbits, farther out, instead of decreasing, the velocities exhibit a constant velocity, or even increase. This can not be explained, without the existence of some matter which does not radiate, but makes up the bulk of the galaxy, while Newtonian physics is considered applicable [13], [57].

Dark matter has also been indirectly "detected" by gravitational lensing, and there is direct evidence of dark matter in the CMB anisotropies. Acoustic oscillations in the photon-baryon plasma account for these

[6] An expanding system can not truly be at thermodynamic equilibrium, however this assumption turns out to be remarkably good.

anisotropies; while baryonic matter interacts well with the radiation, the dark matter does not interact at all, however both will govern the oscillations by their gravitational effects. And these effects can be noted in the power spectrum of the CMB anisotropies [31].

The particle nature of dark matter is completely unknown. Its ability to interact gravitationally, and not electromagnetically is the only inference which can be made. There are several candidates for the unseen matter that must exist in galaxies and galaxy clusters. The earliest of which were heavy baryonic structures which are simply difficult to detect, such as black holes, neutron stars, brown dwarfs etc. These objects are known as massive compact halo objects (MACHOs). While this idea is attractive in its simplicity, MACHOs do not constitute a large enough portion of galaxies or clusters to be responsible for the strange behaviour observed. In fact, Planck constrains the total amount of baryonic matter to about 2.2% [48] of the total mass of the universe, and a statistical analysis of the Milky Way's matter content shows that only 19% can be attributed to MACHOS [13].

Other candidates for dark matter are usually classed, by their energy, into one of the following groups: hot dark matter (HDM) and cold dark matter (CDM) [13], [57].

HDM is composed of particles moving with relativistic speeds, such as massive neutrinos. CDM candidates are hypothetical low energy, slow moving, massive particles, which are thought to interact with baryonic matter only through gravity, known as WIMPS - weakly interacting massive particles. Another proposed cold dark matter candidate is called the axion, which is a low mass boson. However, there is still no observational or experimental proponents for either [38], [13].

CDM is currently the favourite class due to the fact that it aids in the explanation of structure formation within the time constraints of the age of the universe. Neutrinos, or any other form of hot dark matter, is known to have energies too high, and motion too fast to facilitate the gravitational collapse which would inevitably lead to the formation of the large scale structures we see today. On the other hand, cold dark matter does well to explain this, and for this reason the most widely accepted model for the universe incorporates CDM as the matter type which constitutes the bulk of the matter content in the universe [38], [21].

However, there are certain issues with the CDM hypothesis regarding simulations based on this theory which show that galactic structures should have a sharp spike in the density of CDM toward their centers, while observations show behaviour of a spheroid of uniform density [18]. Explanations for this involve the idea of warm dark matter which is an intermediate energy weakly interacting particle.

Of course, the inference of the existence of dark energy is based entirely on the assumption that the laws of physics are acceptable and applicable out to galactic and extragalactic scales. As is natural, there is extensive research being done toward the aspect of the missing mass issue which assumes that the observations are a manifestation of incomplete Newtonian physics. This study has lead to the theory modified Newtonian dynamics, or MOND, and assumes that Newtonian gravity is a low acceleration limit to some more general theory and thus has to be modified at the galactic/extragalactic scales [55], [13].

Dark energy and the cosmological constant, Λ

The astrophysics of Type Ia supernovae have been used successfully as accurate distance indicators of the galaxies which contain them [44]. Such distance observations have lead cosmologists and astrophysicists to believe that the expansion of the universe is undergoing an accelerated phase of expansion. It was found, alarmingly so, that galaxies were further away, moving at speeds faster than that predicted by the Hubble constant. Given that the expansion rate, H, is determined by the energy density content of the universe, a change in H would imply a change in the dominant form of energy.

Further, angular measurements of the temperature anisotropies in the CMB point strongly to the cosmic curvature being extremely close to zero; exhibiting spatial flatness. However, the total amount of matter is constrained[7] to about 26.8% dark matter and 4.9% baryonic matter [13], of the critical density required for flatness. So, in order to have the spatial "degree of flatness" observed, there must exists a form of energy density,

[7] As of 2013, results based on observations made by the Planck spacecraft

making up nearly 68.3% of the total energy density of the universe. For this energy density, we have neither direct means of observing its nature, nor a theory predicting or describing it. It has been named Dark Energy, for its mysterious nature, and is the subject of extensive research in cosmology as a result of its enigmatic and elusive effects. Thus, there are several theoretical perspectives of Dark Energy. The simplest answer involves a constant vacuum energy density, called the cosmological constant, denoted Λ.

Revising Einstein's field equations at (1.2) by adding a stress energy tensor for the vacuum of $T^{\Lambda}_{\mu\nu} = \rho_\Lambda g_{\mu\nu}$, we have:

$$G_{\mu\nu} = 8\pi G(T_{\mu\nu} + \rho_\Lambda g_{\mu\nu}) \ , \tag{1.52}$$

where the energy density of dark energy is:

$$\rho_\Lambda \equiv \frac{\Lambda}{8\pi G} = \text{constant} = \rho_{\Lambda,0} \ , \tag{1.53}$$

and the pressure of the vacuum energy is given by:

$$P_\Lambda = -\rho_\Lambda \ . \tag{1.54}$$

If we assume the density is always positive, the pressure associated with the cosmological constant is negative. It is this negative pressure which facilitates an accelerated expansion. While matter and radiation energy components fall off rapidly with the expansion of the universe, the cosmological constant, by definition, will not. It will, therefore, come to dominate in the late time era *after* the matter density declines.

While the idea of a cosmological constant dominating the evolution of the universe is the simplest answer to the big question of Dark Energy, there are several issues it faces at a very basic level. One of which being the fact that the value which particle physics predicts for the value of the energy density of the vacuum is about 120 orders of magnitudes larger than what is observed for ρ_Λ. The fact that this vacuum energy happens to be dominating at this time, when we are alive to observe it, is also a troubling coincidence.

However, the cosmological constant paired with cold dark matter as the bulk of the matter density component forms a parametrisation of the big bang theory, known as the ΛCDM model, which gives excellent fits to current cosmological observations. It is currently the most widely accepted view of the universe.

The most basic difficulty facing the ΛCDM model is the fact that it makes a universe composed of about 95% of exotic, unknown forms of energy, provided physical laws as they stand are presumed universally acceptable.

1.2.4 Theoretical Shortcomings of the Big Bang model

The horizon problem

One of the issues facing the Big Bang model is the extreme isotropy of the CMB. The fact that the CMB is so delightfully smooth from all regions of the sky indicates that this radiation is in complete thermal equilibrium. However, thermal equilibrium requires interaction; if we consider two photons reaching us now from opposite points in the sky, they are only just *now* coming into contact with each other, so they have had no means of interacting prior to this time. In addition, points in the sky which are separated by more than 2 degrees could not have been in causal contact *at the time of decoupling*, which is what epoch the CMB reveals.

Another problem surfaces when we consider that, actually, there are tiny variations in the temperature of the CMB, which are thought to have been the origins of the structure in the universe. However, there is no theory which allows for the generation of fluctuations in a thermalised bath of photons, which means that somehow these fluctuations in the early universe were already there.

The flatness problem

The flatness problem is a fine-tuning issue. From the cosmological observations, it has been determined that at the present time the total density of the universe is rather similar to the critical density; within one percent.

The geometric implication of this discovery is that the universe at the present epoch is very nearly spatially flat.

In order for the total density parameter, Ω_{total} to be exactly unity today, it would have had to be exactly unity at the beginning of the universe as well. In fact, the density parameter is extremely sensitive to initial conditions, slight deviations from unity initially, would result in extremely magnified deviations from unity today, based on the way the scale factor (and thus density components) changes with time. It follows then, that to have the present total density so close to the critical density ($|\Omega_0 - 1| < 0.01$), would require that the density of the universe was even closer to the value for the critical density at around the Planck time (more like ($|\Omega_0 - 1| < 10^{-62}$)).

The fact that the initial density, ρ_i, of the universe was so close to the critical density is the problem: it requires extreme fine tuning of initial conditions to explain the observed geometry, as the flat universe is unstable. If ρ_i was slightly larger than ρ_{crit}, the density would eventually increase to cause the expansion of the universe to halt and then reverse, resulting in the collapse of the universe, known as the Big Crunch. On the other hand, if ρ_i was slightly smaller than ρ_{crit}, the expansion of the universe would occur so rapidly so as to prevent structure formation, leaving an empty universe, with no humans to question its flatness.

The monopole problem

Another one of the big issues facing the Big Bang theory is its failure to reconcile with certain aspects of Grand Unification Theories (GUTs), which attempt to unify the origin of the electromagnetic, weak and strong forces. One of the strong predictions of some of these theories is the existence of magnetic monopoles. Conditions in the early universe would have been sufficient to produce magnetic monopoles, however at this time these objects remain undiscovered.

The growth of structure

The Big Bang postulates that the universe began from a hot, dense, but smooth homogeneous and isotropic state. However, if this is true, there exists no mechanism to promote the growth of structure observed in the universe today. Explaining this obvious inconsistency is one of the biggest problems facing the Big Bang Theory.

One solution to this problem as well as the flatness fine tuning issue, the horizon problem and the monopole problem is known as cosmic inflation.

1.3 Inflation

In 1980, the idea of a finite period of extreme, rapid accelerated expansion of the universe ($\ddot{a} > 0$), due to its vacuum energy only, as a possible solution to all of the above problems, was proposed independently by A. Linde, A. Guth and A. Starobinsky. This is called *cosmic inflation* and it is an augmentation of the Big Bang hypothesis at very early times. After this inflationary period, the Big Bang theory continues as before.

Considering (1.30), which gives the acceleration of the scale factor, in order for $\ddot{a} > 0$, we require a negative pressure according to

$$\rho + 3P < 0 \Rightarrow P < -\frac{\rho}{3} \, . \tag{1.55}$$

The traditional example of inflation is a universe which is dominated by a constant vacuum energy, like a cosmological constant. Introducing a vacuum energy density to the Friedmann equation and neglecting any other energy components, we obtain the following differential equation

$$\left(\frac{\dot{a}}{a}\right) = \frac{\Lambda}{3} \, . \tag{1.56}$$

We can neglect matter, radiation and curvature components because they decay with expansion, but the

constant vacuum energy will remain. Equation (1.56) has a solution of the form:

$$a(t) \sim e^{\sqrt{\frac{\Lambda}{3}}t} \ , \tag{1.57}$$

therefore, the vacuum energy by itself would cause *exponential* expansion of the universe.

The problem with this very simplistic solution is the fact that cosmic inflation is proposed as a *finite* epoch, and by some means must cease, so that the energy of the particle or field giving rise to inflation "decays" into ordinary fundamental particles and photons, a process known as reheating. After this conversion of energy, the regular big bang hypothesis comes into play, and proceeds to expand and evolve the universe as described in Section 1.2.1. Thus, another more appropriate solution to the problem is the existence of a scalar field, discussed in some detail in Section 1.3.1.

The requirement $\ddot{a} > 0$ implies $\frac{d}{dt}(aH) > 0$. Considering (1.48), this implies as aH increases, the total density of the universe is driven toward unity, which (in a very small, simplified nutshell) solves the flatness problem.

Conceptually, inflation can also resolve the horizon problem. At the time before inflation would have occurred, the universe was far more compact and dense than the Big Bang Theory predicts. In fact, according to inflationary theories, it was so compact that all the points in the universe *were* in causal contact with one another, enabling the thermalisation of the entire universe, *before* the rapid expansion. Thereafter, due to the extreme, rapid growth of the universe over a tiny interval of time, the comoving horizon increased in size more quickly than the Hubble sphere. So, points within causal contact prior to the inflationary epoch, are causally disconnect after it, solving the horizon problem.

Inflation also offers answers to the question of the formation of large scale structure from slight fluctuations observed in the CMB. Initial spontaneous quantum fluctuations in what was the universe prior to inflation, were magnified, and became what would be the origins of structure in the universe.

And finally, regarding the monopole problem, the rapid expansion exhibited by the universe during the inflationary epoch, serves to "dilute" particles which are predicted by particle physics but not observable today, due to the fact that their density falls of with scale factor more efficiently than that of the entity responsible for inflation. Given enough time, this dilution ensures that the predicted monopoles, although created, are not observable at the present epoch [37],[13], [38], [21].

1.3.1 Inflation due to a scalar field

We assume the existence of a scalar field, $\phi(t)$ defined on the space time manifold of the universe, with an associated potential $V(\phi)$ defined everywhere. The action which governs the dynamics of the scalar field, minimally coupled to gravity is given by:

$$S_\phi = \int \sqrt{-g}\left(-\frac{1}{2}\partial^\mu\phi\partial_\mu\phi - V(\phi)\right), \tag{1.58}$$

where, as usual, $g = \det(g_{\mu\nu})$. The corresponding energy momentum tensor, in terms of this scalar field and its potential is given by

$$T_{\mu\nu} = \partial_\mu\phi\partial_\nu\phi - g_{\mu\nu}\left(\frac{1}{2}\partial^\alpha\phi\partial_\alpha\phi + V(\phi)\right) \ . \tag{1.59}$$

Substituting in the FLRW metric, corresponding to a homogeneous and isotropic geometry into the above expression for a perfect fluid, we obtain an expression for the energy density, ρ, and the pressure, P in terms of the scalar field:

$$\rho = \frac{1}{2}\dot{\phi}^2 + V(\phi) \ , \tag{1.60}$$

$$P = \frac{1}{2}\dot{\phi}^2 - V(\phi) \ . \tag{1.61}$$

The term $\frac{1}{2}\dot{\phi}$ can be interpreted as a kinetic energy, and $V(\phi)$ as the potential energy of the inflaton field, ϕ. It is then possible to construct the equation of state of the inflaton field using the above equations:

$$w = \frac{P}{\rho} = \frac{\frac{1}{2}\dot{\phi} - V(\phi)}{\frac{1}{2}\dot{\phi} + V(\phi)} \ . \tag{1.62}$$

Clearly, if the derivative of the field is much smaller than the potential, $\dot{\phi} \ll V(\phi)$, then

$$w = -1 \ , \tag{1.63}$$

so that ϕ enables cosmological constant type behaviour.

The equation of motion of the scalar field is given by the Klein-Gordon equation, which is derived by varying the action (1.58) with respect to the scalar field:

$$\nabla^{\mu}\nabla_{\mu}\phi = \frac{dV}{d\phi}. \tag{1.64}$$

This becomes

$$\ddot{\phi} + 3H\dot{\phi} + V' = 0, \tag{1.65}$$

where the prime denotes a derivative with respect to ϕ. Thus, the interaction between the geometry of space time and the scalar field ϕ, with potential $V(\phi)$, is given by the following dynamical system:

$$H^2 = \frac{8\pi G}{3}\left(\frac{1}{2}\dot{\phi}^2 + V(\phi)\right), \tag{1.66}$$

$$\ddot{\phi} + 3H\dot{\phi} + V' = 0. \tag{1.67}$$

The second term in (1.67) above maybe considered a damping term, resulting from the expansion [37], [30], [38].

1.3.2 The slow roll regime

The dynamical system given by (1.66) and (1.67) only enables accelerated expansion under specific conditions. These conditions are satisfied in what is known as the *slow roll regime*, where the kinetic energy of the scalar field can be neglected in comparison with its potential energy. That is, when the kinetic energy of the scalar field, $\dot{\phi}$ and its acceleration $\ddot{\phi}$ vanish from equations (1.66) and (1.67), respectively, so that the potential energy, V, and the damping, $3H\dot{\phi}$, terms dominate:

$$H^2 \simeq \frac{8\pi G}{3}V, \tag{1.68}$$

$$3H\dot{\phi} + V' \simeq 0. \tag{1.69}$$

This amounts to satisfying the following conditions:

$$\varepsilon_V \equiv \frac{M_P^2}{2}\left(\frac{V'}{V}\right)^2 \ll 1 \quad \text{and} \quad \eta_V \equiv M_P^2\frac{V''}{V} \ll 1 \ , \tag{1.70}$$

where $M_P \equiv \frac{1}{\sqrt{8\pi G}}$ is the reduced Planck mass. The parameters ε_V and η_V measure the slope and the curvature of the potential, respectively. When these are sufficiently small, the rate of change of the scalar inflaton field, and therefore the potential, occurs *slowly* [37], [30].

1.3.3 E-folds

The inflationary epoch must last long enough, in order to establish the properties of the universe which we observe today (and, therefore, solve the problems facing the Big Bang Theory: horizon, flatness, monopole and growth of structure) . It is common, when considering this problem, to refer to a characteristic ratio, called *the number of E-folds*, defined as:

$$N = \ln\left(\frac{a_{end}}{a}\right) , \tag{1.71}$$

a_{end} is the value of the scale factor at the end of inflation, and a is a value of the scale factor during inflation. As inflation progresses, the value of N decreases and approaches zero, as a tends to equal a_{end}. We obtain N as a function of the scalar field in the slow roll approximation as:

$$N(\phi) \simeq \int_{\phi}^{\phi_{end}} \frac{V}{M_P^2 V'} d\phi \ . \tag{1.72}$$

Specifying the potential one can use the above equation to obtain the number of E-folds required to solve the various problems encountered by the Big Bang Theory.

Example: Power-law potential

Here the input potential is defined to be a power law monomial potential, which has been a popular case study in the literature, as an example:

$$V(\phi) = \lambda\phi^p. \tag{1.73}$$

This set includes the case of a free massive scalar field, $V(\phi) = \frac{m^2\phi}{2}$ [37]. In this class of model potentials, the inflation era begins when the inflaton field takes on large values relative to the Planck mass, and slowly rolls down. Inflation is ended when the slow roll parameters no longer satisfy the conditions for slow roll. For this case the slow roll paramaters, ε_V and η_V are:

$$\varepsilon_V = \frac{p^2 M_P}{2\phi^2} , \tag{1.74}$$

$$\eta_V = p(p-1)\frac{M_P^2}{\phi^2} \ . \tag{1.75}$$

Enforcing the slow roll conditions (1.70) upon the above parameters implies that $\phi \gg pM_P$. That is, the scalar field amplitude must be much larger than the Planck mass during the inflationary epoch.

Substituting the potential defined at (1.73) into the slow roll equations of motion (1.68) and (1.69), and integrating, we obtain

$$(\phi - \phi_i)^{2-\frac{p}{2}} = \frac{-2p}{4-p}\sqrt{\frac{\lambda}{3}} M_P (t - t_i) \ , \tag{1.76}$$

when $p \neq 4$ and

$$\phi = \phi_i e^{\left[-4\sqrt{\frac{\lambda}{3}} M_P (t-t_i)\right]} \ , \tag{1.77}$$

when $p = 4$. By making use of the following relation

$$\frac{d\ln a}{d\phi} = \frac{H}{\dot{\phi}} \simeq -\frac{\phi}{pM_P^2} \tag{1.78}$$

it is possible to obtain an expression for the scale factor as a function of ϕ:

$$a = a_{end} e^{\left[-\frac{\left(\phi^2 - \phi_{end}^2\right)}{2pM_P^2}\right]} \ . \tag{1.79}$$

We can find the number of e-folds over which this characteristic inflation lasts by defining the end of inflation

as $\varepsilon_V = 1$, to find

$$\phi_{end} = \frac{pM_P}{\sqrt{2}}. \tag{1.80}$$

It follows that the number of e-folds is given as a function of the scalar field is

$$N(\phi) \simeq \frac{\phi^2}{2pM_P^2} - \frac{p}{4}. \tag{1.81}$$

1.3.4 Classification of models for inflation

Single field models are commonly placed in the following broad classes:

- **Large Field Models**
  These are models for which the inflation parameters obey the condition : $0 < \eta_V \leq \varepsilon_V$. In these models, the scalar field is perturbed from a stabled minimum by an amount $\Delta\phi \approx M_P$.

- **Small Field Models**
  These are models for which the inflation parameters obey $\eta_V < 0 < \varepsilon_V$. Here the scalar field rolls away from an unstable maximum value of the potential $V(\phi)$.

- **Hybrid Models**
  These models are identified by conditions on the second derivative of the potential as well as on the slow roll parameters: $V''(\phi) > 0$ and $0 < \varepsilon_V < \eta_V$. However, in these models, a second scalar field is required to end inflation. Even so, hybrid models are considered *effective* single field models.

Naturally there is a large degeneracy of models which are candidates to describe inflation, as well as a degeneracy amongst the classes which group these models. The task of, at the very least, reducing the number of viable models depends on quality data.

In 2009, the ESA launched its Planck satellite, and very recently, in 2013, the first set of results based on the data were released in a set of papers. One of the most important sets of results are the findings on the constraints imposed by the Planck data on inflationary models.

The results of investigations based on the Planck data are useful for providing information about the early universe, more so, even than particle colliders, which can not always probe the kind of energies important at that era. It has been able to rule out various previously submitted models for inflation. For example, statistical analyses found that inflaton field potentials which exhibit a concave shape are favoured by the data and are accepted with almost 95% confidence [50]. That is to say, the data favour models in which the inflaton potential was initially concave during inflation. At some point this curvature changed, and the potential at this time lies in a convex minimum. Where as, inflaton fields with monomial potentials with power larger than 2, exponential potentials and hybrid potentials which are dominated by a quadratic term, are *disfavoured* by the data at a confidence of greater than 95% [50]. The Planck data coupled with Bayesian statistic analyses are apparently able to *prefer* models within the single field slow roll class quite successfully, and many of the models previously supported by older data have now lost credence. The Starobinsky model $(R + R^2)$[63] is particularly favoured by the Planck data, and these results have stimulated renewed interest in this theory [34]. See [50] for details.

1.4 End Note

This chapter served as a compact description of modern standard cosmology. The ΛCDM version of the Big Bang Theory, built upon the assumption that general relativity is applicable universally, faces observational cosmology very well, explaining light chemical abundances, the observed expansion of the universe, the cosmic microwave background and the measured flatness of the universe. The addition of an inflationary epoch at early times in the universe seems a good solution to many of the problems which the original Big Bang Theory encountered.

But this theory is built upon the assumption that we know *everything* we need to know about gravity, and it is all completely described by Einstein's General Relativity. The assumption that our understanding of physical laws is complete has been to our detriment in the past. It is, therefore, not unnatural to question whether we really have it right from our desks to the solar system to the furthest limits of the cosmos. The next chapter intends to survey the efforts so far to extend the theory of general relativity in the case that it is not yet fit to handle the physics of the universe at cosmological scales.

Chapter 2

Modified Gravity

While the success of the ΛCDM model is undeniable, there remains major room for improvement. Conceptually, it is not a satisfying theory as it requires the existence of unknown forms of energy to complete its explanation of the universe. The physical effects of Dark Energy may be a manifestation of the gravitational force behaving unexpectedly at cosmological scales, implying our understanding of gravity (since, as far as we know, it is the only force which acts over such large distances) is lacking; General Relativity may be the low curvature limit of some more general theory of gravity.

Modified gravity is a field of research concerned with generalising the theory of gravity, and several approaches to this task have been taken over the past few decades. This chapter will attempt a concise review of the specific area of $f(R)$ gravity in the metric formalism, to develop a background for the research presented in this thesis.

2.1 Motivation to modify gravity

Extensions to Einstein's theory of General Relativity were examined since its birth in the early parts of the 20th century, however, without a substantial enough theoretical or experimental motivation, the complexities which emerged from the endeavours of modifying GR proved so arduous, that any generalisation seemed unproductive. Thus, to the end of understanding and curiosity, the concern with modifying General Relativity fizzled out.

Interest in the theoretical qualities of modified gravity was renewed in the early 1960's in the context of a quantum gravity theory. As it stands, the two most successful theories of modern physics are found incongruous; General relativity's geometric description of the gravitational interaction leaves no room for it to be described by a quantum mechanical field theory. This is due to the fact that in GR the theory is not developed against a fixed background, the space-time is the dynamical variable which is determined by its energy contents. In quantum mechanics the positions of particles are probabilities determined by a wave function, therefore particles do not follow geodesics, which are used to *map* the space time.

Quantum field theory predicts that the known, observable particles result from various phase transitions of some superstructure, such as the Higgs bosons. According to GR, the geometry of the space would supposedly impose itself on the quantum matter fields, the result of this interaction having a feedback effect on the geometry. This implies that the combined Lagrangian for the gravitational and quantum matter fields results in a modification of the Einstein-Hilbert action: resulting in some *extended theory of gravity* .

Researchers find further grounds to question the completeness of GR in light of the emergence of cosmological issues such as inflation and the requirement of a dark sector of the universe. As mentioned in Chapter 1, the recent observational evidence, which suggests that the bulk of the energy content of the universe is made up of two "dark components": dark matter - electromagnetically undetectable and appearing to possess the clustering properties similar to that of ordinary matter, and dark energy - an unclustered form of energy that dominates the present epoch, whose nature is mostly unknown, having an apparent negative pressure.

Dark matter is required to solve the missing mass issue of both single galaxies and galaxy clusters. Dark energy is required to solve the problem of the exponentially accelerated expansion of the universe today. An additional, not yet fully understood, component of the standard model of cosmology is an early time cosmic inflation epoch, which has been introduced to explain the flatness, horizon and monopole problems, as well as to generate the primordial fluctuations which are the origins of the large scale structure.

These three parts of the standard model of cosmology are absolutely fundamental to its success in its fit and description of the observational data we have collected. However all three remain on extremely uncertain ground in physics; their origin and nature, for the most part, still unknown. The cosmological constant answer to dark energy fails at a phenomenological level, as its inferred magnitude is egregiously smaller than that predicted by particle physics. Dynamical dark energy models, while they can be constructed to describe the behaviour observed, do not find a deep enough theoretical motivation, as would be expected.

One perspective on the issues above would be to consider an overhaul of the theory of gravity, given that it is this fundamental interaction which acts at cosmological scales. The consideration of both sides of the Einstein's equations at (1.2) can make this, at first, radical idea more palatable : instead of adding unknown, mysterious dark contents to the energy in the universe on the right hand side, we may modify the geometric properties of the equations on the left hand side. There is no reason *a priori* to reject this approach [6]. It may offer valid alternatives to the exotic forms of energy currently constituting our best fit model. Such a pursuit will only benefit the science of gravitation, it offers the potential to enrich the theory by adding important corrections, or safely rule out the requirement for corrections at all.

It seems appropriate to mention, at this stage, that the precession of Mercury's orbit was initially thought to be due to the existence of some unobserved planet whose presence interfered gravitationally with Mercury's. We now know that, in fact, Newtonian theory was simply incompatible with the problem, and it required a new approach to gravitation to explain it [24].

2.2 Criteria for a satisfactory theory of gravity

Arguably, the most important criterion for a good scientific theory of any aspect of nature would be its predictive power; that is, the proposed theory must be able to make falsifiable predictions for the phenomena which it seeks to describe. Accordingly, any proposed theory of gravity must be able to predict the time evolution of the universe which it supposedly governs. Mathematically, this translates to having a well posed Cauchy, or initial value problem.

In order for a proposed theory to even be considered a candidate to describe the gravitational interaction, it must confront and explain several observational facts and produce the predicted results in the appropriate limits, which are already well described by our current theory of gravity. The three considerations are distance scales, gravitational potentials and cosmological perturbations.

Firstly, with regard to the distance scales, a good theory of gravity should echo Newtonian dynamics when its weak-field, non-relativistic limit is considered, as well as reproduce the results of solar system tests which are well described by general relativity. The Newtonian limit is important and applicable when considering large self-gravitating slow moving objects, such as galaxies, and galaxies within clusters, orbits of planets and moons, and therefore these observations must be a benchmark for the Newtonian limit of a proposed theory [24],[6].

The gravitational potential predicted by the theory must be sufficiently similar to the Newtonian potential which well explains the measured amounts of baryonic matter and radiation contained in stars and galaxies.

The proposed theory should be able to give a description of the origin and formation of the large scale structure observed today, such as superclusters, filaments and voids, using perturbation theory. The cosmological perturbations emerging from the theory should be reconcilable with the observational data of the CMB.

Finally, the theory must predict and describe the observed expansion evolution of the universe; that is, it should correctly predict the values of the Hubble parameter, the deceleration parameter, the density parameters

of the various energy components of the universe etc [6],[24].

In addition to being able to contend at a conceptual and observational level with General Relativity, a proposed theory of modified gravity should be able to explain the late time acceleration of the universe, without an explicit cosmological constant term, or even the existence of a Dark Energy fluid.

The assumptions which Einstein used in the formulation of his theory; the principle of relativity, the equivalence principle, the principle of general covariance, and the principle of causality, are still assumed to hold in the class of extended gravity considered here ($f(R)$ theories).

2.3 Streams of Extended Theories of Gravity

Since its conception, several approaches to the modification or generalisation of GR have been considered, many methods are still viable and investigations continue. According to the Lovelock theorem [17], modifying gravity amounts to making one or more of the following changes: considering other fields in the theory, accepting higher derivatives of the curvature and related invariants, or adding dimensions to the space-time. This brought to life theories like Dvali-Gabadadze-Porrati (DGP) gravity, Tensor-Vector-Scalar gravity (TeVeS) and brane-world gravity, and the popular stream called scalar-tensor gravity, in which the geometry can have a non-minimal coupling to the density of standard matter. This thesis is concerned with an approach commonly referred to as higher order theories of gravity (HOGT), which involve a brute force generalization of the Einstein-Hilbert action (1.1). Specifically, the first modification would be to introduce quadratic Lagrangians into (1.1).

In particular we are concerned with a subset of these theories called $f(R)$ theories of gravity, which assert that the generalisation of the gravitational Lagrangian may be completely contained in a generic *nonlinear* function of the scalar curvature, R.

It is natural to assume that this class of theories, $f(R)$, is very special and restrictive among a greater set of more general theories which involve Lagrangians constructed from even higher order invariants than the scalar curvature. However, there are several reasons which make this subset the pragmatic and especially interesting choice. While $f(R)$ theories allow a level of generality which has the potential to improve GR in the specific ways higher order theories are expected to, it also offers a simplicity which enables productive, qualitative and analytic study of the characteristic universes which they govern. Lagrangians involving the other quadratic invariants, such as $R^{\mu\nu}R_{\mu\nu}$ or $R^{\mu\nu\alpha\beta}R_{\mu\nu\alpha\beta}$ prove, in many cases, to produce complexities which hamper the analysis of such theories. The following identities

$$(\delta/\delta g_{ab})\int d^4x\sqrt{-g}(R^{abcd}R_{abcd}-4R^{ab}R_{ab}+R^2)=0, \tag{2.1}$$

$$(\delta/\delta g_{ab})\int d^4x\sqrt{-g}\varepsilon^{abcd}R_{abcd}R^{ef}_{cd}=0, \tag{2.2}$$

and

$$(\delta/\delta g_{ab})\int d^4x\sqrt{-g}(3R^{ab}R_{ab}-R^2)=0, \tag{2.3}$$

which is true for space-times with maximally symmetric spatial sections, imply that the quadratic invariants $R^{\mu\nu}R_{\mu\nu}$ or $R^{\mu\nu\alpha\beta}R_{\mu\nu\alpha\beta}$ can be expressed in terms of R^2, as long as they are combined linearly in the Lagrangian. It follows that any Lagrangian involving a linear combination of these higher order quadratic invariants is equivalent to some form of general power law function of R. A proof of these identities can be found in [20], p134.

And yet another reason to favour the $f(R)$ class is the Ostrogradsky theorem: *A system whose Lagrangian depends non-degenerately on the second- and higher-order derivatives of the dynamical quantities is necessarily unstable.* The Ostrogradsky instability has been shown to be avoidable within the class of $f(R)$ theories due to the fact that any modified Lagrangians which depend on the traces of $R_{\mu\nu}$ or $R_{\mu\nu\alpha\beta}$ should, according to the theorem stated above, be excluded as candidates [52].

It is important to note early on, that $f(R)$ gravity is what is known as a toy theory: it is simple enough to manipulate and general enough to enable the extraction of some useful insights into the deeper workings of both the class of modifications to GR, as well as GR itself. We use it to extend our understanding of the potential which modified gravity holds in the context of solving some of the problems of modern physics as well as its limitations to doing so. There is little doubt that, while there are many shortcomings associated to the theories, the endeavour of its study will be to our benefit.

2.4 $f(R)$-Gravity

$f(R)$ gravity aims to modify GR by making infrared corrections that become significant only at low curvatures. In GR, supposedly, just the spin-2 massless graviton propagates the gravitational field, however, upon the modification of a linear function of R to one which is a nonlinear function, $f(R)$, there appears a massive scalar degree of freedom which can cause the late time accelerated expansion observed today [24].

The field equations describing the gravitational interaction can be derived from a variational principle. There are three variational methods which one can use to derive the Einstein field equations in General Relativity as given at (1.2); the metric formalism, the Palatini formalism and the metric-affine formalism.

Within the standard metric formalism, it is assumed that the metric is the independent variable, and the variation of the action occurs with respect to the metric alone. Whereas, the Palatini variation is performed with respect to both the connection and the metric, which are both taken to be independent variables, while the matter Lagrangian is assumed to be independent of the connection. Metric affine $f(R)$ gravity generalises both of the previously mentioned approaches; the metric and the connection are considered both independent variables, and the action is varied with respect to both, but the matter Lagrangian is assumed to depend explicitly on the connection.

These three methods of varying the gravitational action will result in the same field equations if the action is the Einstein-Hilbert action given at (1.1), where the Lagrangian is linear in R. This is due to the fact that equations for the connection, $\Gamma^{\alpha}{}_{\mu\nu}$, in GR, result in the Levi-Civita connection of the metric, $g_{\mu\nu}$ [6], therefore in GR the metric formalism and the Palatini formalism produce an equivalent set of field equations. However, as soon as slight corrections are made, the various approaches reveal strikingly different physical natures of the theory in question.

The $f(R)$ gravity theories which result from the Palatini formalism are called *Palatini $f(R)$ theories of gravity*, similarly the gravity theory resulting from a metric-affine variation is called *metric-affine f(R) gravity*, and gravity theories which result from standard metric variation are referred to as *metric f(R) theories of gravity* . In this thesis, the last approach is the variational principle which is used.

2.4.1 Difficulties with $f(R)$ gravity

$f(R)$ theories of gravity are not without problems:

- The complex nature of the resulting theories make analysis and understanding quite difficult.
- There is a large degeneracy of available functions which can produce the late time acceleration of the scale factor. There is still no method of identifying preferred theories, as it has not been made clear whether the wide variety of functions which have been considered, can also satisfy the criteria for a good theory of gravity as given in Section 2.2.
    - ⋆ In general, the weak field limits of these theories are unsatisfactory in comparison with those of GR, and give corrections to the Newtonian description.
    - ⋆ The solar system, a well established laboratory for testing GR, poses problems for $f(R)$, as it is difficult to obtain both accelerated expansion as well as satisfy the solar system tests.

⋆ It has been shown that $f(R)$ gravity introduces a very low mass scalar field which manifests as a long range gravity force, resulting in the curvature of space-time and the local energy density of space-time decoupling. That is to say, high density is no longer associated with high curvature [32],[16]. Therefore the predicted metric in the solar system deviates from the observations, which are well described by GR. One consideration is the idea of this scalar field being able to evolve on cosmological scales. The mass of such a scalar field would depend on the local matter density: in regions of high matter density the mass of the field would be large enough to satisfy high local density tests. Whereas at cosmological scales, where the matter density is significantly lower, the mass of the field would be of order of H_0 in order to facilitate the evolution of the field today. In principle, this idea offers a solution as to why cosmological scalar fields are not yet detectable by local tests of the equivalence principle; the environment for testing is simply too dense. These scalar fields are called "chameleons" due to their properties having a severe sensitivity to the local environment[35].

2.4.2 Field Equations of $f(R)$ Gravity in the Metric Formalism

In this section, a derivation of the field equations, produced with the variation of a general function in the scalar curvature R, is presented.

Consider a more general action than the Einstein-Hilbert action (1.1) as follows, in the vacuum:

$$S = \int [f(R)]\sqrt{-g}d^4x, \tag{2.4}$$

which satisfies the variational principle $\delta\int\sqrt{-g}f(R)d^4x = 0$. $f(R)$ is a generic function of the Ricci scalar that, in principle, looks like $R + g(R)$, where $g(R)$ contains corrective terms, so that as $g(R) \to 0$ we regain GR. Varying this action, considering a locally inertial frame:

$$\begin{aligned}\delta\int\sqrt{-g}f(R) &= \int\left[\delta(\sqrt{-g}f(R)) + \sqrt{-g}\delta f(R)\right]d^4x \\ &= \int\sqrt{-g}\left[f'(R)R_{\mu\nu} - \frac{1}{2}g_{\mu\nu}f(R)\right]\delta g^{\mu\nu}d^4x + \int\sqrt{-g}f'(R)g^{\mu\nu}\delta R_{\mu\nu}d^4x.\end{aligned} \tag{2.5}$$

Here, primes indicate derivatives with respect to the scalar curvature, R. Using:

$$\begin{aligned}g^{\mu\nu}\delta R_{\mu\nu} &= g^{\mu\nu}\partial_\alpha(\delta\Gamma^\alpha{}_{\mu\nu}) - g^{\mu\alpha}\partial_\alpha(\delta\Gamma^\nu{}_{\mu\nu}) \\ &= \partial_\alpha(g^{\mu\nu}\delta\Gamma^\alpha{}_{\mu\nu} - g^{\mu\alpha}\delta\Gamma^\nu{}_{\mu\nu}),\end{aligned} \tag{2.6}$$

and if we define :

$$W^\alpha \equiv g^{\mu\nu}\delta\Gamma^\alpha{}_{\mu\nu} - g^{\mu\alpha}\delta\Gamma^\nu{}_{\mu\nu}, \tag{2.7}$$

we can write the second part of (2.5) as:

$$\begin{aligned}\int\sqrt{-g}f'(R)g^{\mu\nu}\delta R_{\mu\nu}d^4x &= \int\sqrt{-g}f'(R)\partial_\alpha W^\alpha d^4x \\ &= \int\partial_\alpha\left[\sqrt{-g}f'(R)W^\alpha\right]d^4x - \int\partial_\alpha\left[\sqrt{-g}f'(R)\right]W^\alpha d^4x.\end{aligned} \tag{2.8}$$

The first term in (2.8) goes to zero, as it represents the total divergence of the field, and we assume the field goes to zero at infinity. Therefore, only the second term remains:

$$\int\sqrt{-g}f'(R)g^{\mu\nu}\delta R_{\mu\nu}d^4x = \int\partial_\alpha\left[\sqrt{-g}f'(R)\right]W^\alpha d^4x. \tag{2.9}$$

The quantity W^α can be determined simply by considering the variation of the connection $\Gamma^\alpha{}_{\mu\nu}$, from its

definition (1.5):

$$\begin{aligned}\delta\Gamma^{\alpha}{}_{\mu\nu} &= \delta\left[\frac{1}{2}g^{\alpha\beta}\left(\partial_\mu g_{\beta\nu}+\partial_\nu g_{\mu\beta}-\partial_\beta g_{\mu\nu}\right)\right]\\ &= \frac{1}{2}g^{\alpha\beta}\left[\partial_\mu(\delta g_{\beta\nu})+\partial_\nu(\delta g_{\mu\beta})-\partial_\beta(\delta g_{\mu\nu})\right].\end{aligned} \tag{2.10}$$

Here, we are considering a locally inertial frame, therefore, the covariant derivative of the metric, which is equal to the partial derivative of the metric, is identically zero, and we have:

$$\delta\Gamma^{\nu}{}_{\mu\nu} = \frac{1}{2}g^{\nu\beta}\partial_\mu(\delta g_{\nu\beta}). \tag{2.11}$$

Using the above equation, and contracting (2.10) with the metric we have:

$$\begin{aligned}g^{\mu\nu}\delta\Gamma^{\alpha}{}_{\mu\nu} &= \frac{1}{2}g^{\mu\nu}\left[-\partial_\mu(g_{\beta\nu}\delta g^{\beta\alpha})-\partial_\nu(g_{\mu\beta}\delta g^{\alpha\beta})-g^{\alpha\beta}\partial_\beta(\delta g_{\mu\nu})\right]\\ &= \frac{1}{2}\partial^\alpha(g_{\mu\nu}\delta g^{\mu\nu})-\partial^\mu(g_{\beta\mu}\delta g^{\nu\beta}) \qquad (2.12)\\ \text{and}\quad \Rightarrow g^{\mu\alpha}\delta\Gamma^{\nu}{}_{\mu\nu} &= -\frac{1}{2}\partial^\alpha(g_{\nu\beta}\delta g^{\nu\beta}). \qquad (2.13)\end{aligned}$$

Substituting the above two expressions into (2.7), and the resulting expression into (2.9) we have:

$$\int\sqrt{-g}f'(R)g^{\mu\nu}\delta R_{\mu\nu}\ d^4x = \int\partial_\alpha\left[\sqrt{-g}f'(R)\right]\left[\partial^\mu(g_{\mu\nu}\delta g^{\alpha\nu})-\partial^\alpha(g_{\mu\nu}\delta g^{\mu\nu})\right]\ d^4x. \tag{2.14}$$

The above expression can be simplified by integrating by parts and neglecting total divergence terms. We get:

$$\int\sqrt{-g}f'(R)g^{\mu\nu}\delta R_{\mu\nu}\ d^4x = \int g_{\mu\nu}\partial^\alpha\partial_\alpha[\sqrt{-g}f'(R)]\delta g^{\mu\nu}\ d^4x - \int g_{\mu\nu}\partial^\mu\partial_\alpha[\sqrt{-g}f'(R)]\delta g^{\alpha\nu}\ d^4x. \tag{2.15}$$

Implying that the variation of the action (2.4) is :

$$\begin{aligned}\delta\int\sqrt{-g}f(R)\ d^4x &= \int\sqrt{-g}\left[f'(R)R_{\mu\nu}-\frac{1}{2}f(R)g_{\mu\nu}\right]\delta g^{\mu\nu}\ d^4x \qquad (2.16)\\ &+\int\left[g_{\mu\nu}\partial^\alpha\partial_\alpha(\sqrt{-g}f'(R))-g_{\alpha\nu}\partial^\mu\partial_\alpha(\sqrt{-g}f'(R))\right]\delta g^{\mu\nu}\ d^4x. \qquad (2.17)\end{aligned}$$

Setting the above variation equal to zero, we obtain the following set of fourth order vacuum field equations:

$$\boxed{f'(R)R_{\mu\nu}-\frac{1}{2}f(R)g_{\mu\nu} = \left(\nabla_\mu\nabla_\nu-g_{\mu\nu}\Box\right)f'(R)} \tag{2.18}$$

We can rearrange the above set of equations to resemble the Einstein equations if we add and subtract $\frac{1}{2}f'(R)g_{\mu\nu}R$ from the left hand side of (2.18):

$$f'(R)R_{\mu\nu}+\frac{1}{2}f'(R)g_{\mu\nu}R-\frac{1}{2}f'(R)g_{\mu\nu}R-\frac{1}{2}f(R)g_{\mu\nu} = \left(\nabla_\mu\nabla_\nu-g_{\mu\nu}\Box\right)f'(R). \tag{2.19}$$

Collecting, we obtain the Einstein tensor equal to a collection of terms in $f(R)$:

$$R_{\mu\nu}-\frac{1}{2}g_{\mu\nu}R\equiv G_{\mu\nu} = \frac{1}{f'(R)}\left[\left(\nabla_\mu\nabla_\nu-g_{\mu\nu}\Box\right)f'(R)+\frac{1}{2}g_{\mu\nu}[f(R)-f'(R)R]\right]. \tag{2.20}$$

We can consider the right hand side of (2.20) as an effective stress energy tensor[1], which acts as a source for the modified field. This source is called the *curvature fluid*; $T^{(curv)}_{\mu\nu}$. Therefore, we can say that the vacuum

[1]This idea should not be taken literally, as the theory derived is completely different from general relativity, and this appearance is imposing an effective GR interpretation on the field. However, rewriting the equations in this way turns out to be rather instructive with regard to the analysis of the equations.

contains a source, generated by the geometry, to which the higher order terms of R, in an otherwise Einstein like field, can be attributed. Is it possible that such a curvature fluid, a property of the vacuum, might be responsible for the observed effects of unknown energy densities such as dark energy and dark matter?

Including a matter stress energy tensor in the Lagrangian, the action becomes:

$$S = \int \sqrt{-g}\,[f(R) + \mathcal{L}_m]\,d^4x, \tag{2.21}$$

where $\mathcal{L}_m$ represents the Lagrangian of ordinary matter sources present. In this case we obtain the following field equations:

$$\boxed{f'(R)R_{\mu\nu} - \frac{1}{2}f(R)g_{\mu\nu} - (\nabla_\mu\nabla_\nu - g_{\mu\nu}\Box)\,f'(R) = T_{\mu\nu}^{matter}} \tag{2.22}$$

This, once again, can be rearranged to resemble the standard Einstein field equations with two fluids source:

$$R_{\mu\nu} - \frac{1}{2}g_{\mu\nu}R = G_{\mu\nu} = T_{\mu\nu}^{(curv)} + \frac{1}{f'(R)}T_{\mu\nu}^{(matter)} \tag{2.23}$$

We regain standard GR in the case when $f(R)$ is exactly equal to R; the stress energy tensor for the curvature fluid will be equal to zero.

The trace of the field equations at (2.22) is given by:

$$f'(R)R + 3\Box f'(R) - 2f(R) = T, \tag{2.24}$$

where $T = g^{\mu\nu}T_{\mu\nu}^{(matter)}$. Note that there is a very different relationship between the curvature and matter density than in standard GR, which gives $R = -T$. Clearly, in this case, $T = 0 \nRightarrow R = 0$.

Given that we are concerned with space-times which offer properties of homogeneity and isotropy (which correspond to maximally symmetric spatial sections), it is interesting to consider the maximally symmetric solutions of these field equations of metric $f(R)$ gravity. For a maximally symmetric solution we have surfaces of constant curvature, that is, $R = Constant$, and $T_{\mu\nu} = 0$. Imposing these conditions on equation (2.24) we have:

$$f'(R)R - 2f(R) = 0. \tag{2.25}$$

The above equation is then some algebraic expression in R[2]. If we accept that $R = 0$ is a root of the above equation, then the field equations at (2.22) become $R_{\mu\nu} = 0$, which represents the maximally symmetric and flat Minkowski space time. If we accept that the root of equation (2.25) is $R = Constant = C$, then the field equations (2.22) become $R_{\mu\nu} = \frac{g_{\mu\nu}C}{4}$ which represents a deSitter space-time or anti deSitter space-time depending on the sign of C, similar to GR with a cosmological constant driving the late time acceleration [59],[60] .

For our purposes, we assume a space-time which is homogeneous and isotropic. In addition, we pick a spatially flat universe to benefit from its simplicity, baring in mind the remarks made in Section 1.1.2 regarding the choice of $k = 0$. Thus, we are selecting a space time governed by the flat, FLRW metric at (1.13). We also assume that the matter contained is completely described by a perfect fluid, for which the stress energy tensor is given by (1.9). Upon the substitition of this metric and this matter stress energy tensor into the field equations (2.22), we obtain the following modified cosmological equations for a general $f(R)$ theory (the specification of the independent variable is dropped for the sake of neatness):

The modified Friedmann Equation

$$H^2 = \frac{1}{3f'}\left(\rho + \frac{1}{2}\left(Rf' - f\right) - 3H\dot{R}f''\right), \tag{2.26}$$

[2]Note that for forms of $f(R)$ which result in complex roots of equation 2.25, maximally symmetric solutions would not be possible. Thus these classes are not of any physical interest to us

The modified Raychauduri Equation

$$2\dot{H} + 3H^2 = -\frac{1}{f'}\left(P + 2H\dot{R}f'' + \frac{1}{2}\left(f - Rf'\right) + \dot{R}^2 f''' + \ddot{R}f''\right). \tag{2.27}$$

We can also calculate the trace of the field equations in this space-time :

The trace equation

$$3\ddot{R}f'' = \rho(1 - 3w) + f'R - 2f - 9Hf''\dot{R} - 3f'''\dot{R}^2. \tag{2.28}$$

Recall the idea of the *curvature fluid*; we can define an *effective energy density* and *effective pressure* attributed to the curvature of the space-time as:

$$\rho_{curv} = \frac{1}{f'}\left[\frac{1}{2}(Rf' - f) - 3H\dot{R}f''\right], \tag{2.29}$$

$$P_{curv} = \frac{1}{f'}\left[2H\dot{R}f'' + \frac{1}{2}(f - Rf') + \dot{R}^2 f''' + \ddot{R}f''\right]. \tag{2.30}$$

We require that the effective density, ρ_{curv}, be positive definite in a spatially flat universe, to preserve the validity of the modified Friedmann equation at (2.26) in the vacuum case.

This takes us to the definition of the effective equation of state of the curvature fluid, w_{curv}:

$$w_{curv} \equiv \frac{P_{curv}}{\rho_{curv}} = \frac{2H\dot{R}f'' + \frac{1}{2}(f - Rf') + \dot{R}^2 f''' + \ddot{R}f''}{\frac{1}{2}(Rf' - f) - 3H\dot{R}f''}. \tag{2.31}$$

The sign of the effective equation of state of the curvature fluid is determined by the sign of its effective pressure. For example, we have reason to believe that the equation of state of the fluid which is currently dominating the energy content of the universe is given by $w \approx -1$, which demonstrates de Sitter expansion; the scale factor exhibits exponential temporal evolution - $a(t) \propto e^{Ht}$. In order for a general function $f(R)$ to exhibit this kind of behaviour, that is to say, in order that it has an equation of state $w_{curv} = -1$, we would require the function to obey:

$$\frac{f'''}{f''} = \frac{\dot{R}H - \ddot{R}}{\dot{R}^2}. \tag{2.32}$$

For this case, we can rewrite the modified cosmological equations (2.26) and (2.27) in a way which extends the interpretation of the effective curvature fluid in the vacuum case by revealing a resemblance to the standard GR Friedmann and Raychaudhuri equations:

$$H^2 = \frac{\rho_{curv}}{3}, \tag{2.33}$$

$$\frac{\ddot{a}}{a} = \frac{1}{6}\rho_{curv}\left[1 + 3w_{curv}\right]. \tag{2.34}$$

2.4.3 Remarks on the form of $f(R)$

So far the only comment made on the function $f(R)$ constituting a "generalized" Lagrangian for the gravitational interaction is that it is nonlinear in the scalar curvature, R. However, the criteria listed in Section 2.2 manifest mathematically in requirements and conditions imposed on the function $f(R)$, when it is this class under consideration for the approach to modified gravity.

An important viability concern is the guarantee that, in the choice of $f(R)$, ghost fields[3] are prevented from appearing. It is also necessary that the resultant effective gravitational coupling is positive. We, therefore, require the first derivative of $f(R)$ to be *positive*; $f' > 0$ [59].

[3] A ghost is a field which introduces a kinetic term in the action which has the wrong sign, and is unbounded below. Such fields in the theory result in a violation of unitarity, as well as the eventual collapse of the theory through instabilities [8].

Concerning the form of the function in relation to the cosmological needs for the modification, the choice of $f(R)$ must

- result in a cosmic history which behaves like the ΛCDM model at high redshifts
- produce a late time accelerated epoch of expansion, fitting the current observational data, without the addition of a true cosmological constant term,
- allow sufficient degrees of freedom in its parametrisation so as to have good predictive power which can be extended to all the low redshift, testable phenomena accessible at this time [32],
- have the standard GR as its low curvature limit,
- ensure that the mass squared of the scalar field introduced in [16] is large and positive at high curvature, to avoid the issue mentioned in Section 2.4.1 [32].

If we choose to look at the function $f(R)$ as the usual linear Lagrangian plus some corrective terms encapsulated in a second function $g(R)$: $f(R) = R + g(R)$, then the above conditions can be expressed as the following limits on the correction, $g(R)$:

$$\lim_{R\to\infty} g(R) = Constant$$
$$\lim_{R\to 0} g(R) = 0. \tag{2.35}$$

With the first limit, as the Ricci scalar grows, the correction term tends to a constant values, forcing the Lagrangian to take on the form of that which is consistent with the ΛCDM; $R+$ *cosmological constant*, so as to describe the late time acceleration of the universe. As the Ricci scalar goes to zero, the second limit enforces the condition that the function $f(R)$ must reduce to R and assume its standard GR form, so as to make its behaviour consistent with solar system tests.

So far, the most compelling models proposed which satisfy these limits are broke power law functions, due to the fact that such functions can be parametrized to assume the required behaviour in the relevant regime. Several models have been proposed which are designed to satisfy the above limits [32],[62]. One popular model is known as the Hu - Sawicki model [32] is discussed below.

2.5 The Hu-Sawicki Model

The Hu-Sawicki model (HS model) for $f(R)$-gravity [32] was designed specifically to over come several problems faced by other functions. It is constructed to satisfy the limits at (2.35). This implies it will, given an appropriate parametrisation, maintain the success of the GR limit at high redshifts, as well as mimic ΛCDM at low redshifts. See [32] for details on this class of models. Below a short summary of the parametrisation details is included, as has aided the research in Section 4.4. The functional form of $f(R)$ is a specification of the correction $g(R)$ which is a general class of broken power laws:

$$f(R) = R - m^2 \frac{c_1 \left(\frac{R}{m^2}\right)^n}{c_2 \left(\frac{R}{m^2}\right)^n + 1}. \tag{2.36}$$

Above, $n > 0$ and the mass scale m^2 is taken to be:

$$m^2 \equiv \frac{\kappa^2 \bar{\rho}_0}{3} = (8315 Mpc)^{-2} \left(\frac{\Omega_m h^2}{0.13}\right), \tag{2.37}$$

where $\bar{\rho}_0$ is the average density of the present epoch and $\kappa^2 = 8\pi G$. As mentioned in Chapter 1, we will use units such that $\kappa^2 = c = 1$. c_1 and c_2 are dimensionless parameters, whose relationship will be shown to be associated with the present matter density parameter, Ω_m.

The sign of the second derivative of the correction, $g(R)$, is required to be strictly positive for large curvatures relative to density to guarantee that, at high density, the solution is stable at high curvature.

$$g_{RR} \equiv \frac{d^2 g(R)}{dR^2} > 0 \quad \text{for} \quad R \gg m^2. \tag{2.38}$$

The above condition is important to ensure the preservation of the GR values of the quantities, measured at high redshifts, such as $\Omega_m h^2$, in the $f(R)$ models as well. For convenience we define:

$$g_R \equiv \frac{dg}{dR}. \tag{2.39}$$

The key appeal of this class of models is that, explicitly, there is no true cosmological constant term. However, if we consider the limit of very high curvature relative to m^2,

$$\lim_{\frac{m^2}{R}\to 0} f(R) \approx R - \frac{c_1}{c_2} m^2 + \frac{c_1}{c_2^2} m^2 \left(\frac{m^2}{R}\right)^n, \tag{2.40}$$

it can be seen that, for a fixed value of $\frac{c_1}{c_2}$, the limiting case of $\frac{c_1}{c_2^2} \to 0$ behaves like a cosmological constant for both local and cosmological scales. At a finite $\frac{c_1}{c_2^2}$ the curvature is frozen to a fixed value and no longer decreases with matter density; this gives rise to a set of models which exhibit late time acceleration similar to ΛCDM. Considering the trace of the modified field equations at (2.28), it is possible to rewrite it in terms of an effective potential using the field g_R, if we define the effective potential to be:

$$\frac{\partial V_{eff}}{\partial g_R} = \frac{1}{3}(R - g_R R + 2g - \rho). \tag{2.41}$$

Then, we can rewrite the trace equation as:

$$\Box g_R = \frac{\partial V_{eff}}{\partial g_R}. \tag{2.42}$$

The effective potential has an extremum at

$$R - g_R R + 2f = \rho. \tag{2.43}$$

In the high curvature regime, wherein $|g_R \ll 1|$ and $|\frac{g}{R}| \ll 1$, the extremum is $R = \rho$, as expected in standard GR. The curvature at this extremum is given by

$$m_{g_R}^2 = \frac{\partial^2 V_{eff}}{\partial g_R^2} = \frac{1}{3}\left(\frac{1 + g_R}{g_{RR}} - R\right). \tag{2.44}$$

In [32] the expansion history of the universe is calculated for a class of models which are parametrized to mimic the ΛCDM model; that is models which do not deviate from ΛCDM in the effective equation of state by more that $|1 + w_{eff}| \lesssim 0.2$. This is done by specifying a value for the field today as $g_{R0} \equiv g_R(\ln a = 0) \ll 1$, or, $R_0 \gg m^2$. Considering this case, the approximation at equation (2.40) supposedly holds for the entire expansion history and the field is always near the minimum of the effective potential, which is (while g_{R0} is small)

$$R = \rho - 2f \approx \rho + 2\frac{c_1}{c_2} m^2 \tag{2.45}$$

Above, it is the $2f$ term (on the right hand side of the approximation sign, it is a term involving c_1 and c_2), which serves as a cosmological constant. Therefore [32] admits the following relationship between the constant and the energy densities of the cosmological constant, $\tilde{\Omega}_\Lambda$, and matter, $\tilde{\Omega}_m$:

$$\frac{c_1}{c_2} \approx 6\frac{\tilde{\Omega}_\Lambda}{\tilde{\Omega}_m}. \tag{2.46}$$

The remaining two parameters n and $\frac{c_1}{c_2^2}$ are free, then, to govern the behaviour of the model, and how well it does to describe the observations, compared to ΛCDM. Larger values of n force the model to mimic ΛCDM until later in the expansion history of the output universe, and smaller values of c_1/c_2^2 enables reduction in general deviations from it. Because both the Hubble parameter and the critical density depend on the correction g_R, $\tilde{\Omega}_m$ only becomes the actual value of the matter density in the following limit:

$$\lim_{\frac{c_1}{c_2^2}\to 0} \tilde{\Omega}_m = \Omega_m \tag{2.47}$$

But, the matter density in the physical units remains unchanged.

Expected Expansion history

Considering the ΛCDM model with flat spatial geometry, we have:

$$R \approx 3m^2 \left(\frac{1}{a^3} + 4\frac{\tilde{\Omega}_\Lambda}{\tilde{\Omega}_m} \right), \tag{2.48}$$

and for the derivative of the correction:

$$g_R = -n\frac{c_1}{c_2^2} \left(\frac{m^2}{R} \right)^{n+1}. \tag{2.49}$$

The values for today are:

$$\begin{aligned} R_0 &\approx m^2 \left(\frac{12}{\tilde{\Omega}_m} - 9 \right), \\ g_{R0} &\approx -n\frac{c_1}{c_2^2} \left(\frac{12}{\tilde{\Omega}_m} - 9 \right)^{-n-1} \end{aligned} \tag{2.50}$$

for $|g_{R0}| \ll 1$. [32] uses the following specific values:

$$\tilde{\Omega}_m = 0.24, \tag{2.51}$$

$$\tilde{\Omega}_\Lambda = 0.76. \tag{2.52}$$

Therefore we have:

$$R_0 = 41m^2 \tag{2.53}$$

$$g_{R0} \approx -n\frac{c_1}{c_2^2} \left(\frac{1}{41} \right)^{n+1} \tag{2.54}$$

Figure 9 in [32] show the range and combinations of parameter values, g_{R0} and n, which are acceptable and enable the model to satisfy both solar system and galaxy tests. The promise of this model lies in its construction which can evade solar system tests with its chameleon properties.

2.6 End Note

This chapter introduced basic ideas in the branch of modified gravity known as $f(R)$-gravity, and explained why this branch is not as specialised as it may first appear. Criteria for a good theory of gravity, and how these criteria constrain the kinds of functions for $f(R)$ which are viable, were reviewed. We presented a derivation of the modified Einstein Field Equations, in the *metric formalism*, and the resulting cosmological equations which correspond to a homogeneous and isotropic flat space universe. A viable model, the Hu-Sawicki broken power-law model, is briefly introduced as per [32], as it is this class of models which is the subject of the research

presented in this thesis.

Chapter 3

Dynamical Systems

The research presented in Chapter 4 has, at its center, a dynamical systems approach to the analysis of the modified cosmological field equations. For this reason, this chapter is dedicated to reviewing the key aspects of the theory of dynamical systems, which are used in acquiring the results of the analysis.

3.1 Basic Theory

A dynamical system is a system whose time evolution can be described by a function of time and the n other independent variables which govern its behaviour. The equations of motion of the system (the equations which describe how it changes with time) are given by a set of differential equations:

$$\begin{aligned}
\dot{x}_1 &= f_1(t, x_1, ..., x_n), \\
\dot{x}_2 &= f_2(t, x_1, ..., x_n), \\
&\vdots \\
\dot{x}_n &= f_n(t, x_1, ..., x_n),
\end{aligned}$$

where, x_i represent the other n independent variables of the system, $x_i \in \mathbb{R}$, $f_i : \mathbb{R} \to \mathbb{R}$, $i = 1, ..n$. We can define $\mathbf{x}= (x_1, ..., x_n)^T$ and $\mathbf{F}(t, \mathbf{x}(t)) = (f_1, ..., f_n)^T$, making it possible to write the n differential equations in the following matrix form:

$$\dot{\mathbf{x}} = \mathbf{F}(t, \mathbf{x}(t)). \tag{3.1}$$

Each x_i represents a degree of freedom of the system, and is a coordinate of a space known as *phase space*. The phase space associated with a given dynamical system is the space of all possible vectors $(x_1, ..., x_n)$, and its boundaries depend on the allowable ranges of each x_i.

A special type of system, called an *autonomous system*, is one in which each f_i has an implicit dependence on time, that is, the time dependence of each f_i is contained only in the time dependence of each $x_i(t)$. In this case, (3.1) can be written:

$$\dot{\mathbf{x}} = \mathbf{F}(\mathbf{x}). \tag{3.2}$$

Solutions to (3.1) trace out time dependent trajectories or *solution curves* in the phase space, and the set of all of these solutions gives the *phase portrait* of the system. Given an initial condition $(t_0, \mathbf{x}_0)$, the initial point of the solution curve is determined, S_0, which determines the next point of the solution curve. In this way, any specific solution curve can be determined given a set of initial conditions.

The field $\mathbf{F}$, which is effectively the velocity field of the given dynamical system is called the *phase flow*; at each time, every vector $\mathbf{F}$ points in the direction of the field at that point, at that time.

Definition 1. Points, $\mathbf{x}_\star$, for which the velocity field $\mathbf{F}(\mathbf{x}_\star) = 0$, that is, $\dot{\mathbf{x}} = 0$, are called equilibrium (critical/fixed/stationary) points. A system which has its initial conditions $\mathbf{x}_0 = \mathbf{x}_\star$ will remain at this state for all time.

3.2 Linear Systems

Linear dynamical systems have all f_i equal to linear combinations of the independent variables, and can therefore be expressed as:

$$\dot{\mathbf{x}} = A\mathbf{x}, \tag{3.3}$$

where the velocity field is described by an $n \times n$ matrix A in the following way:

$$\mathbf{F}(\mathbf{x}) = A\mathbf{x}, \tag{3.4}$$

defining a mapping $\mathbf{F}$:$\mathbb{R}^n \to \mathbb{R}^n$, which defines a vector field on $\mathbb{R}^n$.

The aim of this section is to prove that the solution of the system at (3.3) is given by

$$\mathbf{x}(t) = e^{At}\mathbf{x}_0,$$

where e^{At} is a square matrix function of dimension n defined below.

Definition 2. Let A be an $n \times n$ matrix. For $t \in \mathbb{R}$,

$$e^{At} = \sum_{k=0}^{\infty} \frac{A^k t^k}{k!}. \tag{3.5}$$

Proposition 3.2.1. *If P and B are linear transformations on $\mathbb{R}^n$ and $A = PBP^{-1}$, then $e^A = Pe^BP^{-1}$.*

Proof.
From the definition of e^A we have:

$$e^A = \lim_{n\to\infty} \sum_{k=0}^{n} \frac{(PBP^{-1})^k}{k!} = P \lim_{n\to\infty} \sum_{k=0}^{n} \frac{B^k}{k!} P^{-1} = Pe^BP^{-1}. \qquad \square$$

Proposition 3.2.2. *If A and B are linear transformations on $\mathbb{R}^n$ which commute, that is, they satisfy $AB = BA$, then $e^{A+B} = e^Ae^B$.*

Proof.
If $AB = BA$, by the binomial theorem

$$(A+B)^n = n! \sum_{j+k=n} \frac{A^jB^k}{j!k!}, \tag{3.6}$$

thus,

$$e^{A+B} = \sum_{n=0}^{\infty} \sum_{j+k=n} \frac{A^jB^k}{j!k!} = \sum_{j=0}^{\infty} \frac{A^j}{j!} \sum_{k=0}^{\infty} \frac{B^k}{k!} = e^Ae^B. \qquad \square \tag{3.7}$$

In this section, it is shown that the following initial value problem, where A is an $n \times n$ matrix,

$$\begin{aligned} \dot{\mathbf{x}} &= A\mathbf{x}, \\ \mathbf{x}(0) &= \mathbf{x}_0, \end{aligned} \tag{3.8}$$

has a unique solution for all $t \in \mathbb{R}$, which is given by

$$\mathbf{x}(t) = e^{At}\mathbf{x}_0. \tag{3.9}$$

To prove this, the following lemma is required:

Lemma 3.2.3. *Let A be a square matrix, then*

$$\frac{d}{dt}e^{At} = Ae^{A}t. \tag{3.10}$$

Proof
Since A commutes with itself, considering Proposition 3.2.1 and Definition 2, it follows that

$$\begin{aligned}\frac{d}{dt}e^{At} &= \lim_{h\to 0}\frac{e^{A(t+h)} - e^{At}}{h}\\ &= \lim_{h\to 0} e^{At}\frac{(e^{Ah}) - I}{h}\\ &= e^{At}\lim_{h\to 0}\lim_{k\to\infty}\left(A + \frac{A^2h}{2!} + ... + \frac{A^k h^{k-1}}{k!}\right)\\ &= Ae^{At}. \qquad \square\end{aligned} \tag{3.11}$$

Thus, we arrive at the Fundamental Theorem for Linear Systems:

Theorem 3.2.4 (The Fundamental Theorem for Linear Systems)**.** *Let A be an $n\times n$ matrix. Then, for a given $\mathbf{x}_0 \in \mathbb{R}^n$, the initial value problem*

$$\dot{\mathbf{x}} = A\mathbf{x}, \tag{3.12}$$

$$\mathbf{x}(0) = \mathbf{x}_0, \tag{3.13}$$

has a unique solution given by

$$\mathbf{x}(t) = e^{At}\mathbf{x}_0. \tag{3.14}$$

Proof. By Lemma 3.2.3, if $\mathbf{x}(t) = e^{At}\mathbf{x}_0$, then

$$\dot{\mathbf{x}} = \frac{d}{dt}e^{At}\mathbf{x}_0 = A\mathbf{x}(t) \tag{3.15}$$

for all $t \in \mathbb{R}$. Regarding the initial condition, we have:

$$\mathbf{x}(0) = I\mathbf{x}_0 = \mathbf{x}_0. \tag{3.16}$$

Implying that $\mathbf{x}(t) = e^{At}\mathbf{x}_0$ is a solution to (3.12). To prove its uniqueness, let $\mathbf{x}(t)$ be any solution of the initial value problem at (3.12), and set

$$\mathbf{y}(t) = e^{-At}\mathbf{x}(t).$$

Then, considering Lemma 3.2.3 again and the fact that $\mathbf{x}(t)$ is a solution of (3.12):

$$\begin{aligned}\dot{\mathbf{y}} &= -Ae^{-At}\mathbf{x}(t) + e^{-At}\dot{\mathbf{x}}\\ &= -Ae^{-At}\mathbf{x}(t) + e^{-At}A\mathbf{x}(t)\\ &= 0\\ \Rightarrow \mathbf{y} &= Const\end{aligned} \tag{3.17}$$

throughout time, because A and e^{-At} commute. So, the value of $\mathbf{y}$ can be set when $t = 0$,

$$\mathbf{y}(0) = \mathbf{x}(0) = \mathbf{x}_0.$$

It follows that any solution of the initial value problem (3.12) has to be given by $\mathbf{x}(t) = e^{At}\mathbf{y}(t) = e^{At}\mathbf{x}_0$. □

3.2.1 Diagonalization

Given the linear system at (3.3), it is useful, where possible, to diagonalise the square matrix A, to reduce the system to a set of uncoupled linear differential equations. In the case that A has real and distinct eigenvalues, the following theorem aids the solving of the system.

Theorem 3.2.5. *If the eigenvalues $\lambda_1, \lambda_2, ...\lambda_n$ of an $n \times n$ matrix, A, are real and distinct, then any set of corresponding eigenvectors $\{\boldsymbol{v}_1, \boldsymbol{v}_2, ..., \boldsymbol{v}_n\}$ forms a basis for $\mathbb{R}^n$, the matrix $P = [\boldsymbol{v}_1 \ \ \boldsymbol{v}_2 \ \ ... \ \ \boldsymbol{v}_n]$ is invertible and*

$$P^{-1}AP = diag[\lambda_1, ..., \lambda_n].$$

Using Theorem 3.2.5 to reduce the system (3.3), we make the following linear transformation:

$$\mathbf{y} = P^{-1}\mathbf{x}.$$

Here P is as it is defined in the above theorem. Then,

$$\mathbf{x} = P\mathbf{y},$$
$$\dot{\mathbf{y}} = P^{-1}\dot{\mathbf{x}} = P^{-1}A\mathbf{x} = P^{-1}AP\mathbf{y}.$$

Therefore, by Theorem 3.2.5, we obtain the following system

$$\dot{\mathbf{y}} = \text{diag}[\lambda_1, ..., \lambda_n]\mathbf{y},$$

which has the solution:

$$\mathbf{y}(t) = \text{diag}[e^{\lambda_1 t}, ..., e^{\lambda_n t}]\mathbf{y}(0). \tag{3.18}$$

Now, since $\mathbf{y}(0) = P^{-1}\mathbf{x}(0)$ and $\mathbf{x}(t) = P\mathbf{y}(t)$, we have that (3.3) has the following solution:

$$\mathbf{x}(t) = P\mathcal{D}(t)P^{-1}\mathbf{x}(0), \tag{3.19}$$

where $\mathcal{D}(t) = \text{diag}[e^{\lambda_1 t}, ..., e^{\lambda_n t}]$.

Therefore, according to Theorem 3.2.5, the solution of the linear system (3.3) is given by the function $\mathbf{x}(t)$ defined by (3.19).

Definition 3 (Subspaces of the linear system)**.** Suppose that the n dimensional square matrix A has k negative eigenvalues $\lambda_1, ...\lambda_k$ and $n-k$ positive eigenvalues $\lambda_{k+1}, ..., \lambda_n$, with all the eigenvalues distinct. Let $\{\mathbf{v}_i, ..., \mathbf{v}_n\}$ be the associated eigenvectors. Then the space spanned by $\{\mathbf{v}_1, ..., \mathbf{v}_k\}$, E^s is the stable subspace of the linear system, and the the space spanned by $\{\mathbf{v}_{k+1}, ..., \mathbf{v}_n\}$, E^u, is the unstable subspace of the linear system at (3.3):

$$E^s = \text{span}\{\mathbf{v}_1, ..., \mathbf{v}_k\},$$
$$E^u = \text{span}\{\mathbf{v}_{k+1}, ..., \mathbf{v}_n\}.$$

3.2.2 Complex Eigenvalues

Suppose the real $2n$ dimensional square matrix A has complex eigenvalues, these eigenvalues occur in complex conjugate pairs. If the $2n$ complex eigenvalues are distinct, the following theorem enables the solving of the the linear system (3.3).

Theorem 3.2.6. *If the $2n\times 2n$ real matrix A has $2n$ distinct complex eigenvalues, $\lambda_j = a_j+ib_j$ and $\bar{\lambda_j} = a_j-ib_j$, with corresponding eigenvectors $\boldsymbol{w}_j = \boldsymbol{u}_j + i\boldsymbol{v}_j$ and $\bar{\boldsymbol{w}}_j = \boldsymbol{u}_j - i\boldsymbol{v}_j, j = 1, ..., n$, then $\{\boldsymbol{u}_1, \boldsymbol{v}_1, ..., \boldsymbol{u}_n, \boldsymbol{v}_n\}$ is a basis for $\mathbb{R}^{2n}$, the matrix*

$$P = [\boldsymbol{v}_1 \quad \boldsymbol{u}_1 \quad \boldsymbol{v}_2 \quad \boldsymbol{u}_2 \quad \dots \quad \boldsymbol{v}_n \quad \boldsymbol{u}_n]$$

is invertible and

$$P^{-1}AP = diag\begin{bmatrix} a_j & -b_j \\ b_j & a_i \end{bmatrix},$$

is a real $2n \times 2n$ matrix with 2×2 blocks along the diagonal.

Therefore, according to Theorem 3.2.6, and considering the solution of the linear initial value problem (3.12) is

$$\mathbf{x}(t) = P\text{diag}[e^{a_j t}] \begin{bmatrix} \cos b_j t & -\sin b_j t \\ \sin b_j t & \cos b_j t \end{bmatrix} P^{-1}\mathbf{x}_0.$$

If A has real eigenvalues, which are distinct, λ_j, with their associated eigenvectors, $\mathbf{v}_j, j = 1, .., k$, and distinct complex eigenvalues $\lambda_j = a_j + ib_j$ and $\bar{\lambda_j} = a_j - ib_j$, with their corresponding eigenvectors $\mathbf{w}_j = \mathbf{u}_j + i\mathbf{v}_j$ and $\bar{\mathbf{w}}_j = \mathbf{u}_j - i\mathbf{v}_j, j = k+1, ..., n$ then the matrix

$$P = [\mathbf{v}_1 \quad \dots \quad \mathbf{v}_k \quad \mathbf{v}_{k+1} \quad \mathbf{u}_{k+1} \quad \dots \quad \mathbf{v}_n \quad \mathbf{u}_n]$$

is invertible, and

$$P^{-1}AP = \text{diag}[\lambda_1, ..., \lambda_k, B_{k+1}, ..., B_n]$$

where, B_j is defined for $j = k+1, .., n$ as

$$B_j = \begin{bmatrix} a_j & -b_j \\ b_j & a_j \end{bmatrix} .$$

3.2.3 Multiple Eigenvalues

Definition 4. Let A be an $n \times n$ matrix of multiplicity $m \leq n$, for which λ is an eigenvalue. Then, for $k = 1, ..., m$, any nonzero solution of

$$(A - \lambda I)^k \mathbf{v} = 0$$

is called a *generalised eigenvector of A*.

Definition 5. An n-dimensional square matrix, N, is said to be *nilpotent of order k* if $N^{k-1} \neq 0$ and $N^k = 0$.

Theorem 3.2.7. *Let A be a real $n \times n$ matrix with real eigenvalues $\lambda_1, ..., \lambda_n$, which are repeated according to their multiplicity. Then there exists a basis of generalised eigenvectors for $\mathbb{R}^n$. If $\{\boldsymbol{v}_1, ..., \boldsymbol{v}_n\}$ is any basis of generalised eigenvectors for $\mathbb{R}^n$, the matrix $P = [\boldsymbol{v}_1 \quad \dots \quad \boldsymbol{v}_n]$ is invertible,*

$$A = S + N,$$

where

$$P^{-1}SP = diag[\lambda_j],$$

the matrix $N = A - S$ is nilpotent of order $k \leq n$, and S and N commute, that is, $SN = NS$.

With these conditions, using Theorem 3.2.7 and Propositions 3.2.1 and 3.2.2, the linear initial value problem (3.12) has the following solution:

$$\mathbf{x}(t) = P\text{diag}[e^{\lambda_j t}]P^{-1}\left[I + Nt + ...\frac{N^{k-1}t^{k-1}}{(k-1)!}\right]\mathbf{x}_0.$$

Now, in the case that λ is an eigenvalue of multiplicity n of the $n \times n$ matrix A, the above results are simply

$$\mathbf{x}(t) = e^{\lambda t}\left[I + Nt + ...\frac{N^k t^k}{k!}\right]\mathbf{x}_0 \ ,$$

due to the fact that, in this case, $S = \text{diag}[\lambda]$ with respect to the general basis for $\mathbb{R}^n$, and $N = A - S$.
In the case of multiple *complex* eigenvalues:

Theorem 3.2.8. *Let A be a real $2n \times 2n$ matrix with complex eigenvalues $\lambda_j = a_j + ib_j$ and $\bar{\lambda}_j = a_j - ib_j, j = k+1, ..., n$. Then there exists generated eigenvectors $\boldsymbol{w}_j = \boldsymbol{u}_j + i\boldsymbol{v}_j$ and $\bar{\boldsymbol{w}}_j = \boldsymbol{u}_j - i\boldsymbol{v}_j, j = 1...n$ such that $\{\boldsymbol{u}_1, \boldsymbol{v}_1, ..., \boldsymbol{u}_n, \boldsymbol{v}_n\}$ is a basis for $\mathbb{R}^{2n}$. For any such basis, the matrix $P = [\boldsymbol{v}_1 \ \ \boldsymbol{u}_1 \ \ \ldots \ \ \boldsymbol{v}_n \ \ \boldsymbol{u}_n]$ is invertible,*

$$A = S + N,$$

where

$$P^{-1}SP = diag\begin{bmatrix} a_j & -b_j \\ b_j & a_j \end{bmatrix},$$

the matrix $N = A - S$ is nilpotent of oder $k \leq 2n$, and S and N commute.

So, using the results in the previous section, as well as the fundamental theorem, under the hypothesis of Theorem 3.2.8, the solution to the linear initial value problem at (3.12) is given by the following expression:

$$\mathbf{x}(t) = P\text{diag}[e^{a_j t}]\begin{bmatrix} \cos b_j t & -\sin b_j t \\ \sin b_j t & \cos b_j t \end{bmatrix} P^{-1}\left[I + ... + \frac{N^k t^k}{k!}\right]\mathbf{x}_0.$$

3.2.4 Stability Theory

This section defines the stable, unstable and center subspaces of the linear system at (3.3).

Definition 6. Let $\mathbf{w}_j = \mathbf{u}_j + i\mathbf{v}_j$ be a generalised eigenvector associated with the eigenvalue $\lambda_j = a_j + ib_j$ of the real matrix A. In the case that $b_j = 0$ then $v_j = 0$. Let

$$B = \{\mathbf{u}_1, ..., \mathbf{u}_k, \mathbf{u}_{k+1}, \mathbf{v}_{k+1}, ..., \mathbf{u}_m, \mathbf{v}_m\}$$

be a basis of $\mathbb{R}^n$ with $n = 2m - k$. Then

$$\begin{aligned} E^s &= span\{\mathbf{u}_j, \mathbf{v}_j | a_j < 0\} \ , \\ E^c &= span\{\mathbf{u}_j, \mathbf{v}_j | a_j = 0\} \ , \\ \text{and} \quad E^u &= span\{\mathbf{u}_j, \mathbf{v}_j | a_j > 0\} \ . \end{aligned}$$

In other words, the subspace of $\mathbb{R}^n$ which is spanned by the generalised eigenvectors $\mathbf{w}_j$, for which their associated eigenvalues have negative real parts, is called the stable subspace, and denoted E^s. Likewise, in the cases where the corresponding eigenvalues of $\mathbf{w}_j$ are zero and positive, the subspaces are known as the center and unstable subspaces respectively, and denoted E^c and E^u.

As was shown previously, the general solution to the initial value problem (3.12), is given by

$$\mathbf{x}(t) = e^{At}\mathbf{x}_0.$$

The set of functions $e^{At} : \mathbb{R}^n \to \mathbb{R}^n$ describes the motion (evolution) of the initial points $\mathbf{x}_0 \in \mathbb{R}^n$ along the trajectories (solution curves) of (3.12). This set of functions, or maps, is called the *flow of the system* at (3.12).

Definition 7. Given the $n \times n$ matrix A, in the linear initial value problem at (3.12); if all its eigenvalues have nonzero real part, then the flow at $e^{At} : \mathbb{R}^n \to \mathbb{R}^n$ is called *hyperbolic flow*, and the system (3.12) is said to be a *hyperbolic linear system*

An equilibrium point $\mathbf{x}_\star$ is said to be a *hyperbolic equilibrium point* of (3.12) if all the eigenvalues have non-zero real parts.

Invariant subspaces

Definition 8. A subspace $E \subset \mathbb{R}^n$ is said to be *invariant with respect to the flow* $e^{At} : \mathbb{R}^n \to \mathbb{R}^n$ if $e^{At}E \subset E$ for all $t \in \mathbb{R}^n$.

So, the trajectory of any point $\mathbf{x}_0$ originating in an *invariant subspace* is confined to that subspace for all time.

Lemma 3.2.9. *If E is the generalised eigenspace of A corresponding to the eigenvalue λ , then $AE \subset E$*

Theorem 3.2.10. *Let A be an $n \times n$ real matrix. Then,*

$$\mathbb{R}^n = E^s \oplus E^u \oplus E^c,$$

where E^s, E^c and E^u are the stable, center and unstable subspaces of (3.12)*. Also, E^s, E^c and E^u are invariant with respect to the flow e^{At} of* (3.12)*, respectively.*

Proof. Since $B = \{\mathbf{u}_1, ..., \mathbf{u}_k, \mathbf{u}_{k+1}, \mathbf{v}_{k+1}, ..., \mathbf{u}_m, \mathbf{v}_m\}$, as in Definition 6, is a basis for $\mathbb{R}^n$, it is clear, considering the definitions of E^s, E^c and E^u that

$$\mathbb{R}^n = E^s \oplus E^u \oplus E^c.$$

Now, if the initial point is an element of the stable subspace; if $\mathbf{x}_0 \in E^s$, then

$$\mathbf{x}_0 = \sum_{j=1}^{n_s} c_j \mathbf{w}_j,$$

where $\mathbf{w}_j$ is either $\mathbf{v}_j$ or $\mathbf{u}_j$, and the set $\{\mathbf{w}_j\}_{j=1}^{n_s} \subset B$ is a basis for the subspace E^s. Because the function e^{At} satisfies conditions for linearity, we have

$$e^{At}\mathbf{x}_0 = \sum_{j=1}^{n_s} c_j e^{At}\mathbf{w}_j.$$

But

$$e^{At}\mathbf{w}_j = \lim_{k\to\infty} \left[I + At + ... + \frac{A^k t^k}{k!} \right] \mathbf{w}_j \in E^s,$$

since, by Lemma 3.2.9 we have that $A^k\mathbf{w}_j \in E^s$ for $j = 1, ..., n_s$, and since E^s is complete (E^s is closed and $\mathbb{R}^n$ is complete). Thus, for all $t \in \mathbb{R}^n, e^{At}\mathbf{x}_0 \in E^s \Rightarrow e^{At}E^s \subset E^s$. So, the projection of any element of E^s on a trajectory e^{At} will also be an element of E^s : $e^{At}E^s \subset E^s \Rightarrow$ the space E^s is invariant under the flow e^{At}.

Similarly E^u and E^c are invariant under the flow e^{At}. □

Stability of equilibrium points

Definition 9. The fixed point $\mathbf{x}_\star$ is said to be *stable* or an *attractor* of some motion $\mathbf{x}(t)$ if

$$\lim_{t\to\infty} \mathbf{x}(t) = \mathbf{x}_\star \ . \tag{3.20}$$

- If all solutions $e^{At}\mathbf{x}_0$, where $\mathbf{x}_0 \in b(\mathbf{x}_\star; \varepsilon)$, the open ball, b, for sufficiently small ε, remain close to $\mathbf{x}_\star$ throughout time, then the point $\mathbf{x}_\star$ is *stable*.
- If all solutions $e^{At}\mathbf{x}_0$ where $\mathbf{x}_0 \in \mathbb{R}^n$ converge to $\mathbf{x}_\star$ as $t \to \infty$, then $\mathbf{x}_\star$ is *asymptotically stable*; asymptotically stable implies that it is stable.

Definition 10. If a fixed point $\mathbf{x}_\star$ is not stable, then it is *unstable*.

Equilibrium points of a system can be classified based on the eigenvalues of the matrix A.

- If the eigenvalues of the $n \times n$ matrix A given by (3.12) all have nonzero, distinct real parts such that $Re\{\lambda_i\} < 0, i = 1, .., n$ at the fixed point $\mathbf{x}_\star$, then $\mathbf{x}_\star$ is a *stable node*.
- If the eigenvalues of A all have nonzero, distinct real parts such that $Re\{\lambda_i\} > 0, i = 1, .., n$ at the fixed point $\mathbf{x}_\star$, then $\mathbf{x}_\star$ is an *unstable node*.
- If all the eigenvalues of the $n \times n$ matrix A have nonzero, distinct real parts such that $Re\{\lambda_i\} > 0, i = 1, .., k$ and $Re\{\lambda_i\} < 0, i = k+1, .., n$ at the fixed point $\mathbf{x}_\star$, then $\mathbf{x}_\star$ is known as a *saddle point* (unstable).
- In the case that only the complex parts of the eigenvalues of A are nonzero, that is $Re\{\lambda_i\} = 0, i = 1, .., k$, at the equilibrium point $\mathbf{x}_\star$, then $\mathbf{x}_\star$ is an elliptic point.

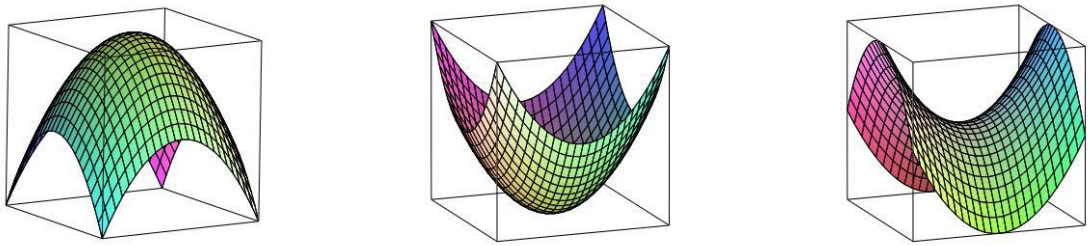

I II III

Figure 3.1: Above shows the basic scenarios of stability, depending on the sign and value of the real parts of the eigenvalues of A. I corresponds to the case where the matrix A has eigenvalues with all positive real parts. II corresponds to the case where the matrix A has eigenvalues with all negative real parts. III corresponds to the case where the matrix A has eigenvalues with some negative and some positive real parts.

3.3 Nonlinear systems

Nonlinear systems are given by the following expression:

$$\dot{\mathbf{x}} = \mathbf{f}(\mathbf{x}) \ , \tag{3.21}$$

here $\mathbf{f} : E \to \mathbb{R}^n$, and E is an open set of $\mathbb{R}^n$. While, in general, it is not possible to solve the system (3.21), there are several extremely useful and enlightening approximation theorems which enable the qualitative analysis of the local features of nonlinear dynamical systems. Below, the theorems which directly relate to the research presented in Part II are discussed, preceding a short summary of important definitions and preliminary theorems.

For our purposes, the analysis of only autonomous systems is sufficient, therefore it is assumed that any time dependence of $\mathbf{f}$ is implicit and contained in the time dependence of $\mathbf{x}$. Below, the derivative of $\mathbf{f}$ at $\mathbf{x}_0$ is denoted $D\mathbf{f}(\mathbf{x}_0)$.

Theorem 3.3.1. *If $\mathbf{f}$: $\mathbb{R}^n \to \mathbb{R}^n$ is differentiable at $\mathbf{x}_0$, then the partial derivatives $\frac{\partial f_i}{\partial x_j}$, for $i, j = 1...n$, all exist at $\mathbf{x}_0$ and for all $\mathbf{x} \in \mathbb{R}^n$,*

$$D\mathbf{f}(\mathbf{x}_0)\mathbf{x} = \sum_{j=1}^{n} \frac{\partial f}{\partial x_j}(\mathbf{x}_0) x_j \ .$$

So, for the differentiable function $\mathbf{f}$, the derivative $D\mathbf{f}$ is given by the following $n \times n$ matrix:

$$D\mathbf{f} = \begin{bmatrix} \frac{\partial f_1}{\partial x_1} & \frac{\partial f_1}{\partial x_2} & \cdots & \frac{\partial f_1}{\partial x_n} \\ \frac{\partial f_2}{\partial x_1} & \frac{\partial f_2}{\partial x_2} & \cdots & \frac{\partial f_2}{\partial x_n} \\ \vdots & \vdots & \ddots & \vdots \\ \frac{\partial f_n}{\partial x_1} & \frac{\partial f_n}{\partial x_2} & \cdots & \frac{\partial f_n}{\partial x_n} \end{bmatrix},$$

known as the Jacobian matrix. We assume that the function $\mathbf{f}$ is continuously differentiable.

Definition 11. A function $\mathbf{f}$:$E \to \mathbb{R}^n$ is said to be analytic in the open set $E \subset \mathbb{R}^n$ if, for $j = 1, ...n$, $\mathbf{x}_0 \in E$, $f_j(\mathbf{x})$ has a Taylor series which converges to $f_j(\mathbf{x})$ in some neighbourhood of $\mathbf{x}_0$ in E.

Analogously to the linear system, an equilibrium point of the nonlinear system at (3.21) is defined as follows:

Definition 12. If the flow of the differential equation (3.21) is given by $\phi_t : E \to \mathbb{R}^n$, then the point $\mathbf{x}_\star$ is called an equilibrium point of the system (3.21) if $\phi_t \mathbf{x}_\star = \mathbf{x}_\star$, for all $t \in \mathbb{R}^n$.

Similarly we can classify the equilibrium points of the nonlinear system at (3.21) based on the eigenvalues of the *Jacobian* matrix of the system at that point. The equilibrium point $\mathbf{x}_\star$ of (3.21) is called a *sink* if all the eigenvalues of $D\mathbf{f}(\mathbf{x}_\star)$ have negative real parts, a *source* if all the eigenvalues of $D\mathbf{f}(\mathbf{x}_\star)$ have positive real part, and a *saddle* point if all the eigenvalues have nonzero real part, with at least one with a positive and at least one with a negative real part.

3.3.1 Linearization

Definition 13. Given (3.21), a point $\mathbf{x}_\star$ is called an equilibrium point of the nonlinear system if $\mathbf{f}(\mathbf{x}_\star) = 0$. The point $\mathbf{x}_\star$ is a hyperbolic equilibrium point if all eigenvalues of the matrix $D\mathbf{f}(\mathbf{x}_\star)$ have nonzero real part. The linear system:

$$\dot{\mathbf{x}} = A\mathbf{x},$$

where the matrix $A = D\mathbf{f}(\mathbf{x}_\star)$ is called the *linearization* of (3.21) at $\mathbf{x}_\star$.

A simple change of coordinates can relocate any equilibrium point of (3.21) to the origin, so for simplicity let us consider the equilibrium point to be the origin; $\mathbf{x}_\star = \mathbf{0}$. So, if the origin is an equilibrium point of (3.21), it implies $\mathbf{f(0)} = \mathbf{0}$. Using a Taylor series to expand $\mathbf{f}$ around the origin (the equilibrium point) we can write:

$$\mathbf{f(x)} = D\mathbf{f(0)x} + \frac{1}{2}D^2\mathbf{f(0)(x,x)} + ... \tag{3.22}$$

It turns out that the linear term of the Taylor expansion, $D\mathbf{f(0)x}$, produces a reasonably good first approximation to the nonlinear function $\mathbf{f(x)}$ in a small neighbourhood around the equilibrium point $\mathbf{x=0}$. That is, the behaviour of (3.21) near the point $\mathbf{x}_\star = \mathbf{0}$ is well approximated by the behaviour of its linearization around $\mathbf{x}_\star$.

The Hartman-Grobman Theorem

The Hartman-Grobman theorem is a remarkably valuable tool for use in nonlinear systems of differential equations. It proves that a hyperbolic equilibrium point of a nonlinear system (3.21) has the same qualitative structure as the linear system (3.3) if the matrix A and the Jacobian matrix $D\mathbf{f}(\mathbf{x}_\star)$ are equal. Below we will always assume that the origin is the fixed point $\mathbf{x}_\star$; that we have performed an appropriate translation to move the fixed point to the origin.

Definition 14. Let X be a metric space, and let P and Q be subsets of X. A continuous, one-to-one map of P onto Q; $h : P \to Q$, such that $h^{-1} : Q \to P$ is continuous, is called a *homeomorphism.*

Definition 15. U, V are open sets containing the origin, $\mathbf{x}_1$, $\mathbf{x}_2 \in U$. If there exists a homeomorphism $H : U \to V$, which maps trajectories of (3.21) in U onto trajectories of (3.3) in V, such that the image of the

trajectory directed from $\mathbf{x}_1$ to $\mathbf{x}_2$ in U is the trajectory directed from $H(\mathbf{x}_1)$ to $H(\mathbf{x}_2)$ in V, then the systems (3.21) and (3.3) are said to be *topologically equivalent.* That is, they have the *same qualitative structure near the origin.*

If the homeomorphism, H, preserves the parametrisation from U to V with respect to time, then the systems (3.21) and (3.3) are said to be *topologically conjugate* in the neighbourhood of the origin.

Theorem 3.3.2 (The Hartman-Grobman Theorem)**.** *Let E be an open subset of $\mathbb{R}^n$ which contains the origin, and let U, V be open sets containing the origin. Let $\mathbf{f} \in C^1(E)$, and let ϕ_t be the flow of the nonlinear system* (3.21)*. Suppose that $\mathbf{f}(\mathbf{0}) = \mathbf{0}$, and that the matrix $A = D\mathbf{f}(\mathbf{0})$ has all eigenvalues with nonzero real part. Then, there exists a homeomorphism, H, of an open set U onto an open set V, such that for each $\mathbf{x}_0 \in U$ there is an open interval $I_0 \subset \mathbb{R}^n$ containing zero, such that for all $\mathbf{x}_0 \in U$ and $t \in I_0$,*

$$H \circ \phi_t(\mathbf{x}_0) = e^{At} H(\mathbf{x}_0).$$

That is, H maps trajectories of (3.21) *near the origin on to trajectories of* (3.3) *near the origin, such that the parametrisation with respect to time in preserved.*

3.3.2 The Stable Manifold Theorem

The stable manifold theorem is an extremely important result and very useful in the analysis of the local qualitative features of a nonlinear system of ordinary differential equations. Below, it is assumed that the equilibrium point in question $\mathbf{x}_\star$ is located at the origin of the coordinate system.

Theorem 3.3.3 (The Stable Manifold Theorem)**.** *Let E be an open subset of $\mathbb{R}^n$ containing the origin, let $\mathbf{f} \in C^1(E)$, and let ϕ_t be the flow of the nonlinear system at* (3.21)*. Suppose that* **$\mathbf{f(0)=0}$** *and that $D\mathbf{f(0)}$ has k eigenvalues with negative real part and $n-k$ eigenvalues with positive real part. Then there exists a k-dimensional differentiable manifold S tangent to the stable subspace E^s of the* linear system *at* (3.3) *at* $\mathbf{0}$ *such that for all $t \geq 0, \phi_t(S) \subset S$ and for all $\mathbf{x}_0 \in S$,*

$$\lim_{t \to \infty} \phi_t(\mathbf{x}_0) = \mathbf{0};$$

and there exists an $n-k$ dimensional differentiable manifold, U, tangent to the unstable subspace E^u of (3.3) *at* $\mathbf{0}$ *such that for all $t \leq 0, \phi_t(U) \subset U$ and for all $\mathbf{x}_0 \in U$,*

$$\lim_{t \to -\infty} \phi_t(\mathbf{x}_0) = \mathbf{0}.$$

The proof of the above theorem can be found in Perko (2001) "*Differential Equations and Dynamical Systems*" (p107).

Theorem 3.3.4. *If $\mathbf{x}_\star$ is a sink of the nonlinear system* (3.21) *and $Re(\lambda_j) < -\alpha < 0$ for all of the eigenvalues λ_j of the matrix $D\mathbf{f}(\mathbf{x}_\star emph)$, then , given $\varepsilon > 0$ there exists a $\delta > 0$ such that for all $\mathbf{x} \in b(\mathbf{x}_\star, \delta)$, the flow $\phi_t(\mathbf{x})$ of* (3.21) *satisfies:*

$$|\phi_t(\mathbf{x}) - \mathbf{x}_\star| \leq \varepsilon e^{-\alpha t}$$

for all $t \geq 0$.

Because hyperbolic points are either asymptotically stable or unstable, the only case in which an equilibrium point of (3.21) can be stable but not asymptotically stable is if the equilibrium point is non-hyperbolic, that is, when it has either at least one zero eigenvalue or a pair of pure imaginary eigenvalues. In order for the point to be stable, all other eigenvalues must have $Re(\lambda_j) \leq 0$.

Theorem 3.3.5. *Let $\mathbf{f} \in C^r(E)$, where E is an open subset of $\mathbb{R}^n$ containing the origin, and $r \geq 1$. Suppose that* **$\mathbf{f(0)} = \mathbf{0}$** *and that $D\mathbf{f(0)}$ has k eigenvalues with negative real parts, j eigenvalues with positive real part,*

and $m = n-k-j$ eigenvalues with zero real part. Then there exists an m-dimensional center manifold $\mathbf{W}^c(\mathbf{0})$ of class C^r which is tangent to the center subspace E^c of (3.3) at $\mathbf{0}$, there exists and k-dimensional stable manifold $W^s(\mathbf{0})$ of class C^r which is tangent to the stable subspace, E^s, of (3.3), and finally there also exists a j-dimensional unstable manifold of class C^r which is tangent to the unstable subspace E^u of (3.3) at $\mathbf{0}$. The manifolds $W^c(\mathbf{0})$, $W^s(\mathbf{0})$ and $W^u(\mathbf{0})$ are invariant under the flow of ϕ_t of (3.21).

This leads naturally to the next section which summarises a technique which makes use of the center manifold of a non-hyperbolic fixed point to infer the local behaviour in a neighbourhood around such a fixed point.

3.3.3 Center Manifold Theory

The Hartman-Grobman Theorem can completely identify and classify the behaviour of the hyperbolic fixed point of (3.21). The following theorem, called the Local Center Manifold theorem enables the qualitative analysis and classification of a non-hyperbolic fixed point of the nonlinear system, by showing that the local qualitative behaviour of a fixed point $\mathbf{x}_\star$ of (3.21) is completely determined by its behaviour on the center manifold.

Theorem 3.3.6 (The Center Manifold Theorem)**.** *Take $\mathbf{f} \in C^r(E), r \geq 1$, with the origin being an equilibrium point, i.e $\mathbf{f}(\mathbf{0})=\mathbf{0}$, then the system (3.21) can be written in diagonal form:*

$$\begin{pmatrix} \dot{x} \\ \dot{y} \\ \dot{z} \end{pmatrix} = \begin{pmatrix} A_s & 0 & 0 \\ 0 & A_u & 0 \\ 0 & 0 & A_c \end{pmatrix} \begin{pmatrix} x \\ y \\ z \end{pmatrix} + \begin{pmatrix} \mathbf{F}_s(x,y,z) \\ \mathbf{F}_u(x,y,z) \\ \mathbf{F}_c(x,y,z) \end{pmatrix},$$

*where (x,y,z) $\in \mathbb{R}^c \times \mathbb{R}^s \times \mathbb{R}^u$, and $s+u+c=n$. The square matrix A_s is an s-dimensional matrix, of which all the eigenvalues have negative real parts, representing the stable manifold. The square matrix A_u is a u-dimensional matrix of which all the eigenvalues have positive real part, associated with the unstable manifold. The square matrix A_c is a c-dimensional matrix of which all the eigenvalues have*zero *real parts, associated with the* center manifold*, and $\mathbf{F}_s$ $(\mathbf{0})=\mathbf{F}_u$ $(\mathbf{0})=\mathbf{F}_c(\mathbf{0})=\mathbf{0}$, $D\mathbf{F}_s(\mathbf{0}) = D\mathbf{F}_u$ $(\mathbf{0}) = D\mathbf{F}_c(\mathbf{0})=\mathbf{0}$. Also, for $\delta > 0$, there exist the functions $\mathbf{h}_x$, $\mathbf{h}_y$, $\mathbf{h}_z \in b(\mathbf{0},\delta)$, that define the local stable, unstable and center manifolds as:*

$$\begin{aligned}
\mathbf{W}^s_{loc}(\mathbf{0}) &= \{(x,y,z) \in \mathbb{R}^s \times \mathbb{R}^u \times \mathbb{R}^c | y = \mathbf{h}^s_y(x), z = \mathbf{h}^s_z(x); D\mathbf{h}^s_y = \mathbf{0}, D\mathbf{h}^s_z = \mathbf{0}; |x| < \delta\}, \\
\mathbf{W}^u_{loc}(\mathbf{0}) &= \{(x,y,z) \in \mathbb{R}^s \times \mathbb{R}^u \times \mathbb{R}^c | x = \mathbf{h}^u_x(y), z = \mathbf{h}^u_z(y); D\mathbf{h}^u_x = \mathbf{0}, D\mathbf{h}^u_z = \mathbf{0}; |y| < \delta\}, \\
\mathbf{W}^c_{loc}(\mathbf{0}) &= \{(x,y,z) \in \mathbb{R}^s \times \mathbb{R}^u \times \mathbb{R}^c | x = \mathbf{h}^c_x(z), y = \mathbf{h}^c_y(z); D\mathbf{h}^c_x = \mathbf{0}, D\mathbf{h}^c_y = \mathbf{0}; |z| < \delta\},
\end{aligned}$$

where all of $\mathbf{h}^m_i (m = s,u,c$ and $i = x,y,z) \in C^r$, which satisfy, for the center manifold:

$$D\mathbf{h}^c_x(z)\left[A_c z + F_c(\mathbf{h}^c_x(z), \mathbf{h}^c_y(z), z)\right] - A_s\mathbf{h}^c_x(z) - F_s\left(\mathbf{h}^c_x(z), \mathbf{h}^c_y(z), z\right) = \mathbf{0}, \tag{3.23}$$

$$D\mathbf{h}^c_y(z)\left[A_c z + F_c(\mathbf{h}^c_x(z), \mathbf{h}^c_y(z), z)\right] - A_u\mathbf{h}^c_y(z) - F_u\left(\mathbf{h}^c_x(z), \mathbf{h}^c_y(z), z\right) = \mathbf{0}, \tag{3.24}$$

for $|z| < \delta$. The flow on the center manifold $\mathbf{W}^c_{loc}(\mathbf{0})$ is then defined by, solving (3.23) and (3.24), the following system of differential equations:

$$\dot{\mathbf{z}} = A_c\mathbf{z} + \mathbf{F}_c(\mathbf{z}, \mathbf{h}^c_x(\mathbf{z}), \mathbf{h}^c_y(\mathbf{z})). \tag{3.25}$$

for all $\mathbf{z} \in \mathbb{R}^c$ with $|\mathbf{z}| < \delta$.

The Center Manifold Theorem helps to reduce the dimensionality of the nonlinear system, since in general $c < n$. And while, equations (3.23) and (3.24) may be difficult to solve for $\mathbf{h}^c_x(\mathbf{z})$ and $\mathbf{h}^c_y(\mathbf{z})$, the above theorem

outlines a method which can be used to approximate these functions, provided r is sufficiently high. This can be done by substituting power series expansions of $\mathbf{h}_x^c(\mathbf{z})$ and $\mathbf{h}_y^c(\mathbf{z})$ into (3.23) and (3.24); the more terms included, the better the approximation.

In general, the flow on the center manifold takes on the following form:

$$\dot{\mathbf{z}} = a_m \mathbf{z}^m + a_{m+1}\mathbf{z}^{m+1}... \tag{3.26}$$

near the origin. So, considering a non-hyperbolic fixed point $\mathbf{x}_\star$, located at the origin, of the the nonlinear system

$$\dot{\mathbf{x}} = \mathbf{f}(\mathbf{x}), \tag{3.27}$$

which is topologically conjugate to the linear system

$$\dot{\mathbf{x}} = A\mathbf{x} \quad \text{with} \quad A = D\mathbf{f}(\mathbf{x}_\star), \tag{3.28}$$

if the flow on the center manifold of the system at the origin is given by (3.26), the following rules apply:

- If m is even, then the fixed point at the origin has saddle-node stability.
- If m is odd, then it is necessary to consider both $\dot{x}$ and $\dot{y}$.

$$\dot{x} = b_k x^k + b_{k+1}x^{k+1} + ... \tag{3.29}$$
$$\dot{y} = c_r y^r + c_{r+1}y^{r+1} + ... \tag{3.30}$$

  where b_k and c_r are coefficients of the $k-th$ and $r-th$ order (lowest order) terms of x and y, respectively.

  - if all of $a_m, b_k, c_r < 0$ then the equilibrium point is a topological attractor
  - if all of $a_m, b_k, c_r > 0$ then the equilibrium point is a topological repellor
  - if the signs of a_m, b_k, c_r are different, then the equilibrium point is a topological saddle.

The Center Manifold Theorem can also treat non-hyperbolic fixed points which produce more than one eigenvalue for the matrix A which have zero real parts. If, for example considering a 3-dimensional system of differential equations, for which two of the eigenvalues of the matrix $A = D\mathbf{f}(\mathbf{x}_\star)$ have their real parts equal to zero, and one eigenvalue with a negative real part. We can write the system in the following diagonalised form:

$$\begin{pmatrix} \dot{x} \\ \dot{z}_1 \\ \dot{z}_2 \end{pmatrix} = \begin{pmatrix} A_s & 0 & 0 \\ 0 & A_{c_1} & 0 \\ 0 & 0 & A_{c_2} \end{pmatrix} \begin{pmatrix} x \\ z_1 \\ z_2 \end{pmatrix} + \begin{pmatrix} \mathbf{F}_s(x, z_1, z_2) \\ \mathbf{F}_{c_1}(x, z_1, z_2) \\ \mathbf{F}_{c_2}(x, z_1, z_2) \end{pmatrix},$$

above, z_1 and z_2 are the components of (3.21) which correspond to the double eigenvalues with zero real parts and x is the component which corresponds to the eigenvalue with the negative real part. From the local Center Manifold Theorem, in this case, a 2-dimensional invariant center manifold exists:
For some $\delta > 0$,

$$\mathbf{W}^c_{loc}(\mathbf{0}) = \{(x, z_1, z_2) \in \mathbb{R}^s \times \mathbb{R}^c | x = \mathbf{h}(z_1, z_2); \mathbf{h}(\mathbf{0}) = D\mathbf{h}(\mathbf{0}) = \mathbf{0}; |z_1|, |z_2| < \delta\}, \tag{3.31}$$

where, $\mathbf{h} \in B(\mathbf{0}, \delta)$, where B is an open ball centered on the origin.

In this case, finding the flow on the center manifold involves solving the following matrix equation:

$$\begin{bmatrix} \frac{\partial \mathbf{h}(z_1,z_2)}{\partial z_1} & \frac{\partial \mathbf{h}(z_1,z_2)}{\partial z_2} \end{bmatrix} \begin{bmatrix} A_{c_1} z_1 \\ A_{c_2} z_2 \end{bmatrix} - A_s \mathbf{x} - \mathbf{F}_s(x, \mathbf{h}(z_1, z_2)) \ .$$

We have the following boundary conditions:

$$\mathbf{h}(z_1, z_2) = D\mathbf{h}(z_1, z_2) = 0. \tag{3.32}$$

A power series approximation for $\mathbf{h}$ which is consistent with the above boundary conditions is

$$\mathbf{h}(z_1, z_2) = az_1^2 + bz_1z_2 + dz_2^2, \tag{3.33}$$

Thus, the flow defined on the center manifold in the neighbourhood of the origin, which is a non-hyperbolic point, in the case of a double zero eigenvalue is:

$$\begin{aligned} \dot{z}_1 &= A_{c_1} z_1 + \mathbf{F}_s(x, \mathbf{h}(z_1, z_2)), \\ \dot{z}_2 &= A_{c_2} z_2 + \mathbf{F}_s(x, \mathbf{h}(z_1, z_2)). \end{aligned} \tag{3.34}$$

3.4 End note

This chapter summarised the basics of linear dynamical systems theory, and presented techniques which can be used to study the local qualitative behaviour of nonlinear systems. The Hartman-Grobman Theorem and linearisation technique can be used to study local features of hyperbolic equilibrium points of nonlinear systems, and the Center Manifold Theorem states that the behaviour near a non-hyperbolic fixed point is completely described by the flow on the center manifold at that point. The research presented in Chapter 4 uses the theory outlined in this chapter to study the cosmological dynamics of a fourth order gravity model and to obtain a qualitative appreciation of the properties of its phase space. In particular, we make use of the Hartman-Grobman Theorem and the Center Manifold Theorem to analyse the local behaviour of the stationary points of the nonlinear system which represents the modified cosmological field equations.

Part II

Dynamics of the Hu & Sawicki model for $f(R)$ gravity

Chapter 4

Dynamical systems approach to $f(R)$ gravity

The object of this chapter is to present a detailed account of a dynamical systems analysis applied to the Hu-Sawicki model introduced above. In Section 4.1, I give a brief overview of how the qualitative theory of dynamical systems has been used in standard cosmology. In Section 4.2 the details of the compact analysis and its results are presented. A non-compact analysis was also performed in order to aid an integration of the dynamical systems equations to obtain the background evolution of the resulting universe, in Section 4.3. In Section 4.4 the expansion history resulting from an integration of the non-compact dynamical system is presented, along with a comparison of these results with the ΛCDM model.

The work contained and detailed in Sections 4.2.3, 4.2.4, 4.3 and 4.4 is an original contribution - unless otherwise stated - submitted as the basis for this thesis. Section 4.5 examines the success of a fitting function used in [7] to match the behaviour of the Hu-Sawicki model over a range of redshifts; this is also an original perspective.

4.1 Dynamical Systems approach to cosmology

Over the years, the development of a theoretical description of the cosmos has come to require some sort of modification to the theory of gravity, to the end of developing an improved understanding of quantum gravity, establishing a theoretical motivation for early time cosmic inflation, as well as explaining the late time domination of the Dark Energy fluid. It is now clear that studying more general cosmological models, whether in the sense of generalizing the gravitational Lagrangian or questioning the FLRW background, is part of the future of cosmology. It has become important to extract quality information from very complicated systems, and because this task can, at most times, be formidable, researchers have been nudged into the application of the qualitative theory of dynamical systems to elicit physical insights about various cosmological models.

The dynamical systems approach has been used successfully in the past to acquire information regarding the global features and properties of a variety of cosmologies, both in standard GR and, more recently in the context of modified theories of gravity. This analysis enables the study of interesting cosmological solutions of especially complicated field equations, without the need to directly solve the system (which may otherwise be very difficult). From such an analysis, we can draw the nature of these solutions, and construct a view of the entire phase space of the cosmology [64].

While the exact solutions obtained in this way represent asymptotic behaviour, the qualitative description of the resulting universe gives a method to prefer some models over others, and indicate which warrant more attention [10].

The technique relies on the ability to express the cosmological equations, in terms of a suitable choice of *generalised dynamical variables*, as a set of autonomous differential equations. Up to now, there has been much

work done in the application of dynamical systems to cosmology, see for example [64], [27], [2], [10], [12]. A popular method is to define a set of expansion normalised (or Hubble normalized) variables along with a time variable normalised in the same way. A state space constructed with such variables is compact for simple, expanding models, where the specific theory does not allow for recollapsing, bouncing or static universes, that is, there are no contributions to the modified Friedmann equation which would allow for zero valued or negative H.

Complications arising from the modification of the Einstein field equations usually result in additional degrees of freedom, allowing the volume expansion, Θ, and therefore H, to pass through zero. This will usually result in the dynamical variables becoming unbounded, and cause the expansion normalised time variable to change sign, i.e. it will no longer be monotonically increasing [27]. In these cases, an additional analysis is required, such as the Poincaré projection, to study the equilibrium points which lie at infinity, by projecting these points onto a unit sphere and studying their stability.

Another way to deal with these additional degrees of freedom is to divide the phase space into compact subsectors, where the dynamical variables, the normalisation and the normalised time variable are defined separately in each. The full phase space is then constructed by aligning the boundaries of the various sectors [29], [19], [64], [28], [27].

4.1.1 Example : Stability of Friedmann-Lemaître cosmologies

In this section, a dynamical systems analysis is applied to the set of models in standard GR known as *Friedmann-Lemaître* (FL) models[1], which describe universes that are homogeneous and isotropic about every point, with a cosmological constant Λ. For a detailed analysis, see [29], [64]. Λ is interpreted as the vacuum energy, and is assumed never to be negative; $\Lambda \geq 0$. Further assumptions made for this analysis is that the matter source is described completely by a perfect fluid, with an equation of state $P = \rho(w-1)$ [29] .

The field equations are

$$G_{\alpha\beta} + \Lambda g_{\alpha\beta} = T_{\alpha\beta}. \tag{4.1}$$

Using the line element

$$ds^2 = -dt^2 + a^2(t)d\Omega^2, \tag{4.2}$$

where the spatial sections correspond to maximally symmetric 3-space of constant curvature:

$$d\Omega^2 = dr^2 + f^2(r)(d\theta^2 + \sin^2\theta d\phi^2), \tag{4.3}$$

where

$$f(R) = \begin{cases} \sin r & \text{if } \ k = +1 \\ r & \text{if } \ k = 0 \\ \sinh r & \text{if } \ k = -1. \end{cases}$$

Then, the cosmological field equations are

The Friedmann Equation

$$H^2 = \frac{1}{3}\rho - \frac{1}{6}{}^3R + \frac{1}{3}\Lambda \ \ , \tag{4.4}$$

The Raychaudhuri Equation

$$\frac{\ddot{a}}{a} \equiv -qH^2 = -\frac{3w-2}{6}\rho + \frac{1}{3}\Lambda \ \ , \tag{4.5}$$

The continuity equation

$$\dot{\rho} = -3wH\rho \ \ , \tag{4.6}$$

[1]This section is adapted from [29]

where $H \equiv \frac{\dot{a}}{a}$ and ${}^3R = 6k/a^2$ gives the 3-curvature of symmetry surfaces. Assuming the Hubble rate obeys $H \neq 0$, we can quite naturally define the following dimensionless dynamical coordinates:

$$K = \frac{k}{3H^2}, \quad \Omega = \frac{\rho}{3H^2}, \quad \Omega_\Lambda = \frac{\Lambda}{3H^2} \ . \tag{4.7}$$

It follows that the Friedmann equation defines the following constraint on the system:

$$1 = \Omega - K + \Omega_\Lambda. \tag{4.8}$$

The deceleration parameter, q is determined by the Raychaudhuri equation in terms of the dynamical variables as:

$$q = \frac{3w-2}{2}(1+K) - \frac{3w}{2}\Omega_\Lambda \ . \tag{4.9}$$

The ranges of the dynamical variables can be obtained by imposing a weak energy condition on the system and assuming $\Lambda \geq 0$. The system can be made compact by assuming that the spatial curvature is non-positive:

$$0 \leq \Omega \leq 1, \quad -1 \leq K \leq 0, \quad 0 \leq \Omega_\Lambda \leq 1. \tag{4.10}$$

If the normalised time variable is defined as:

$$\frac{1}{H}\frac{d}{dt} \equiv \ ', \tag{4.11}$$

the system can be written as a set of first order autonomous differential equations, in terms of the dynamical variables as follows:

$$K' = 2K\left[\frac{3w-2}{2}\Omega - \Omega_\Lambda\right] \ , \tag{4.12}$$

$$\Omega' = \left[2\left[\frac{3w-2}{2}\Omega - \Omega_\Lambda\right] - (3w-2)\right]\Omega \ , \tag{4.13}$$

$$\Omega_\Lambda' = 2\left[1 + \frac{3w-2}{2}\Omega - \Omega_\Lambda\right]\Omega_\Lambda \ , \tag{4.14}$$

along with a decoupled differential equation for the Hubble expansion rate:

$$H' = -(1 + \left[\frac{3w-2}{2}\Omega - \Omega_\Lambda\right])H. \tag{4.15}$$

The Friedmann constraint can be used to eliminate Ω and reduce the dimension of the problem from 3 to 2. The differential equations of the 2-dimensional system are

$$\begin{aligned} K' &= 2K\left[\frac{3w-2}{2}(1+K) - \frac{3w}{2}\Omega_\Lambda\right] \ , \\ \Omega_\Lambda' &= 2\left[1 + \frac{3w-2}{2}(1+K) - \frac{3w}{2}\Omega_\Lambda\right]\Omega_\Lambda \ . \end{aligned} \tag{4.16}$$

The equilibrium points identified [29], along with a stability classification and the exact solution associated with each point, from the dynamical systems analysis of the equations (4.16) are presented in Table (4.1).

Note that all of $K, \Omega_\Lambda, \Omega = 0$ are invariant submanifolds, corresponding to the flat submanifold, the vacuum boundary and the submanifold containing GR with no cosmological constant, respectively.

The above analysis, however, is finite, and neglects to identify any equilibrium points which lie at infinity. It would therefore be advantageous to perform a dynamical systems analysis on the same system written in terms of a set of compact coordinates, constructing a phase space which is constrained by this compact basis.

Point	Coordinates $(K, \Omega_\Lambda, \Omega)$	Eigenvalues	Stability		Solution
			$0 < w < 2/3$	$2/3 < w < 2$	
F	$[0, 0, 1, \frac{3w-2}{2}]$	$[3w-2, 3w]$	saddle	source	Flat Friedmann solution
M	$[-1, 0, 0, 0]$	$[-(3w-2), 2]$	source	saddle	Milne solution
dS	$[0, 1, 0, -1]$	$[-2, -3w]$	sink	sink	de Sitter solution

Table 4.1: Summarising the equilibrium points identified, along with their corresponding exact solution, and their local stability classification [29].

Keeping this in mind, the Friedmann equation is written as follows [29]:

$$\rho = 3H^2 + \frac{1}{2}{}^3R - \Lambda \ . \tag{4.17}$$

If the curvature is taken to be positive, ${}^3R > 0$, we can define the following positive definite normalisation:

$$D \equiv \sqrt{H^2 + \frac{{}^3R}{6}} \ , \tag{4.18}$$

as well as the normalised time variable $' \equiv \frac{1}{D}\frac{d}{dt}$, and a compact set of dynamical variables:

$$Q = \frac{H}{D}, \quad \tilde{\Omega}_\Lambda = \frac{\Lambda}{3D^2}. \tag{4.19}$$

Thus, the following set of first order coupled differential equations for the dynamical variables emerge:

$$\begin{aligned} \tilde{\Omega}'_\Lambda &= 3w(1-\tilde{\Omega}_\Lambda)\tilde{\Omega}_\Lambda Q \ , \\ Q' &= \left[1 - \frac{3w}{2}\left(1-\tilde{\Omega}_\Lambda\right)\right](1-Q^2) \ . \end{aligned} \tag{4.20}$$

Setting the above derivatives equal to zero we obtain the fixed points corresponding to the compact dynamical system, these are summarised in Table 4.2.

Point	Coordinates (Q, Ω_Λ)	Stability	Solution
${}_+F$	$[1, 0]$	source	Flat Friedmann solution
${}_-F$	$[-1, 0]$	sink	Flat Friedmann solution
${}_+dS$	$[1, 1]$	sink	de Sitter solution
${}_-dS$	$[-1, 1]$	source	de Sitter solution
E	$[0, \frac{3w-2}{3w}]$	saddle	Einstein static solution

Table 4.2: Summarising the equilibrium points identified, along with their corresponding exact solution, and their local stability classification for the compact dynamical systems analysis of FL cosmologies with a cosmological constant. The sign associated with the F and dS points indicate whether it lies within the expanding or contracting sector of the phase space corresponding to positive or negative Q, respectively [29].

The complete dynamical phase space can be constructed by matching the $K > 0$ phase space with the contracting and expanding $K < 0$ phase spaces. The phase space is constrained by $\Omega_\Lambda = 0$ at the bottom and by the vacuum submanifold $\Omega = 0$ on the other sides.

Solution trajectories of $w > 2/3$ have the following behaviour:

- Universes for which $K < 0$, $H > 0$, $\Omega, \Omega_\Lambda > 0$ (lie *within* the left triangular region), evolve from ${}_+F$, an initial big bang singularity and evolve toward the the de Sitter expansion phase solution at ${}_+dS$.
- Universe for which $K > 0$, $H > 0$:
  - If Λ is sufficiently small, the trajectories move into the contracting half of the phase space and represent recollapsing universes which terminate at ${}_-F$ in a 'big crunch'. These are known as

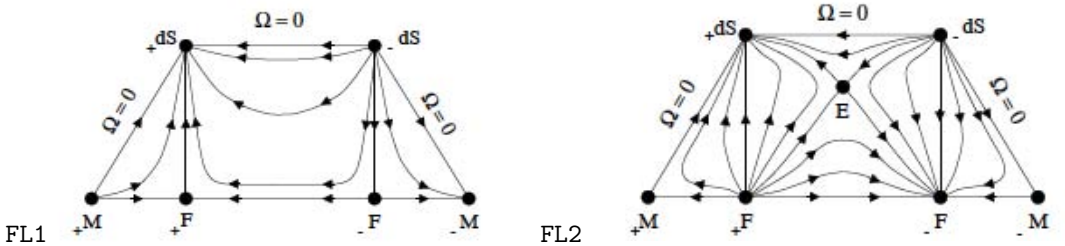

Figure 4.1: The completed state space portraits of Friedmann-Lemaître cosmologies for $0 < w < 2$ (M. Goliath and G.F.R. Ellis, 1999 *Phys. Rev.* D **60** 023502 [29]). The above phase plots show the entire phase space different ranges of w: FL1 - $0 < w < 2/3$ and FL2 - $2/3 < w < 2$. The left half of each of FL1 and FL2 correspond to the expanding sector of the phase spaces ($H, Q > 0$) and the right half correspond to the contracting sector ($H, Q < 0$). The triangular sections represent regions for which $K < 0$, where the horizontal axis corresponds to K and the vertical axis corresponds to Ω_Λ. The rectangular sections represent the regions for which $K > 0$, where along the vertical axis runs $\tilde{\Omega}_\Lambda$ and the horizontal axis corresponds to Q. The Einstein static solution appears only in the phase space when $w > 2/3$.

Friedmann-Lemaître models.

- If Λ is sufficiently large, the trajectory evolves towards the de Sitter model, ${}_+dS$. These are called Lemaître models.
- If $\Lambda = \Lambda_c \equiv \frac{3w-2}{w}\frac{k}{a_c^2}$, then trajectories evolve towards the Einstein static universe, E. For every value of the scale factor a_c there is a corresponding Λ_c which results in an Einstein static universe. Therefore, E actually represents a set of static universes.

Because the submanifold corresponding to static universe, $H = 0$, is non-invariant, trajectories are, in principle, allowed to cross from the expanding sector of the phase space to the contracting sector without running into a singularity.

It can be seen that, from the diagrams of the compact phase space, the local stability around the equilibrium points vary according to the equation of state parameter, w, therefore, the phase space for the range $0 < w < 2/3$ is different to the phase space for the range $2/3 < w < 2$. The Einstein static solution only appears in the analysis when $w > 2/3$ [29], [64].

4.2 Compact phase space analysis of $f(R)$ gravity

The general strategy for the application of dynamical systems to the cosmology of fourth order gravity is detailed in [12], [10], [2], [1]. This approach enables the analysis of any analytic function $f(R)$, that is invertible for the Ricci scalar. Following the considerations of [2], [28], [27], a compact analysis of the phase space for such a general theory is performed, by defining a strictly positive normalization to pull the solutions at infinity into a finite volume, which may then be studied conveniently.

To facilitate this, a normalized time variable is required, defined as follows [2]:

$$\frac{d}{d\tau} \equiv \frac{1}{D}\frac{d}{dt} \,. \tag{4.21}$$

Ensuring that this time variable is strictly non-decreasing (monotonic) amounts to guaranteeing that the expansion-normalization adopted, D, is strictly positive [2], [27]. This means that any negative contribution to the Friedmann equation must be absorbed into the normalization. In the case where a quantity is possibly negative or positive, each option must be studied in a separate sector of the phase space. The full phase space can then be reconstructed by simply aligning the various sectors along their common boundaries. A phase space which is constructed in this way can include all of static, bouncing and re-collapsing models [27]. Following this prescription for the definition of the normalisation, the sign of time can be maintained whether studying expanding or collapsing cosmologies.

Recall the modified cosmological equations are given by:

The modified Friedmann Equation

$$H^2 = \frac{1}{3f'}\left(\rho_m + \frac{1}{2}\left(Rf' - f\right) - 3H\dot{f'}\right), \tag{4.22}$$

The modified Raychauduri Equation

$$2\dot{H} + 3H^2 = -\frac{1}{f'}\left(P_m + 2H\dot{f'} + \frac{1}{2}\left(f - Rf'\right) + \dot{R}^2 f''' + \ddot{R}f''\right), \tag{4.23}$$

The trace of the modified field equations

$$3\ddot{R}f'' = \rho(1-3w) + f'R - 2f - 9Hf''\dot{R} - 3f'''\dot{R}^2, \tag{4.24}$$

where the subscript m indicates a property of matter.

The conservation of standard matter is given by the continuity equation:

$$\dot{\rho} = -3H(1+w)\rho. \tag{4.25}$$

The Ricci scalar is given in terms of the Hubble rate as:

$$R = 6\dot{H} + 12H^2. \tag{4.26}$$

We are only concerned with the sectors of the phase space where $R \geq 0$, simply because negative Ricci scalar values are not of any real physical interest. As mentioned previously, we require $f', f'' > 0$, and the matter density is assumed to be nonnegative. The function f, as shall be seen is always positive. Therefore, in (4.22) the term which contains f attached to a negative sign must be absorbed into the positive-definite normalization.

4.2.1 Compact phase space

Rewriting the modified Friedmann equation (4.22) in the following way allows convenient definition of the normalized variables:

$$\left(3H + \frac{3}{2}\frac{\dot{f'}}{f'}\right)^2 + \frac{3}{2}\frac{f}{f'} = \frac{3\rho_m}{f'} + \frac{3}{2}R + \left(\frac{3}{2}\frac{\dot{f}}{f'}\right)^2. \tag{4.27}$$

The left hand side of the above equation is a positive definite quantity. Quite naturally, assigning each term in (4.27) a name as done in [2], we obtain the following dynamical variables:

$$\begin{aligned} x &= \frac{3}{2}\frac{\dot{f'}}{f'}\frac{1}{D}, \qquad v = \frac{3}{2}\frac{R}{D^2}, \\ y &= \frac{3}{2}\frac{f}{f'}\frac{1}{D^2}, \qquad \Omega = \frac{3\rho_m}{f'}\frac{1}{D^2}, \qquad Q = \frac{3H}{D}, \end{aligned} \tag{4.28}$$

where D represents the normalization which compactifies the phase space, and takes the form

$$D^2 = \left(3H + \frac{3}{2}\frac{\dot{f'}}{f'}\right)^2 + \frac{3}{2}\frac{f}{f'}. \tag{4.29}$$

Then, (4.27) and (4.29) establish two independent constraint equations for our system:

$$1 = \Omega + x^2 + v, \tag{4.30}$$

$$1 = (Q + x)^2 + y. \tag{4.31}$$

The above dynamical variables (4.28) constitute the coordinates of our compact phase space, and the boundaries of this phase space are defined by the above two constraints as follows:

$$-1 \leq x \leq 1, \quad 0 \leq \Omega \leq 1, \quad -2 \leq Q \leq 2, \quad 0 \leq v \leq 1, \quad 0 \leq y \leq 1.$$

The construction of D ensures that the dynamical variables are well defined when $H = 0$, thus we expect all of static, expanding, collapsing and bounce solutions to be included. Expanding and collapsing universes will be connected via the non-invariant submanifold $Q = 0$.

4.2.2 The General Propagation Equations

Following the method laid out in [12], [10], [2], [1], [64], [29], to obtain the dynamical system , we differentiate the dynamical variables (4.28) with respect to the the normalized time variable, τ. Substituting the independent cosmological equations, (4.22)−(4.24), produces a set of 5 first order autonomous differential equations. The dimensionality of the system can be reduced by using the constraint equations (4.30) and (4.31) to eliminate y and Ω. Below, we show the general propagation equations for the 3-dimensional autonomous system:

$$\frac{dv}{d\tau} = -\frac{1}{3} v \left[(Q + x) \left(2\, v + 4\, xQ - \left(1 - v - x^2 \right) (1 + 3\, w) \right) - 2\, Q - 4\, x + 2\, x\Gamma\ (v - 1) \right], \tag{4.32}$$

$$\begin{aligned} \frac{dx}{d\tau} =& \frac{1}{6} \left[-2\, x^2 v\Gamma + \left(1 - v - x^2 \right) (1 - 3\, w) + 2v + 4\ \left(x^2 - 1 \right) \left(1 - Q^2 - xQ \right) \right. \\ & \left. + x\, (Q + x) \left(\left(1 - v - x^2 \right) (1 + 3\, w) - 2\, v \right) \right], \end{aligned} \tag{4.33}$$

$$\begin{aligned} \frac{dQ}{d\tau} =& \frac{1}{6} \left[-4\, xQ^3 + (5 + 3\, w)\, Qx\, (1 - xQ) - Q^2\, (1 - 3\, w) - Qx^3\, (1 + 3\, w) \right. \\ & \left. - 3\, vQ\, (1 + w)\, (Q + x) + 2\, v\, (1 - \Gamma\, Qx) \right]. \end{aligned} \tag{4.34}$$

where

$$\Gamma \equiv \frac{f'}{f''R}. \tag{4.35}$$

The term Γ specifies the model which is to be input into the above general propagation equations. In order to close the system, Γ must be expressible in terms of the dynamical variables [2]. This implies that the above system characterizes a general dynamical system for any modified gravity cosmology defined by a function $f(R)$, which is invertible in terms of the dynamical variables, so as to be able to find Γ as a function of (x, Q, v).

Clearly, $v = 0$ corresponds to an invariant submanifold; solutions which originate there will remain there forever. This submanifold corresponds to a universe for which the Ricci scalar vanishes. Due to the existence of an invariant submanifold, no global attractor can exist for cosmological systems defined by the above compact dynamical variables.

The cosmological equations can be expressed in terms of the variables. The modified Friedmann equation is given by (4.30). The second time derivative of f', given by the trace equation, in terms of the dynamical variables is:

$$\frac{\ddot{f}'}{f'} = \frac{\ddot{R} f''}{f'} + \frac{\dot{R}^2 f'''}{f'} = \frac{H^2}{Q^2} \left[(1 - 3w)\Omega + 2v - 4y - 2xQ \right]. \tag{4.36}$$

So, using (4.36) and the constraint equations, we can write the modified Raychaudhuri equation (4.23) in terms of the dynamical variables as:

$$\dot{H} = -\frac{H^2}{Q^2}\left(1 + \Omega - 2\,y - x^2\right). \tag{4.37}$$

4.2.3 The Dynamical Systems Analysis of the Hu-Sawicki model

In this thesis, we focus on the HS model as described in [32], given by:

$$f(R) = R - m^2 \frac{c_1 \left(\frac{R}{m^2}\right)^n}{c_2 \left(\frac{R}{m^2}\right)^n + 1}. \tag{4.38}$$

We define the following relations:

$$m^2 \equiv C H_0^2, \tag{4.39}$$

$$r \equiv \frac{R}{H_0^2}, \tag{4.40}$$

$$h \equiv \frac{H}{H_0}, \tag{4.41}$$

hence, we can write (4.38) as:

$$f(R) = C H_0^2 \left[\left(\frac{r}{C}\right) - \frac{c_1 \left(\frac{r}{C}\right)^n}{c_2 \left(\frac{r}{C}\right)^n + 1}\right]. \tag{4.42}$$

where c_1, c_2 and n are constant parameters to be constrained by observations, and the dimensionless parameter C is related to the ratio of m^2 defined at (2.37) and the Hubble rate today.

The compact dynamical systems analysis outlined in the previous section is applied to the Hu-Sawicki model (4.38) or (4.42) for the case $n = 1$. It has been shown that n remains unconstrained by current cosmological data [54] and, therefore, the case $n = 1$ does not compromise generality at this stage. To benefit from simplicity, we set $c_1 = 1$ to facilitate the inversion of the function $f(R)$ for R.

For this case, R can be obtained in terms of the variables as:

$$R = -\frac{C {H_0}^2 (v - 2\,y)}{c_2 (v - y)}\ , \tag{4.43}$$

and Γ is given by:

$$\Gamma \equiv \frac{f'}{f'' R} = \frac{1}{2}\,\frac{v y}{(v - y)^2}\ . \tag{4.44}$$

The expression for Γ associated with this specific model (4.44) is substituted into equations (4.32) - (4.34), and a dynamical systems analysis is performed to obtain the equilibrium points of the system. The equilibria, as well the exact solutions of the scale factor corresponding to the stationary points are combined in Table 4.3.

The Hartman-Grobman theorem is used to assess the stability of these fixed points, where possible. Some points obtained are non-hyperbolic, and in this case we resort to the Center Manifold Theorem.
Below several illustrative orbits in the 3-D phase space (Q, x, v) are presented to show the general behaviour around the stationary points.

4.2.4 Stationary points, stability and exact solutions

For the HS model, when $n = c_1 = 1$, keeping an arbitrary equation of state, w, the fixed points for the entire phase space, as well as the exact solution of the scale factor at each point, are summarized in Table 4.3.

Note that although Table 4.4 includes a stability classification of the fixed points identified for universes dominated by each of radiation, matter and a cosmological constant, the analysis is primarily concerned with a universe dominated by a dust fluid ; $w = 0$. Accordingly, the plots below are all generated for dust universes.

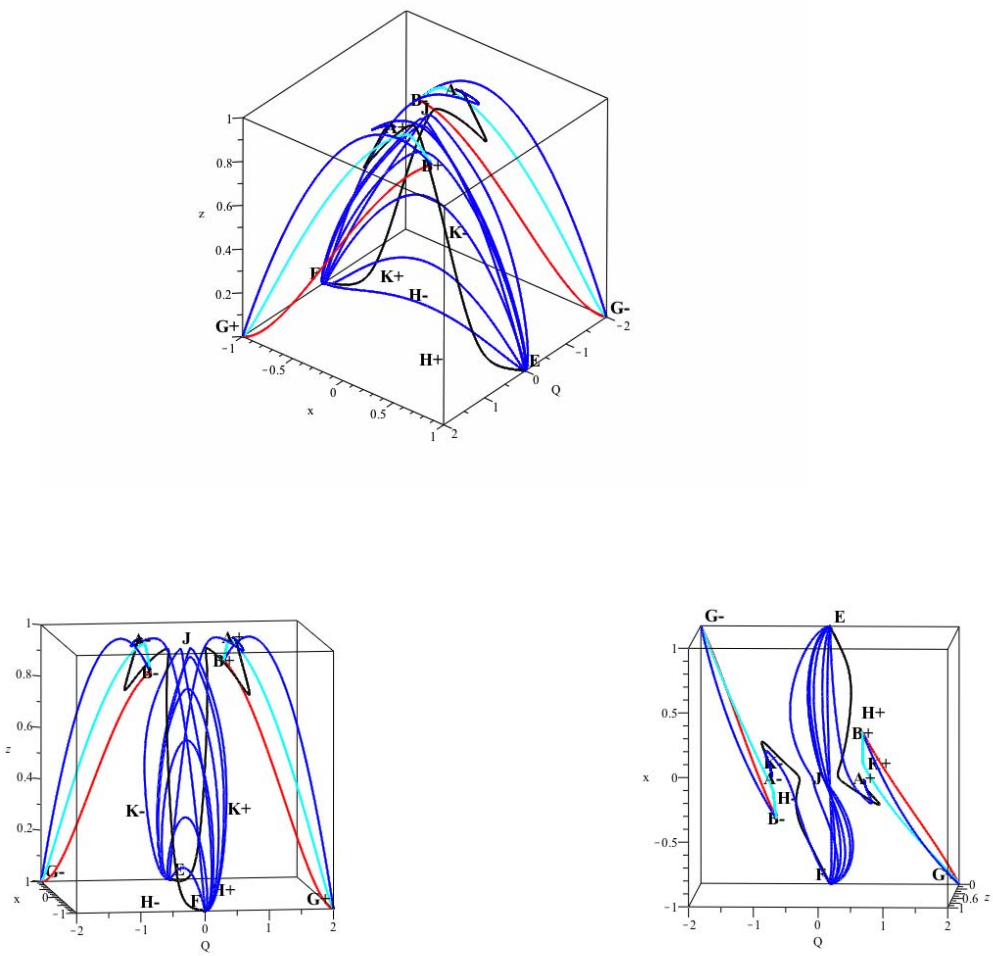

Figure 4.2: The above plots show various angular perspectives of the 3-dimensional compact phase space of the Hu-Sawicki model for $n = 1, c_1 = 1$. What is clear from these illustrative plots is the anti-symmetry between the expanding and contracting sides of the phase space, the $Q = 0$ plane, as well as the fact that orbits can cross this plane, implying the acceptance of universes with bounce behaviour.

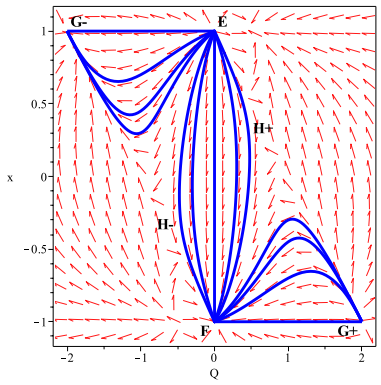

Figure 4.3: Showing the phase plane of the invariant submanifold $v = 0$, corresponding to the plane of universes with zero curvature.

The points for which the v and/or y coordinate is exactly zero make up a subset of fixed points which will appear in the dynamical systems analysis for an arbitrary $f(R)$ analysed in terms of the variables at (4.28), due to the fact that zero values for v and/or y reduce the specific $f(R)$ contribution term, Γ, to zero. We find

the corresponding fixed points for which $v = 0$ that appear in [2] for $f(R) = R + \alpha R^n$.

Point	Coordinate (Q, x, y, v, Ω)	Scale factor evolution, $a(t)$
$\mathcal{A}_\pm$	$\left[\pm\frac{1}{\sqrt{2}}, 0, \frac{1}{2}, 1, 0\right]$	$a(t) = a_0 e^{H_0(t-t_0)}$
$\mathcal{B}_\pm$	$\left[\pm\frac{2}{3}, \pm\frac{1}{3}, 0, \frac{8}{9}, 0\right]$	$a(t) = a_0 e^{H_0(t-t_0)}$
$\mathcal{C}(w=-1)$	$\left[0, \sqrt{\frac{3(w+1)}{1+3w}}, -\frac{2}{1+3w}, 0, -\frac{2}{1+3w}\right]$	$a(t) = a_0$
$\mathcal{D}(w=-1)$	$\left[0, -\sqrt{\frac{3(w+1)}{1+3w}}, -\frac{2}{1+3w}, 0, -\frac{2}{1+3w}\right]$	$a(t) = a_0$
$\mathcal{E}$	$[0, 1, 0, 0, 0]$	$a(t) = a_0$
$\mathcal{F}$	$[0, -1, 0, 0, 0]$	$a(t) = a_0$
$\mathcal{G}_\pm$	$[\pm 2, \mp 1, 0, 0, 0]$	$a(t) = a_0 \left(2H_0(t-t_0) + 1\right)^{\frac{1}{2}}$
$\mathcal{H}_\pm(w \leq \frac{2}{3})$	$\left[\mp\frac{2}{3(w-1)}, \pm\frac{3w-1}{3(w-1)}, 0, 0, -\frac{4}{9}\frac{3w-2}{(w-1)^2}\right]$	$a(t) = a_0 \left(2H_0(t-t_0) + 1\right)^{\frac{1}{2}}$
$\mathcal{J}$	$[0, 0, 1, 1, 0]$	$a(t) = a_0$
$\mathcal{K}_\pm$	$\left[\pm\frac{\sqrt{6}}{3}, 0, \frac{1}{3}, \frac{1}{3}, \frac{2}{3}\right]$	$a(t) = a_0 \left(\frac{3}{2}H_0 \left(t - t_0\right) + 1\right)^{\frac{2}{3}}$

Table 4.3: Each equilibrium point in the phase space has an expanding and collapsing version, denoted by a subscript +/-. Fixed points with $Q = 0$, correspond to static universes. The points $\mathcal{H}_\pm, \mathcal{C}$ and $\mathcal{D}$ depend on the equation of state parameter, w; $\mathcal{H}_\pm$ only lies in the phase space for $-1 \leq w \leq \frac{2}{3}$, and while $\mathcal{C}$ and $\mathcal{D}$ lie in the phase space for all values of $w \leq -1$. For our purposes $-1 \leq w \leq 1$, therefore we only consider the case when $w = -1$ for these points. The points $\mathcal{C}, \mathcal{D}, \mathcal{E}, \mathcal{F}, \mathcal{G}_\pm, \mathcal{H}_\pm$ all lie on the invariant submanifold $v = 0$. Other w dependent fixed points were found, but are not included in this analysis as they only lie within the bounds of the phase space for un-physical values of the equation of state parameter.

Stability

The stability of all the fixed points, save $\mathcal{A}_\pm$, $\mathcal{K}_\pm$ and $\mathcal{J}$, could be inferred using the Hartman-Grobman theorem stated and discussed in Section 3.3.1. The fixed points $\mathcal{A}_\pm$ are non-hyperbolic, so the Center Manifold Theorem was used to determine the stability of $\mathcal{A}_+$[2], and perturbation theory was employed to find the stability near $\mathcal{A}_-$[3].

Non analytic points $\mathcal{K}_+$ and $\mathcal{J}$

Considering the structure of Γ, as expressed in (4.44) in terms of the variables, it is clear that when $v = y$, this term becomes undefined. Thus, analytically, it is not possible to identify and analyse stationary states in the phase space, when this occurs. The matter-like points $\mathcal{K}_\pm$, which lie on the intersection of the $y = v$ and $x = 0$ planes as detailed in [2] is also identified here. The point $\mathcal{J}$ which lies on the $v = y = 1$ surface appears as a saddle, static universe, stationary phase state.

The respective stabilities of these points were inferred by inspection of the behaviour of solutions near each. In particular, the time evolution of the coordinates, when initial conditions were chosen close to the fixed points, were considered. Figures 4.4 and 4.5 are presented to justify the inferred stability of $\mathcal{K}_+$ and $\mathcal{J}$.

When initial conditions are chosen near the point $\mathcal{K}_+$, in the expanding half of the phase space, clear oscillations about this point can be seen, after which the orbit then converges to a nearby attractor. For example the plots below at Figure 4.4 show an orbit converging to the de Sitter attractor $\mathcal{A}_+$ at $Q = \frac{\sqrt{2}}{2}$, $x = 0$, $v = \frac{1}{3}$.

In the case of $\mathcal{J}$, it is especially useful and illustrative to plot orbits in the 3D phase space, presented in Figure 4.5.

[2]The system is significantly less complicated using the finite variables defined in Section 4.3.1 given by (4.50), therefore the flow of the Center Manifold at $\mathcal{A}_+$ is analysed using this coordinate system. Details are in Appendix A

[3]The details of this analysis is included in Appendix A

Point	Eigenvalues of Jacobian	Stability		
		$w=0$	$w=\frac{1}{3}$	$w=-1$
$\mathcal{A}_+$	$\left[0,-\frac{1}{\sqrt{2}},-\frac{1}{\sqrt{2}}-\frac{1}{\sqrt{2}}w\right]$	ATTRACTOR	ATTRACTOR	ATTRACTOR
$\mathcal{A}_-$	$\left[0,\frac{1}{\sqrt{2}},\frac{1}{\sqrt{2}}+\frac{1}{\sqrt{2}}w\right]$	REPELLOR	REPELLOR	REPELLOR
$\mathcal{B}_+$	$\left[-\frac{8}{9},-\frac{1}{9},-\frac{8}{9}-\frac{2}{3}w\right]$	ATTRACTOR	ATTRACTOR	ATTRACTOR
$\mathcal{B}_-$	$\left[\frac{8}{9},\frac{1}{9},\frac{8}{9}+\frac{2}{3}w\right]$	REPELLOR	REPELLOR	REPELLOR
$\mathcal{C}$	$\left[\frac{2}{3}\sqrt{\frac{3(1+w)}{1+3w}},-\frac{2}{3}\sqrt{\frac{3(1+w)}{1+3w}},\frac{1}{3}\sqrt{\frac{3(1+w)}{1+3w}}\right]$	□	□	SADDLE
$\mathcal{D}$	$\left[\frac{2}{3}\sqrt{\frac{3(1+w)}{1+3w}},-\frac{2}{3}\sqrt{\frac{3(1+w)}{1+3w}},-\frac{1}{3}\sqrt{\frac{3(1+w)}{1+3w}}\right]$	□	□	SADDLE
$\mathcal{E}$	$\left[1,\frac{4}{3},\frac{2}{3}\right]$	REPELLOR	REPELLOR	REPELLOR
$\mathcal{F}$	$\left[-\frac{2}{3},-\frac{4}{3},-1\right]$	ATTRACTOR	ATTRACTOR	ATTRACTOR
$\mathcal{G}_+$	$\left[\frac{8}{3},3,\frac{4}{3}-2w\right]$	REPELLOR	REPELLOR	REPELLOR
$\mathcal{G}_-$	$\left[-\frac{8}{3},-3,-\frac{4}{3}+2w\right]$	ATTRACTOR	ATTRACTOR	ATTRACTOR
$\mathcal{H}_+$	$\left[-\frac{8}{9(w-1)},-\frac{3w+7}{9(w-1)},-\frac{6w-4}{9(w-1)}\right]$	SADDLE	SADDLE	SADDLE
$\mathcal{H}_-$	$\left[\frac{3w+7}{9(w-1)},\frac{8}{9(w-1)},\frac{6w-4}{9(w-1)}\right]$	SADDLE	SADDLE	SADDLE
$\mathcal{J}$		SADDLE	SADDLE	SADDLE
$\mathcal{K}_+$		UNSTABLE (SPIRAL)	UNSTABLE	UNSTABLE
$\mathcal{K}_-$		STABLE (SPIRAL)	UNSTABLE	UNSTABLE

Table 4.4: Summarized above is the stability of each stationary state, for equation of state parameters corresponding to dust, radiation and a cosmological constant. $\mathcal{A}_+$ and $\mathcal{A}_-$ are non-hyperbolic; the Center Manifold Theorem and examining the behaviour of small perturbations are used to obtain their stability, respectively. Points $\mathcal{C}$, $\mathcal{D}$ only exist physically in the phase space for $w=-1$, and the eigenvalues for these points for $w=-1$ are all equal to zero. The stability of these points were inferred by inspection; they are self-evidently saddle points. The points $\mathcal{J}$ and $\mathcal{K}_\pm$ lie on the plane $y=v$; for these points Γ, and thus the system, is undefined, therefore there are no analytic eigenvalues for these points. The classification of these points was done by inspection of time evolution plots. For the cases $w=\frac{1}{3},-1$, it was only possible to determine whether or not the points were stable.

Exact solutions

The rate of expansion, H, and the deceleration parameter, q, are related by the following expression:

$$\dot{H}=-(1+q)H^2, \tag{4.45}$$

where $q=-\frac{\ddot{a}a}{\dot{a}^2}$. This relationship can be used to determine the time evolution of the scale factor at an equilibrium point, if the deceleration parameter at that equilibrium point is known. In order to find the value of q at the i^{th} equilibrium point, and therefore the exact solution at that equilibrium point, we need to express q in terms of the compact variables x, y, v, Q, Ω .

It follows, from the Raychaudhuri equation (4.37) and the constraint equations, that

$$q_i=1-\frac{z_i}{Q_i^2}\ . \tag{4.46}$$

For the cases in which $Q\neq 0$, direct integration of (4.45) results in an expression describing the evolution of the scale factor for each equilibrium point of the compact dynamical system. This can be done for the points $\mathcal{A}_\pm, \mathcal{B}_\pm, \mathcal{G}_\pm, \mathcal{H}_\pm$, and $\mathcal{K}_\pm$.

Fixed points with deceleration parameter $q=-1$ represent de Sitter universes, with the scale factor evolving exponentially with time, while fixed points for which $q=1$ represent universes which appear to be "radiation-like"[4], as the scale factor is proportional to the square root of time.

[4]Note that this "radiation-like" behaviour refers to the properties of the curvature fluid; at these points the curvature fluid causes the expansion of the universe to scale with time in the same way that ordinary radiation would: $a(t)\propto\sqrt{t}$, exhibiting

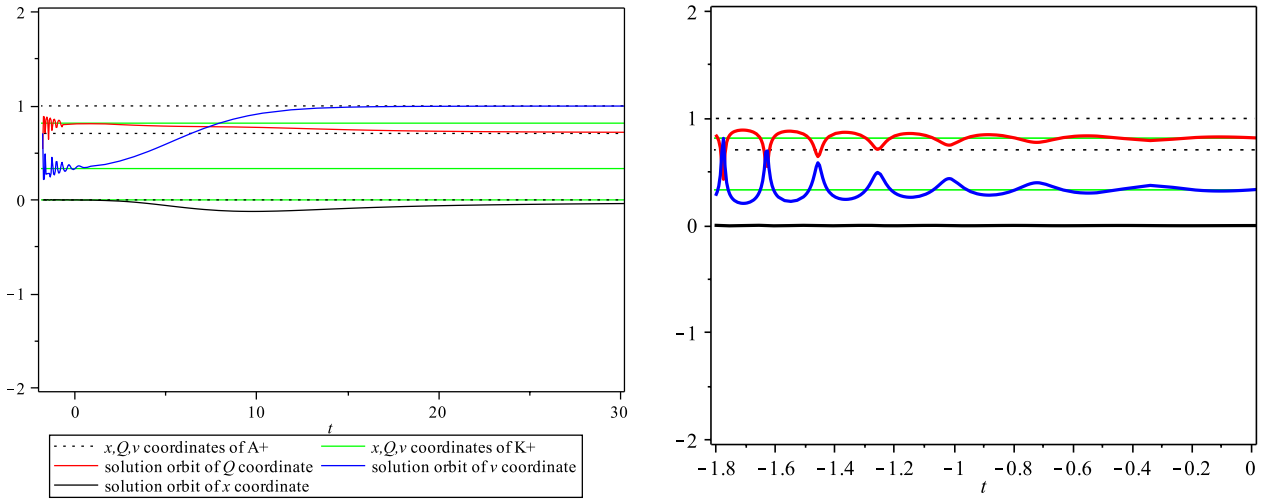

Figure 4.4: The above plots show a time evolution of each compact coordinate x, Q and v, as a solution orbit evolves (backward and forward in time) from a set of initial conditions very close to the stationary state at $\mathcal{K}_+$, when $w = 0$. The vertical axis runs through the various values each of the coordinates may take, and the horizontal axis represents time as the phase space evolves. The figure on the right shows a magnification of the "backward" time evolution. Oscillations, out of phase, of the v and Q coordinates are obvious. These oscillations about the coordinates of $\mathcal{K}_+$ indicate its spiral nature within the phase space on the v-Q plane. The coordinate values of the orbit eventually converge to a stationary phase state corresponding to a de Sitter like attractor, $\mathcal{A}_+$.

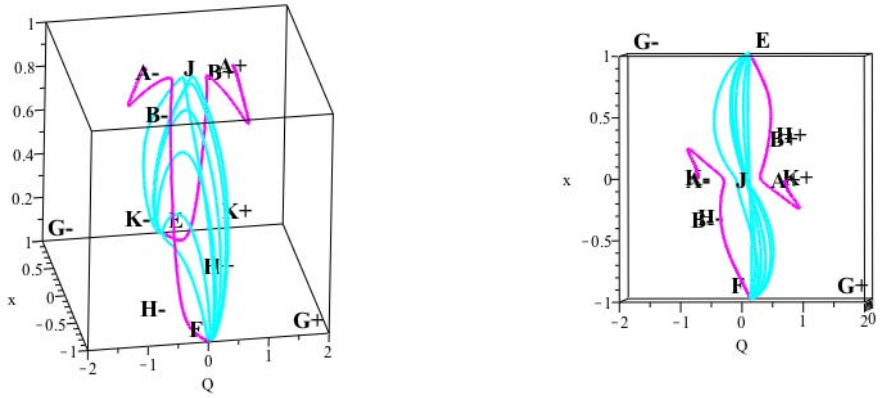

A B

Figure 4.5: For clarity, only a few solution trajectories are featured in the above plot of the phase space, to illustrate the saddle nature of the point $\mathcal{J}$ in a dust dominated universe. The solution orbits presented in boxes A and B all have initial conditions very close to the point $\mathcal{J}$. Each of the cyan orbits begin near the local repeller $\mathcal{E}$, fall toward $\mathcal{J}$ and terminate at the local attractor $\mathcal{F}$. The magenta orbit in the expanding section of the phase space ($Q > 0$) begins at $\mathcal{E}$ and evolves toward the local attractor $\mathcal{A}_+$, a de Sitter point. The magenta orbit originating in the collapsing section of the phase space begins at the local de Sitter repeller state, is pulled toward $\mathcal{J}$ and evolves toward $\mathcal{F}$.

One of the short-comings of the dynamical systems approach to cosmology, as outlined in [11], is that it is possible for the analysis to admit fixed points which correspond to solutions of the dynamical system (as defined, for example, by (4.32)-(4.34)) but *do not* satisfy the cosmological equations. In many cases, constants of integration, which emerge in families of solutions to the cosmological equations, result in additional constraints, which must be satisfied by all physical points of the system. Setting the derivatives of the dynamical variables

"radiation-like" behaviour. From now on we refer to points which fall into this class as "radiation" points, but emphasise that they do not represent universes dominated by ordinary radiation, but by a curvature fluid whose properties are similar to ordinary radiation.

equal to zero;

$$x' = F(x) = 0 \tag{4.47}$$

implies either of

$$F(x) = 0 \tag{4.48}$$

or

$$x' = 0 \Rightarrow x = constant \tag{4.49}$$

Solutions to (4.47) may result from solving either of the equations (4.48) or (4.49), where the latter now represents a set of constraints imposed on the system [11].

For this reason, it is important to verify that the solutions obtained satisfy the cosmological equations.

The points $\mathcal{C}, \mathcal{D}, \mathcal{E}, \mathcal{F}, \mathcal{J}, \mathcal{K}$, all lie on the non-invariant $Q = 0$ submanifold, describing solutions for which the scale factor has no time dependence, and so represent static universes.

For the HS model, for $n = 1, c_1 = 1$, we find that the non-static, analytic fixed points belong to one of two scale factor solutions : a radiation-like expansion and a de Sitter like expansion. The fact that other cosmological evolutions do not appear as stationary phase states does not imply that this model does not allow them, it may be that the choice of variables places analytic limitations on what can appear as stationary solutions.

The non-invariant submanifold $Q = 0$ divides the phase space into expanding and collapsing universes.

The expanding versions of $\mathcal{A}$ and $\mathcal{B}$ are stable equilibrium phase states, and correspond to de Sitter scale factor evolutions. Several interesting orbits exist, which originate near an unstable "radiation-like" point, for example $\mathcal{G}_+$ or $\mathcal{H}_+$, and evolve toward one of these accelerated expansion points.

In Figure 4.6 four such orbits are presented.

Extremely fine tuned initial conditions are required for a trajectory initialised near the non-analytic, unstable expanding matter point $\mathcal{K}_+$ to evolve toward either of the de Sitter equilibria. It is more natural for trajectories to begin near one of the radiation like points, $\mathcal{G}_+$ or $\mathcal{H}_+$ and asymptote toward an exponentially expanding state. This model phenomenon will be clarified in Section 4.4.

4.3 Non-compact phase space analysis of an HS model

4.3.1 Finite Analysis

Integrating the compact dynamical system at (4.32)−(4.34), it is possible to obtain an expansion history (values of the cosmological parameters at all times in the universe) for the HS model. This will enable a quantitative *and* qualitative appreciation for the potential behaviour of a universe governed by the HS model for modified gravity. From such an integration, we are able to see how well the HS model compares to the Concordance Model and its predictions for parameters such as the Hubble parameter, H, the deceleration parameter, q, the total density, Ω, the equation of state, w, etc. It is interesting to pick initial conditions near one of the stationary phase states obtained in the dynamical systems analysis, and watch the behaviour of the resulting expansion history.

The orbits shown in Figure 4.6 serve as starting points for such an investigation − orbits beginning near an unstable radiation like state and evolving toward a stable de Sitter expansion phase − because the chronological order of these phase states resemble the history of our universe as we observe it today. Determining what happens between these states is essential to gaining insight into the behaviour of the HS model as a theory for gravity.

Above, several stationary points were identified using a compact dynamical systems analysis, which include points pulled in from infinity to sit in the phase space compactified by the normalization D defined by (4.29). However, it turns out that four of these fixed points, $\mathcal{A}_\pm, \mathcal{B}_\pm, \mathcal{G}_\pm$ and $\mathcal{H}_\pm$, are *finite* and exist even in a *non-compact* phase space. As mentioned above, $\mathcal{A}_\pm$ and $\mathcal{B}_\pm$ are equilibria that have scale factors evolving

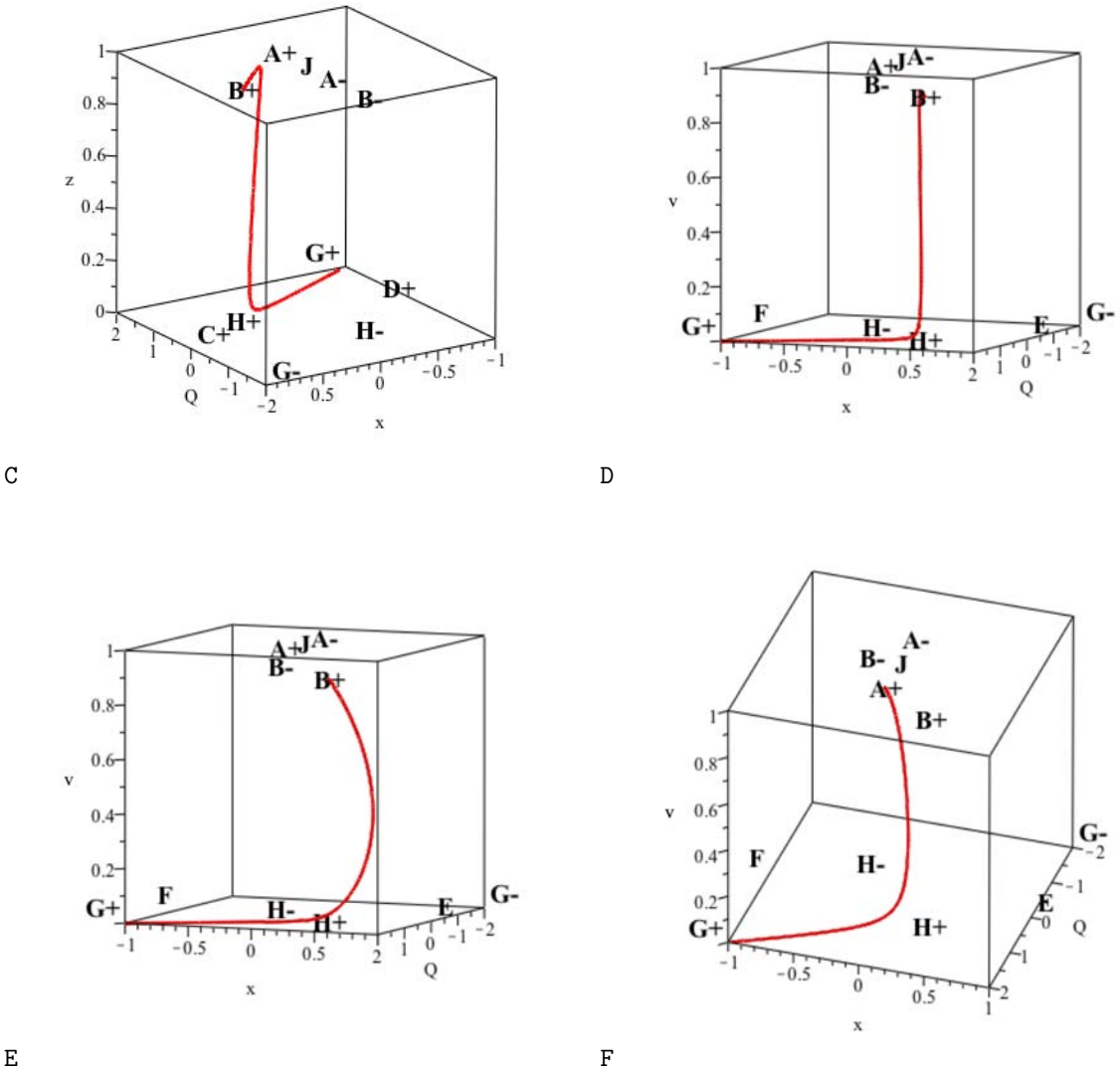

Figure 4.6: Above are four example solution orbits. The orbits represented at C, D and E all begin near the radiation like repeller point $\mathcal{G}_+$, are pulled toward the saddle radiation like point $\mathcal{H}_+$ and eventually evolve toward the de Sitter like attractor $\mathcal{B}_+$. C shows an orbit which after passing by $\mathcal{H}_+$ proceeds toward the stable de Sitter equilibrium point $\mathcal{A}_+$, after which, the trajectory falls away, and is pulled to the de Sitter fixed point $\mathcal{B}_+$. The orbit represented at F also begins near $\mathcal{G}_+$, but evolves towards the de Sitter point, $\mathcal{A}_+$. The existence of these orbits show that this model allows solutions which have a late time de Sitter expansion, which can produce expansion histories which look like a Dark Energy fluid is dominating the universe at late times.

exponentially with time, and each of $\mathcal{G}_\pm$ and $\mathcal{H}_\pm$ resemble the scale factor evolution of a "radiation-like" era. The fact that these four points exist in the non-compact phase space implies that a non-compact analysis is sufficient to study the expansion behaviour of a universe evolving between them. It is, therefore, convenient to make a simple change of coordinates, to facilitate this analysis to study only the finite stationary points. We make use of the following non-compact coordinates:

$$\tilde{x} = \frac{\dot{f}'}{f'}\frac{1}{H}, \qquad \tilde{v} = \frac{1}{6}\frac{R}{H^2}, \qquad \tilde{y} = \frac{1}{6}\frac{f}{f'}\frac{1}{H^2}, \qquad \tilde{\Omega}_m = \frac{1}{3}\frac{\rho_m}{f'}\frac{1}{H^2}. \tag{4.50}$$

The coordinate transformation between compact and non-compact variables is as follows:

$$\tilde{x} = 2\frac{x}{Q}, \qquad \tilde{u} = \frac{u}{Q^2}, \tag{4.51}$$

where $\tilde{u}$ represents all of $\tilde{y}, \tilde{v}$ and $\tilde{\Omega}$ in turn.

The dimensionality of the dynamical system has been reduced as there is no dynamical variable which represents the normalized volume expansion. The Friedmann equation at (4.22) can be reshuffled to give a constraint equation in terms of the above variables:

$$1 = \tilde{\Omega} + \tilde{v} - \tilde{x} - \tilde{y}\ . \tag{4.52}$$

Since we are interested in integrating the system with respect to redshift, the differential equations corresponding to the non-compact dynamical system can be obtained by differentiating the non-compact variables (4.50) with respect to redshift, z:

$$\frac{d\tilde{x}}{dz} = \frac{1}{(z+1)}\left[(-1+3\,w)\,\tilde{\Omega} + \tilde{x}^2 + (1+\tilde{v})\,\tilde{x} - 2\tilde{v} + 4\tilde{y}\right], \tag{4.53}$$

$$\frac{d\tilde{y}}{dz} = -\frac{1}{(z+1)}\left[\tilde{v}\tilde{x}\Gamma - \tilde{x}\tilde{y} + 4\,\tilde{y} - 2\,\tilde{y}\tilde{v}\right], \tag{4.54}$$

$$\frac{d\tilde{v}}{dz} = -\frac{\tilde{v}}{(z+1)}\left[(\tilde{x}\Gamma + 4 - 2\,\tilde{v})\right], \tag{4.55}$$

$$\frac{d\tilde{\Omega}}{dz} = \frac{1}{(z+1)}\left[\tilde{\Omega}\ (-1+3\,w + \tilde{x} + 2\,\tilde{v})\right], \tag{4.56}$$

where Γ is still given by (4.44), due to the fact that the relationship between v and y, and $\tilde{v}$ and $\tilde{y}$ is preserved during the coordinate transformation from compact to non-compact variables. The above equations have been used to aid a later study of the geodesic deviation equation in $f(R)$ gravity, [22].

In terms of the dynamical variables, we also have an expression for the dimensionless expansion rate of the universe, h,

$$\frac{dh}{dz} = \frac{h}{z+1}\left[(2-\tilde{v})\right], \tag{4.57}$$

where $h = \frac{H}{H_0}$.

The four interesting *non-boundary* points and their coordinates in the compact and non-compact phase spaces are tabulated below in Table 4.5, along with their stability and their scale factor evolution, in a universe dominated by dust. The purpose of this finite analysis is to produce an expansion history for the particular HS model under investigation with which the ΛCDM model can be compared. It is, thus, only important to consider the *expanding* version of the fixed points. That is to say, we need only look at the non-compact fixed points corresponding to the *expanding* versions of the compact fixed points obtained earlier. These points are presented in Table 4.5.

Point	Non-Compact $(\tilde{x},\tilde{y},\tilde{v},\tilde{\Omega})$	Compact (Q,x,y,v,Ω)	Stability $(w=0)$	Scale factor solution
$\tilde{\mathcal{A}}_+$	$[0,1,2,0]$	$[\frac{\sqrt{2}}{2},0,\frac{1}{2},1,0]$	ATTRACTOR	$a(t)=a_0e^{H_0(t-t_0)}$
$\tilde{\mathcal{B}}_+$	$[1,0,2,0]$	$[\frac{2}{3},\frac{1}{3},0,\frac{8}{9},0]$	ATTRACTOR	$a(t)=a_0e^{H_0(t-t_0)}$
$\tilde{\mathcal{G}}_+$	$[-1,0,0,0]$	$[2,-1,0,0,0]$	REPELLOR	$a(t)=a_0\left(2H_0(t-t_0)+1\right)^{\frac{1}{2}}$
$\tilde{\mathcal{H}}_+$	$[1-3w,0,0,2-3w]$	$\left[\frac{2}{3(w-1)},\frac{3w-1}{3(w-1)},0,0,-\frac{4}{9}\frac{3w-2}{(w-1)^2}\right]$	SADDLE	$a(t)=a_0\left(2H_0(t-t_0)+1\right)^{\frac{1}{2}}$
$\tilde{\mathcal{K}}_+$	$\left[0,\frac{1}{2},\frac{1}{2},1\right]$	$\left[\frac{\sqrt{6}}{3},0,\frac{1}{3},\frac{1}{3},\frac{2}{3}\right]$	UNSTABLE SPIRAL	$a(t)=a_0\left(\frac{3}{2}H_0\left(t-t_0\right)+1\right)^{\frac{2}{3}}$

Table 4.5: There exist two stable phase states for which the scale factor increases exponentially into the future; $\tilde{\mathcal{A}}_+$ and $\tilde{\mathcal{B}}_+$. It follows that these states can be associated with the late time accelerated expansion of the universe attributed to Dark Energy. The scale factor evolution of the points, $\tilde{\mathcal{G}}_+$ and $\tilde{\mathcal{H}}_+$ depend on the square root of time, and therefore represent "radiation dominated" -like universes. The non-analytic matter point is included, as it also appears in the non-compact phase space on the plane $\tilde{y}=\tilde{v}$.

4.4 Expansion History for the Hu-Sawicki model, with $n=1$, $c_1=1$

To reiterate, the purpose of the finite analysis is to aid a numerical integration of the universe described by this model between two, preferably finite, points. This expansion history can then be compared to the ΛCDM model to ascertain whether this model behaves well at solar systems scales as well as in the cosmological regime. The success of this model in matching ΛCDM depends sensitively on the selection of the parameters which describe it.

4.4.1 Initial conditions

The expansion history for a universe governed by the HS model with $n=1$ and $c_1=1$ is calculated by performing an integration of the differential equations representing the dynamical system (4.53) − (4.56). The model was parametrized based on the considerations of [32] wherein fiducial restrictions were placed on the relationship between c_1 and c_2 [32]:

$$\frac{c_1}{c_2}\approx 6\frac{\Omega_\Lambda}{\Omega_m}, \tag{4.58}$$

to control the ratio of matter density to the cosmological constant via the parameters c_1 and c_2. As done in [32], the following values for the densities at the present epoch are used [32]:

$$\Omega_\Lambda=0.76, \qquad \Omega_{m0}=0.24\ . \tag{4.59}$$

As shown previously in Section 2.5, the initial values (at the present epoch) for the Ricci scalar, R, and the derivative of the function, $f'(R)\equiv f_R$, can be given by [32]

$$\begin{aligned} R_0&\approx m^2\left(\frac{12}{\Omega_{m0}}-9\right),\\ f_{R0}&\approx 1-g_{R0}=1-n\frac{c_1}{c_2^2}\left(\frac{12}{\Omega_{m0}}-9\right)^{-n-1}, \end{aligned} \tag{4.60}$$

for $|g_{R0}|\ll 1$. Substituting (4.59) into (4.60), we have:

$$R_0=41m^2=41CH_0^2. \tag{4.61}$$

In order to calculate the initial values for the dynamical variables $(\tilde{x},\tilde{y},\tilde{v},\tilde{\Omega})$, expressions for each are required in terms of the quantities q, r and h (with r and h defined by (4.39)), for which the initial values can

be obtained by using (4.60) and (4.59). With $n = 1, c_1 = 1$ we obtain:

$$f'(r_0) = \frac{c_2 r_0 (c_2 r_0 + 2C)}{(c_2 r_0 + C)^2}, \tag{4.62}$$

$$r_0 = 6(1 - q_0)h_0^2, \tag{4.63}$$

$$\Rightarrow q_0 = \frac{6h_0^2 - r_0}{6h_0^2}. \tag{4.64}$$

It follows that, in terms of the Ricci scalar, the Hubble parameter, the deceleration parameter and c_2 and C, the dynamical variables are :

$$\tilde{v}_0 = 1 - q_0 = \frac{r_0}{6h_0^2}, \tag{4.65}$$

$$\tilde{\Omega}_0 = \frac{\Omega_{m0}(z_0 + 1)^3}{h_0^2 f'(r_0)} = \frac{\Omega_{m0}(r_0 c_2 + C)^2}{h_0^2 r_0 c_2 (r_0 c_2 + 2C)}(z_0 + 1)^3, \tag{4.66}$$

$$\tilde{y}_0 = \frac{1}{6}\frac{r_0(r_0 c_2 + C)}{h_0^2(r_0 c_2 + 2C)}, \tag{4.67}$$

$$\tilde{x}_0 = \Omega_0 + v_0 - y_0 - 1 = \frac{\Omega_{m0}(r_0 c_2 + C)^2}{h_0^2 r_0 c_2 (r_0 c_2 + 2C)}(z_0 + 1)^3 + \frac{r_0}{6h_0^2} - \frac{1}{6}\frac{r_0(r_0 c_2 + C)}{h_0^2(r_0 c_2 + 2C)} - 1 \ . \tag{4.68}$$

Ω_0 denotes the initial value of the dynamical variable Ω, and is not to be confused with Ω_{m0}, which represents the matter density parameter of the universe at the present epoch. Using (4.58) and (4.60), and the fact that $m^2 \equiv CH_0^2$, we find the following values for the parameters:

$$\begin{aligned} n &= 1 \ , \\ c_1 &= 1 \ , \\ c_2 &= \frac{1}{19} \ , \\ C &= 0.24 \ , \end{aligned} \tag{4.69}$$

and the following initial values:

$$\begin{aligned} H_0 = 67.8 \Rightarrow h_0 &= \frac{H}{H_0} = 1 \ , \\ R_0 = 45232.906 \Rightarrow r_0 &= \frac{R_0}{H_0^2} = 9.840 \ , \\ \Rightarrow \tilde{x}_{0,HS} &= -0.339 \ , \\ \tilde{y}_{0,HS} &= 1.246 \ , \\ \tilde{v}_{0,HS} &= 1.640 \ , \\ \tilde{\Omega}_{0,HS} &= 0.267 \ . \end{aligned} \tag{4.70}$$

The above set of coordinates correspond to the *present epoch*, $\mathbf{z_0 = 0}$, as calculated from the parameter values and constraints outlined in [32]. We can obtain the compact version of these coordinates by obtaining the Q coordinate from the constraint equations for the compact system in terms of the non-compact variables using

the coordinate transformations at (4.51):

$$\begin{aligned} 1 &= \Omega + v + x^2 \\ &= \tilde{\Omega}Q^2 + \tilde{v}Q^2 + \left(\frac{\tilde{x}^2}{2}\right)^2 Q^2. \end{aligned} \tag{4.71}$$

Substituting the initial values for the non-compact variables at (4.70) into the above relation and solving for Q, the values for the present epoch in the compact phase space are found to be:

$$Q_{0,HS} = 0.719, \quad x_{0,HS} = -0.122, \quad y_{0,HS} = 0.644, \quad v_{0,HS} = 0.847, \quad \Omega_{0,HS} = 0.138\ . \tag{4.72}$$

Below, in Figure 4.7, an orbit in the 3D *compact phase space* is presented, which has its initial values at (Q_0, x_0, v_0) as given by (4.72).

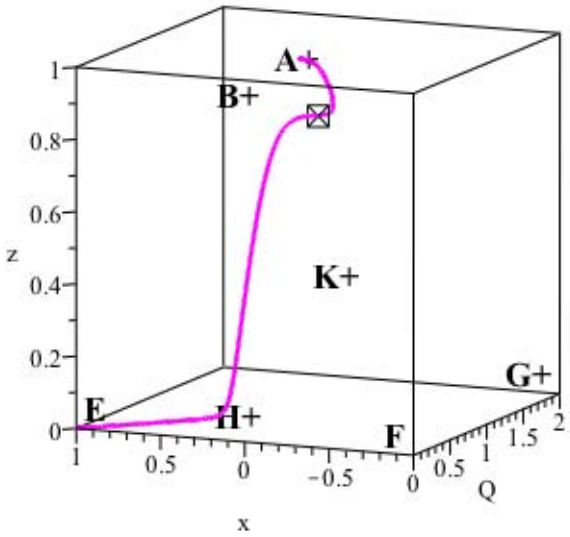

Figure 4.7: The fixed points represented by $\mathcal{A}_+$, $\mathcal{B}_+$, $\mathcal{G}_+$, $\mathcal{H}_+$ and $\mathcal{K}_+$ in the above plot correspond to the compact fixed points given in Table 4.3. The matter point $\mathcal{K}_+$ lies on the plane $y = v$ for which Γ is undefined. The crossed square indicates the point which corresponds to the present epoch as given by (4.72), *today* ($z_0 = 0$), for the model defined by the parameters defined in [32]. It can be seen that this point is close to the de Sitter stationary solution $\mathcal{A}_+$. From ⊠ the orbit evolves forward in time toward $\mathcal{A}_+$. In its past, it passed by the unstable radiation-like stationary state, $\mathcal{H}_+$. Preceding the point $\mathcal{H}_+$, the orbit evolves from the unstable static universe phase state $\mathcal{E}$.

4.4.2 Comparing the Hu-Sawicki Model ($n = 1, c_1 = 1$) with ΛCDM

Figures 4.8 - 4.10 show the redshift evolution of the dimensionless Hubble parameter, the deceleration parameter and the matter density parameter, for the specific HS model considered above, in comparison with a ΛCDM model parametrized by the same values for Ω_m and Ω_Λ as above, i.e. $z_0 = 0$ or "today".

Hubble parameter, h

The dimensionless Hubble rate for the ΛCDM model is givel by:

$$h(z) = \sqrt{\Omega_{m0}(1+z)^3 + \Omega_\Lambda}\ . \tag{4.73}$$

and is compared to the solution of the differential equation for $h(z)$ given by (4.57).

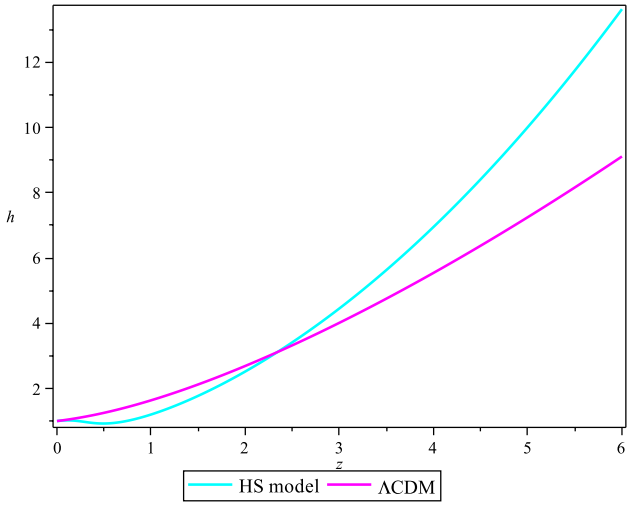

Figure 4.8: The dimensionless Hubble parameter for ΛCDM given by equation (4.73) compared with the dimensionless Hubble rate obtained from the integration of the equations extracted from the non-compact dynamical systems analysis (the solution to the dynamical system (4.53) −(4.57)). At very low redshifts, the two models coincide for a short interval, but after around $z = 0.05$ they deviate substantially.

Deceleration parameter, q

The deceleration parameter for the ΛCDM model is given by the following expression:

$$q = \frac{1}{H^2}\left(\frac{1}{2}\Omega_{m0}(1+z)^3 - 2\Omega_\Lambda\right), \tag{4.74}$$

where as the deceleration parameter calculated for this specific HS model is given in terms of the dynamical variables as

$$q = 1 - v. \tag{4.75}$$

Matter density, ρ_m

We also compare the matter density as calculated by the integration of HS model, given by the dynamical variable, Ω,

$$\rho_{m,DS} = 3\Omega f' H^2, \tag{4.76}$$

with the matter density given by the ΛCDM critical density;

$$\rho_{m,\Lambda CDM} = \Omega_{m0}(1+z)^3. \tag{4.77}$$

Effective Dark Energy equation of state, w_{DE}

It is interesting to consider the redshift evolution of the Dark Energy equation of state parameter, w_{DE}. We can interpret the modified Friedmann equation as being composed of a matter density term and an *effective*

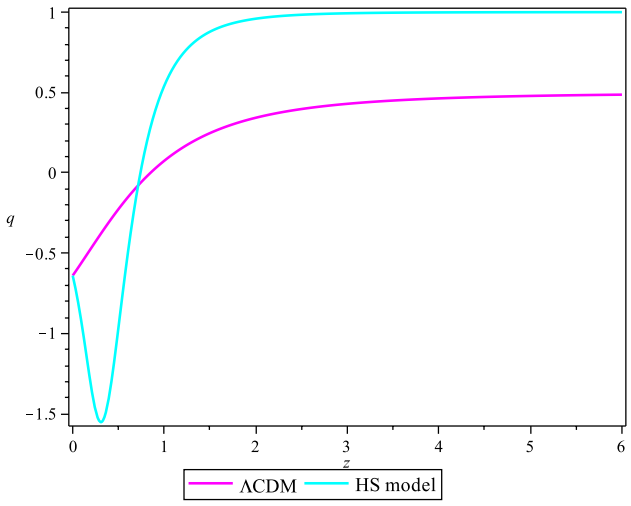

Figure 4.9: The deceleration parameter for ΛCDM given by equation (4.74) is compared with the deceleration parameter determined by the solution of the dynamical system at (4.53) −(4.57), given by equation (4.75). The deceleration parameter determined by this specific HS model supports late time acceleration as well as a stabilised deceleration at higher redshifts. However, there is a large discrepancy in the values for q predicted by the HS model and that predicted by ΛCDM for this choice of parameters.

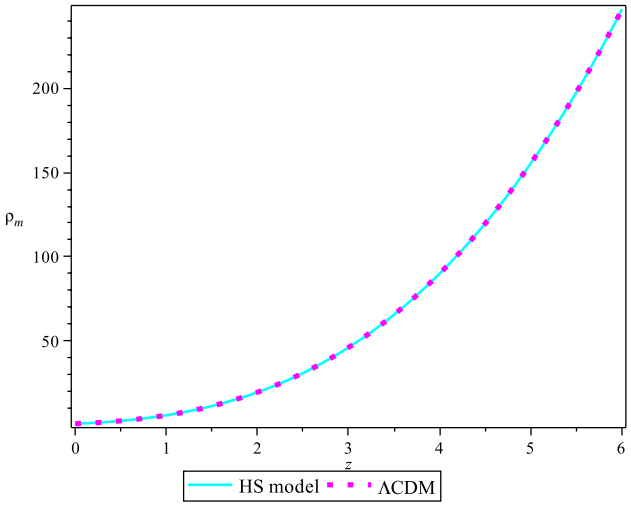

Figure 4.10: Plotting equations (4.76) and (4.77) to compare the matter density redshift evolution shows excellent agreement between the dynamical systems analysis results and the matter density parameter.

dark energy density term:

$$H^2 = \frac{\rho_m}{3f'} + \frac{R}{6} - \frac{1}{6}\frac{f}{f'} - H\frac{\dot{f}'}{f'}$$
$$\Rightarrow 3H^2 = \frac{\rho_m}{f'} + 3H^2\,[v - y - x] = \frac{\rho_m}{f'} + \rho_{DE,eff}\ . \tag{4.78}$$

We can, therefore, say

$$\rho_{DE,eff} = 3H^2 - \frac{\rho_m}{f'} = 3H^2[v - y - x]. \tag{4.79}$$

Toward the construction of a total equation of state parameter from the effective dark energy (or *curvature*) density, we can use the flat ΛCDM Raychaudhuri equation to obtain an expression for the effective dark energy pressure as follows, assuming a flat universe, such that the total energy density is equal to the critical density;

$\rho = \frac{3H^2}{8\pi G}$, ($\rho_{tot} = \rho_c, P_{tot} = P_{DE} + P_m = P_{DE}$):

$$\frac{\ddot{a}}{a} = -\frac{8\pi G}{6}(\rho_{tot} + 3P_{tot}) \quad \text{(recall } c = 8\pi G = 1\text{)}$$
$$2\frac{\ddot{a}}{a} = -H^2 - P_{tot}$$

Note that

$$\frac{\ddot{a}}{a} = -\left(-\frac{\ddot{a}a}{\dot{a}^2}\right)\left(\frac{\dot{a}^2}{a^2}\right) = -qH^2 \Rightarrow -2qH^2 = -H^2 - P_{tot}$$
$$\Rightarrow P_{tot} = H^2(2q - 1),$$

expressed in terms of the dynamical variables is

$$P_{tot} = P_{DE} = H^2(1 - 2v). \tag{4.80}$$

The total equation of state is then constructed by calculating:

$$w_{total} = \frac{P_{total}}{\rho_{total}} = \frac{P_{tot}}{\rho_m + \rho_{DE,eff}}. \tag{4.81}$$

Figure 4.11 shows the behaviour of the total equation of state parameter. It is interesting to note that this total equation of state parameter asymptotes toward the value of $w = \frac{1}{3}$, indicating a universe which is dominated, for most of its history, by a curvature fluid exhibiting "radiation-like" behaviour , and only *now*, at *very* low redshifts does a change in the form of the dominant energy density take place. This result is counterintuitive, owing to the fact that the entire analysis was performed with respect to a duct only universe. However, it is consistent with the dynamical systems analysis which have unstable radiation like phase states from which the corresponding solution orbit begins. This model produces a late time negative equation of state which is consistent with the dynamical systems analysis showing an approach toward a universe having scale factor which evolves exponentially with time.

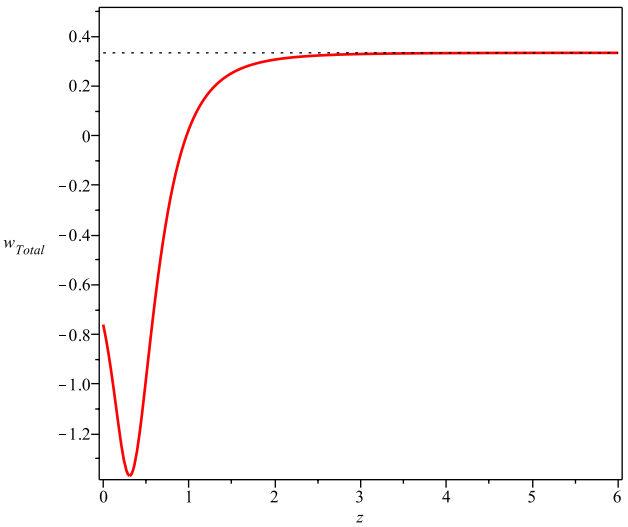

Figure 4.11: Above is the redshift evolution of the total equation of state parameter determined by the HS model. It exhibits odd behaviour; at high redshifts it tends towards a constant value of $\frac{1}{3}$ indicating radiation domination-like behaviour, even though the entire analysis was performed assuming a dust filled universe of $w = 0$. At low redshifts it decreases sharply to indicate the domination of a fluid with negative pressure, which reaches a minimum at -1.37 and begins to increase towards the present epoch to about -0.76. This is consistent with the dynamical systems analysis which shows an early time radiation-like repeller, no matter point, and a late time stable de Sitter phase state, as a result of the fluid with equation of state $w \approx -0.76$.

However, this result is not consistent with idea that the HS model approximation holds throughout the expansion history of the universe, as it predicts that a radiation fluid energy density dominates even at relatively low redshifts. This is a highly unsatisfactory match to observations and, of course, ΛCDM predictions. This result is specific to the model considered, where $n = 1, c_1 = 1$.

Choosing the initial parameter values to be exactly equal to their ΛCDM values today ($z_0 = 0$) is what compromises the agreement between this Hu-Sawicki model and the ΛCDM model. To obtain a better match, an appropriate adjustment of these initial values from their corresponding ΛCDM values is required.

In order to understand why this is so, consider a plot of the correction $g(R)$ generated by the model with initial values specified at (4.70) for $\mathbf{z_0} = \mathbf{0}$, i.e. the ΛCDM values corresponding to "today", in Figure 4.12.

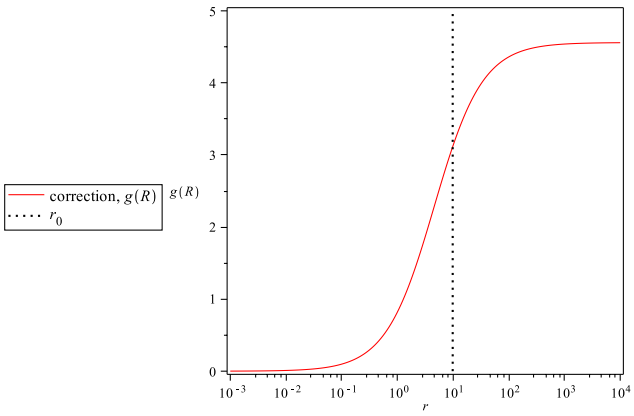

Figure 4.12: Showing the behaviour of the correction. To fulfil its purpose, $g(R)$ is constructed to tend toward zero at low curvature in order to be compatible with GR, which is very well tested at solar system scales, and it should approach a constant value at higher curvatures to mimic the observed cosmological constant behaviour, which is well described, so far, by the ΛCDM model. The plateau of constant $g(R)$ offers a simulated cosmological constant term to the gravitational Lagrangian. The dotted black line indicates the initial value of the Ricci scalar, $R/H_0^2(z = 0)$.

In order for the model investigated to mimic ΛCDM behaviour, that is, exhibit a GR+*cosmological constant* nature, the initial value of the Ricci scalar should lie on the plateau corresponding to a constant value of $g(R)$. However, for the specific model and density parameters above, the initial value of R/H_0^2 at $z_0 = 0$, the present epoch, is 9.84 as stated in (4.70). This value of R/H_0^2 is not high enough to place the correction *initially* on the plateau, and therefore it does not allow the model ($n = 1, c_1 = 1$) to mimic ΛCDM behaviour. In fact, as can be seen in Figure 4.13, the Ricci scalar determined by this model, for initial parameter values given by (4.70), *decreases* with redshift. This indicates that integrating from $z_0 = 0$ only drives the value of $g(R)$ further away from its ΛCDM plateau limit.

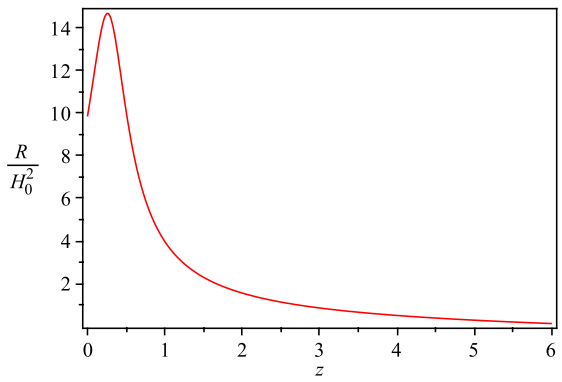

Figure 4.13: A plot of the behaviour of the Ricci scalar with redshift.

4.4.3 Initial conditions at $z_0 = 20$

To remedy this, we can choose initial values which increase the initial value of r so that it lies comfortably on the plateau of $g(R)$, representing a model which, at high r, resembles a version of ΛCDM. To begin, for example, we can calculate the values of the parameters as calculated by ΛCDM at $z_0 = 20$, which, after numerical experimentation, was found to be sufficiently high for our purposes, as can be seen from Figure 4.14. In this

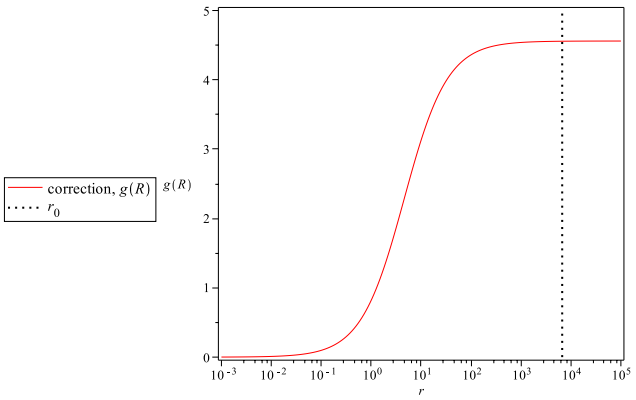

Figure 4.14: Clearly, the initial value of $g(R)$ sits on the constant valued plateau of $g(R)$ which represents a simulated cosmological constant.

case, the initial values for the Ricci scalar, R_0 and the non-compact dynamical variables are :

$$\begin{aligned} h_0 &= \frac{H}{H_0} = 47.153 \ , \\ r_0 &= \frac{R_0}{H_0^2} = 6677.040 \ , \\ \tilde{x}_{0,HS} &= 0.0 \ , \\ \tilde{y}_{0,HS} &= 0.500 \ , \\ \tilde{v}_{0,HS} &= 0.501 \ , \\ \tilde{\Omega}_{0,HS} &= 0.999 \ . \end{aligned} \tag{4.82}$$

The above initial values are extremely close to the matter point $\mathcal{K}_+$, which is consistent with the fact that, at higher redshifts, we expect the dust fluid will dominate the equation of state of the universe. To illustrate this point, the solution trajectory with initial values given by (4.82) is presented in Figure 4.15.

At this point, it is worth noting that the value of $z_0 = 20$ is sufficiently high in redshift to begin the integration of the dynamical system. As we increase redshift, the values of the coordinates tend closer and closer to the matter point $\mathcal{K}_+$, more and more quickly, to such an extent that it makes little difference whether we begin at $z = 1000$ or $z = 20$, as we have chosen. Figure 4.16 demonstrates this fact, showing the dynamical variables as a function of redshift. The asymptote of the variables toward their respective matter point, $\mathcal{K}_+$, coordinates is obvious.

To demonstrate the effects of placing the initial value of the correction initially on its function's plateau, the corresponding plots of the dimensionless Hubble parameter, the deceleration parameter and the equation of state parameter is presented.

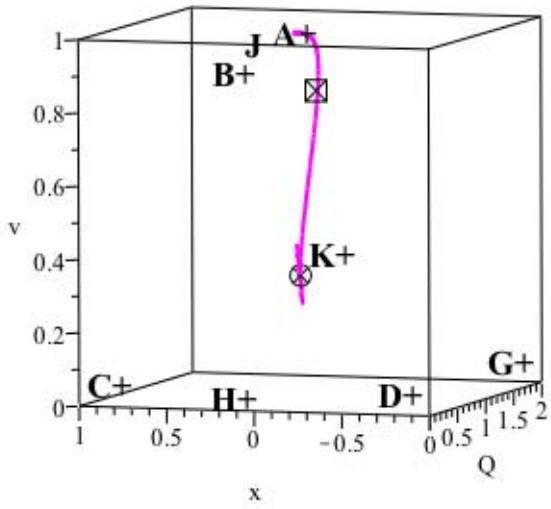

Figure 4.15: The above 3D plot shows the solution trajectory of the compact dynamical systems equations, integrated from the initial values specified at (4.82) for $z_0 = 20$. The crossed circle symbol represents the starting point ($z_0 = 20$) and the crossed square symbol represents the coordinate values at the present epoch ($z_0 = 0$). The fixed point $\mathcal{K}_+$ represents the matter fixed point at $(x, y, v, \Omega) = (0, \frac{1}{2}, \frac{1}{2}, 1)$. The fixed point $\mathcal{A}_+$ represents a de Sitter point. This trajectory clearly begins extremely close to the matter point, is affected by the spiral nature of the neighbourhood of $\mathcal{K}_+$ on the Q - v plane and then evolves neatly toward the de Sitter point. This shows an expansion evolution which is similar to ΛCDM, in that it evolves from a state which is matter dominated to a state which is filled with a fluid causing exponentially accelerated late time expansion.

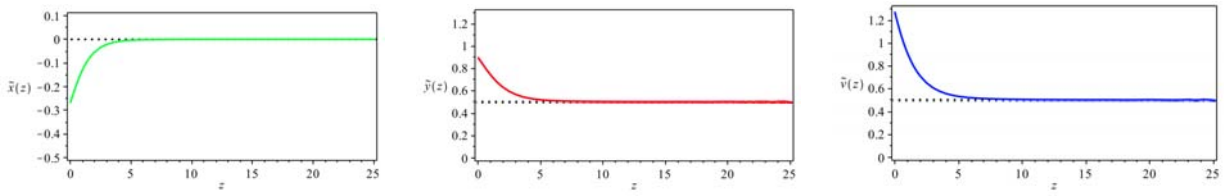

Figure 4.16: The $(\tilde{x}, \tilde{y}, \tilde{v})$ coordinates of the matter points, $\mathcal{K}_+$ are $\left(0, \frac{1}{2}, \frac{1}{2}\right)$. The difference between these values and the initial values of the dynamical variables $\tilde{x}, \tilde{y}$ and $\tilde{v}$ is too small to resolve at a redshift greater than 20. We therefore assert that beginning the integration at this redshift is sufficient to determine the behaviour of this model in the ΛCDM regime.

It is clear that placing the correction $g(R)$ *initially* on the constant valued plateau permits the specific HS model analysed to mimic the ΛCDM model relatively well. By doing this, we have corrected the asymptote of the equation of state from $\frac{1}{3}$ to 0, we have managed to simulate the Hubble parameter, h, of the ΛCDM model very closely, and there is an improvement in the early time behaviour of the deceleration parameter. From these results it can be concluded that the HS model considered here ($n = 1, c_1 = 1$) can produce a very good simulation of the ΛCDM model, however, this occurs at the expense of the present ΛCDM values of q, h and r. In order to obtain the desired behaviour; for the cosmology to be dominated by a dust fluid in the past, the values of $q_{\Lambda CDM}$, $h_{\Lambda CDM}$ and $r_{\Lambda CDM}$ corresponding to the present epoch ($z = 0$) can not be used as starting values for the integration. These parameters must be adjusted to enable $g(R)$ to initially assume its plateau value.

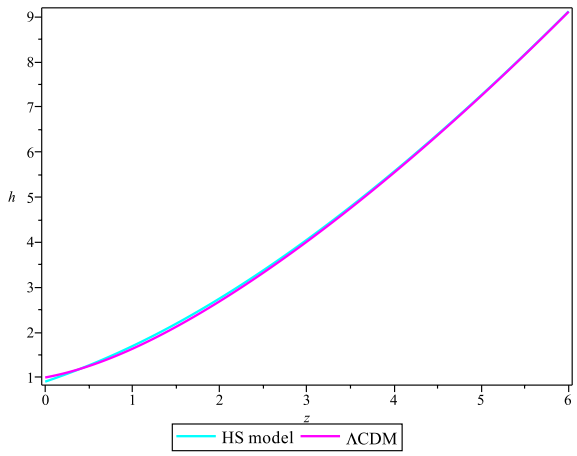

Figure 4.17: Showing a comparison of the dimensionless Hubble parameter, h, generated by ΛCDM (4.73) and the HS model ($n = 1, c_1 = 1, c_2 = 1/19, C = 0.24$) with the integration with respect to redshift initialised at $\mathbf{z_0 = 20}$. The two models are nearly indistinguishable. This is a dramatic improvement from Figure 4.8

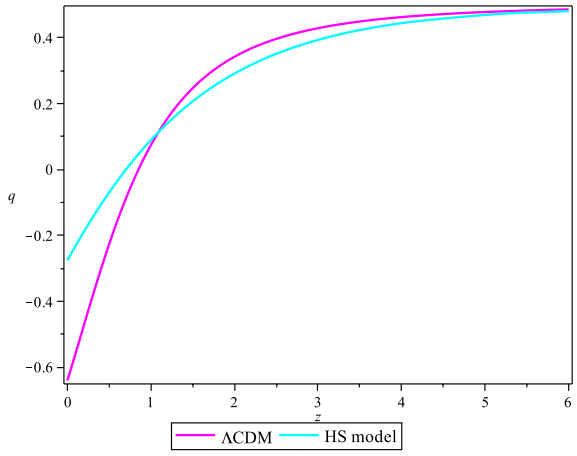

Figure 4.18: Showing the comparison of the deceleration parameter, q, generated the ΛCDM model and the HS model specified above. It is clear that adjusting the initial values of the parameters to those determined at $z_0 = 20$ instead of $z_0 = 0$ improves the behaviour of q_{HS} significantly with respect to ΛCDM model. It exhibits late time acceleration, and at higher redshifts, $q_{HS} \Rightarrow q_{\Lambda CDM} \approx \frac{1}{2}$.

Effects of increasing n

Note that the model parameter n plays an important role in the derivative of $g(R)$. Large values of n result in a tighter, or *steeper*, slope of the transition between the limiting values of $g(R)$. Therefore increasing n − making the transition from $g(R) \to 0$ to $g(R) \to Const$ more rapid − could place the initial value for $g(R)$ at the present epoch ($z_0 = 0$) on the constant plateau of the correction function. Figure 4.20 shows a plot of the correction, $g(R)$ for $n = 3$. In this plot, it is clear that the initial value of r at $z_0 = 0$ results in a value of $g(R)$ which sits well on the constant part of the function, enabling a model which closely resembles the ΛCDM model at high curvature and low curvature. However, given that, in terms of the dynamical variables at (4.28) or (4.50), any HS model with $n > 1$ is not invertible for the Ricci scalar, it is not possible to obtain a qualitative analysis using a dynamical systems approach for $n > 1$, thus, other methods must be considered.

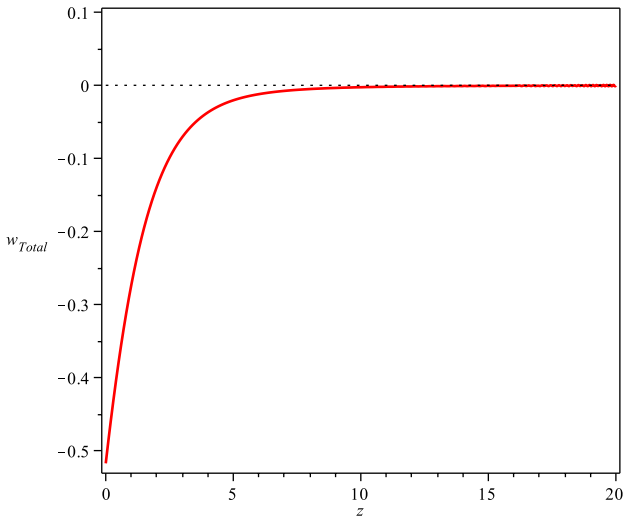

Figure 4.19: Showing a plot of the total equation of state parameter, w_{Total} generated by the HS model $(n = 1, c_1 = 1, c_2 = 1/19, C = 0.24)$, where the initial values of the parameters h, q and r were calculated for $z_0 = 20$. Upon comparison of this curve with that shown in Figure 4.11, it is clear that this is an improvement. We here have an equation of state clearly assymptoting towards $w_{Total} = 0$ at high redshifts (as expected) as well as tending toward a negative value in the low redshift regime: behaving as a Dark Energy fluid.

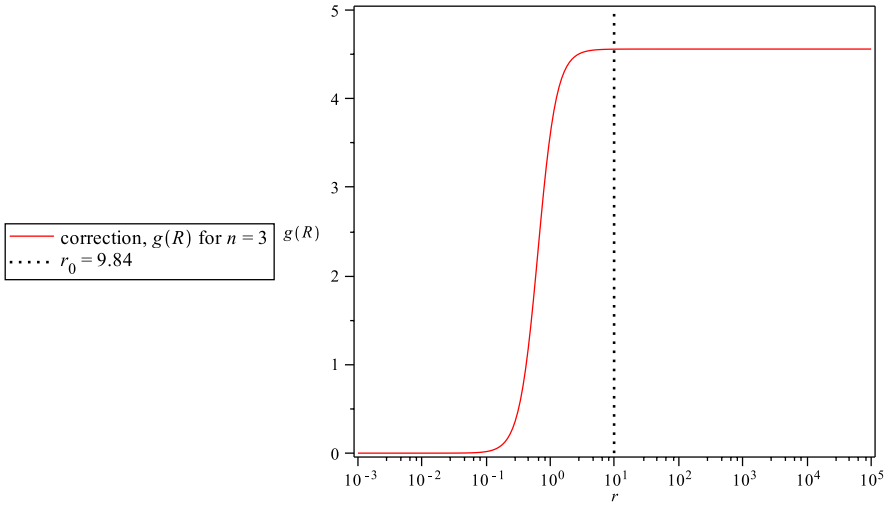

Figure 4.20: Above is a plot of the correction $g(R)$ for $n = 3$. It shows a significantly steeper slope, enabling a more rapid transition from the GR limit to the ΛCDM limit of the function. This slope enables the HS model (for $n > 1$) to mimic the ΛCDM model even with initial values set at the present epoch, $\mathbf{z_0 = 0}$. However, $n \neq 1$ is not permitted by a dynamical systems analysis performed with the variables defined by (4.28) or (4.50), therefore other means must be used to compute its resulting expansion history.

4.5 Fitting function for the Hu-Sawicki model

In this section, a fitting function approximation introduced by Cardone et al [7] and the results of the integration, of the non-compact dynamical system presented above, are compared.

Because of the complexities introduced into the modified cosmological field equations, brute force numerical integration can be computationally expensive. When it comes to estimating the model parameters using some nonlinear optimisation routine against large sets of data, it can prove highly inefficient and numerically taxing.

The Cardone fitting function [7], which is a piecewise function of redshift, is constructed with the intention to provide a more *efficient* means to obtain the expansion history for the HS model, with an analytic approximation to the solution of the cosmological equations for the Hu-Sawicki function (2.36), which reduce to a second order nonlinear differential equation in the Ricci scalar. The design of the analytic approximation is based on the

expectation that at higher redshifts the HS model is well described by ΛCDM (standard general relativity plus a cosmological constant). Therefore, the following is assumed [7]:

$$h(z >> z_\Lambda) \simeq h_\Lambda(z) = \left[\Omega_{m,eff}(1+z)^3 + \Omega_r(1+z)^4 + (1-\Omega_{m,eff}-\Omega_r)\right]^{\frac{1}{2}}, \tag{4.83}$$

where, z_Λ is a characteristic redshift at which the transition to the ΛCDM regime occurs, Ω_r is the radiation density parameter, $h = H/H_0$, as defined previously. $\Omega_{m,eff}$ is the effective matter density parameter determined by the *effective* cosmological constant term, Λ_{eff}, which the HS model supposedly introduces in this limit, and is determined by the model parameters as follows:

$$\Omega_{m,eff} = \frac{6c_2}{c_1 + 6c_2}. \tag{4.84}$$

Considering the background evolution, the equation of state can be approximated by the Chevallier-Polarski-Linder parametrization [15], [39],[7], given by

$$w(z) = w_0 + w_a(1-a). \tag{4.85}$$

So, at redshifts lower than the characteristic redshift, z_Λ, the dimensionless Hubble parameter becomes:

$$h_{CPL}(z) = \left[\Omega_m(1+z)^3 + (1-\Omega_m)(1+z)^{3(1+w_0+w_a)}e^{-\frac{3w_a z}{1+z}}\right]. \tag{4.86}$$

Cardone et al [7], therefore, propose the following function as an approximation to the numerical solution of the cosmological field equations for the HS model:

$$h(z) = \begin{cases} \mathcal{E}(z)h_{CPL}(z,\Omega_m) + [1-\mathcal{E}(z)]h_\Lambda(z,\Omega_m) & z \le z_\Lambda \\ h_\Lambda(z,\Omega_{m,eff}) & z \ge z_\Lambda \end{cases}$$

where

$$\mathcal{E} = \sum_{i=1}^{3} e_i(z-z_\Lambda)^i, \tag{4.87}$$

with the parameters $(z_\Lambda, e_i, w_0, w_a)$ to be determined by the fit.

Below, we fit this function to the dimensionless Hubble parameter, $h(z)$, as determined by integration of the equations from the dynamical systems analysis, above. First, the case with the initial redshift, $z_0 = 0$ (Figure 4.8) is considered, and to compare, the case with $z_0 = 20$ (Figure 4.17) is presented, thereafter.

For the present epoch (where the integration began at $z_0 = 0$), the values for the fit parameters are summarised below:

$$\begin{aligned} z_\Lambda &= 2.336\ , \\ w_0 &= 0.503\ , \\ w_a &= -2.147\ , \\ e_1 &= 0.444 \times 10^{-1}\ , \\ e_2 &= -0.116 \times 10^{-1}\ , \\ e_3 &= 0.105 \times 10^{-2}\ . \end{aligned} \tag{4.88}$$

In Figure 4.21, the Cardone approximation to the dimensionless Hubble rate is fitted to that obtained by the dynamical systems analysis of the HS model, the prediction of ΛCDM is over-plotted for comparison. Because the HS model with initial values at $z_0 = 0$ is not a good match to the ΛCDM model, the Cardone fitting function fails to approximate it at redshifts higher than the characteristic redshift, at which ΛCDM becomes effective, z_Λ. Recall this failure is due to the fact that the initial value for the correction $g(R)$ does not lie on

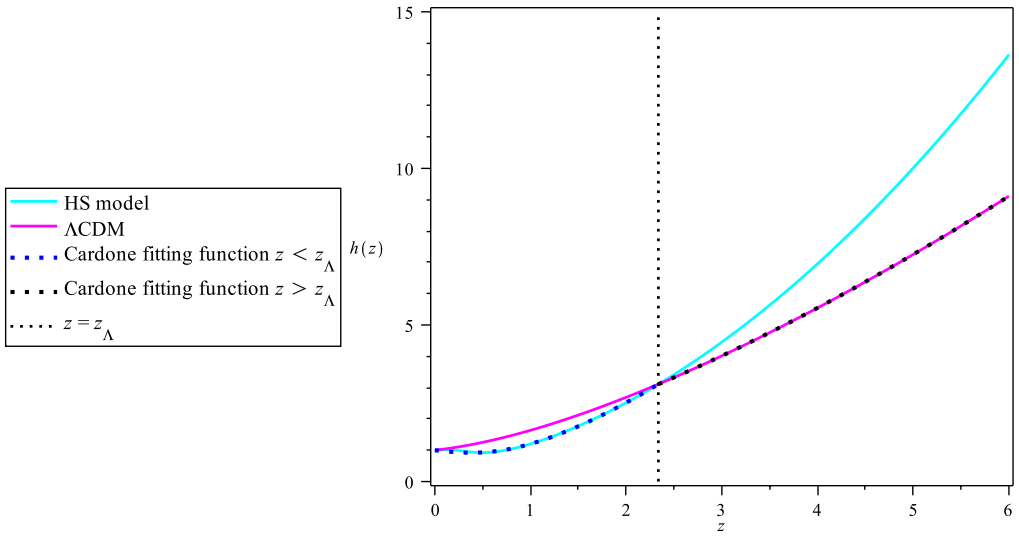

Figure 4.21: For the HS model parametrized by the values discussed above it can be seen that the Cardone fitting function (parametrized by the values (4.88)) does very well to approximate the HS model at low redshifts $z < z_\Lambda$, and the ΛCDM model at high redshift, $z > z_\Lambda$. But the fitting function fails to approximate the HS model at high redshifts due to its construction having heavy dependence on the idea that the HS model is a good approximation to the ΛCDM model in this regime.

the constant plateau which is supposed to characterise the ΛCDM regime. We can, therefore, expect that if we compare the Cardone approximation to the dimensionless Hubble parameter obtained from the integration with the correction initially on the plateau (for example at $z_0 = 20$), that the fit will be significantly more successful.

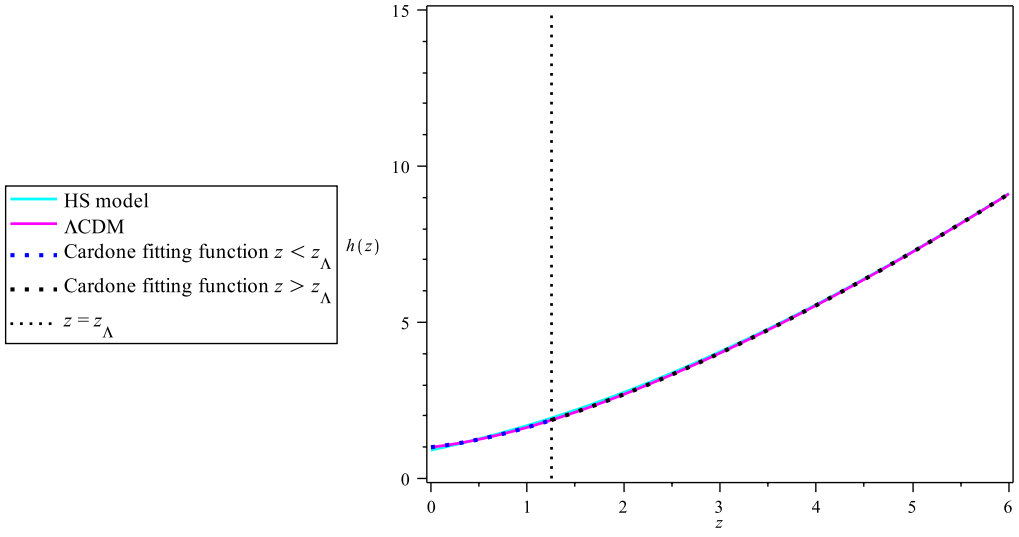

Figure 4.22: This shows the Cardone approximation parameterised by (4.89) fitted to the dimensionless Hubble parameter obtained by an integration of the dynamical systems equations for the HS model ($n = 1, c_1 = 1$) - where initial parameter values are determined by $z_0 = 20$. The Cardone approximation does excellently in this case; h determined by the HS model is almost indistinguishable from h predicted by the ΛCDM model. Thus, the approximation, which fits to the HS model for the redshift regime lower than z_Λ using the CPL equation of state parameter, and is equal to the ΛCDM model for redshifts higher than z_Λ, is an excellent approximation in this case.

A similar plot is presented for the expansion history generated by an integration of the dynamical system

equations with initial values fixed at $z_0 = 20$. In this case, $\mathbf{z_0 = 20}$, the fit parameters are

$$\begin{aligned} z_\Lambda &= 1.272 \ , \\ w_0 &= 0.883 \ , \\ w_a &= 1.024 \ , \\ e_1 &= 5.920 \times 10^{-12} \ , \\ e_2 &= -7.101 \times 10^{-13} \ , \\ e_3 &= 2.106 \times 10^{-14} \ . \end{aligned} \tag{4.89}$$

Figure 4.22 illustrates the success of the Cardone fitting function approximation to the HS model. The dimensionless Hubble parameter characterised by the CPL equation of state in the redshift regime $z < z_\Lambda$ reveals an excellent fit to the lower redshift regime of the Hubble parameter. Thus, it can be expected that when $n > 1$ the HS model will be well approximated by the Cardone fitting function.

4.6 End Note

This chapter presents the results of the original work done toward this thesis. From the results detailed above, it can be said that the specific HS model under investigation ($n = 1, c_1 = 1$) with initial values set to the present epoch as calculated by ΛCDM ($z_0 = 0$) does not mimic the ΛCDM model well. This is due to the fact that the correction $g(R)$ does not initially lie on the constant valued plateau, which represents the cosmological constant limit of the function. In fact, as redshift evolves, the Ricci scalar, in this case, becomes smaller and smaller, resulting in the eventual evolution *away* from the ΛCDM regime. On the other hand, picking initial values for the Hubble and deceleration parameters which differed from their corresponding ΛCDM values today, specifically at $z = 20$, almost completely rectifies the issue, indicating that the general Hu-Sawicki model can give the desired properties, if the correction is within its ΛCDM regime. Thus, for the case $n = 1, c_1 = 1$ a universe close to ΛCDM *can* be obtained, at the expense of the present values of q_0 and h_0.

Chapter 5

Concluding Remarks

5.1 Brief review of the problem

In Chapter 1, a very compact discussion of the state of standard cosmology was presented. It is accepted, with wide consensus in the community, that the universe, largely homogeneous and isotropic, began, by some unknown mechanism, from an extremely hot and dense state, into an epoch of rapid inflation. This rapid inflation facilitated the cooling of the energy content of the universe, and was proposed as a resolution to issues such as the monopole, flatness and horizon problems. The potential energy of the inflaton field, which caused the rapid inflation, eventually decays into the relativistic particles described by the standard model of particle physics, leading to the end of the inflationary epoch, and the beginning of the radiation dominated era. This process is known as reheating [36].

The universe continues to expand according to the dominating energy form in the universe at the time: first radiation, then a cold dark matter dominated phase and most recently what seems to be an unclustered fluid having negative pressure which is forcing the universe into a phase of accelerated expansion, called Dark Energy.

One of the most serious problems facing cosmology, and the field of modern physics, is understanding the nature of this mysterious new Dark Energy, which has taken over the expansion evolution of the universe. Probably the biggest question regarding this issue is whether or not the observation of the accelerated expansion, and the deduction of this new form of energy, is *real*. Is it possible that Dark Energy is a signal that our assumptions or our physics are wrong or incomplete?

There are two main ways to be skeptical about standard cosmology: (1) Assume Einstein's gravitational theory is correct, and abandon the assumption of homogeneity and isotropy, or (2) assume that the Cosmological Principle holds, but standard General Relativity is incomplete.

Modified gravity is a field of research concerned with the latter, aiming to generalise the field equations of General Relativity in order to explain the late time acceleration phenomenon. In this thesis, a specific branch of modified gravity was considered, known as $f(R)$-gravity, treated in the metric formalism.

5.2 Summary and overview of results

The Hu-Sawicki model was considered as a correction to the standard Einstein-Hilbert action in the context of a dynamical systems analysis.

The HS model is constructed, as several other broken power law models, with the intention to evade the solar system tests of GR by design.

The purpose of the work presented in this thesis was to analyse the Hu-Sawicki model, using the dynamical systems approach to cosmology, to elicit qualitative information about the universe which it governs.

By the technical requirements of the dynamical systems approach, the cosmological equations must be

expressed in terms of a set of generalised dimensionless dynamical variables which span the phase space of the dynamical systems problem. The model is specified by the term Γ, which must be expressible in terms of the dynamical variables in order to close the system. For the variables considered, the HS model can only be inverted for the Ricci scalar (to obtain Γ in terms of the variables) for $n = 1$, and therefore our investigation was restricted with respect to this parameter. While it was shown above that $n > 1$ improves the way the HS model matches the ΛCDM predictions, at this stage there are no observational constraints on the value of n [54]. Thus, technically, we do not compromise the generality of the study by choosing $n = 1$.

The model parameter c_1 was also set to 1 in this analysis to facilitate the inversion of the function $f(R)$ for the Ricci scalar.

The following summarises the original work completed as the basis of this thesis. A compact dynamical systems analysis was performed using a positive definite normalisation to pull the equilibria at infinity into a finite volume constrained by the normalised ranges of the dynamical variables. From this analysis, twelve equilibrium points were identified, each having an expanding ($Q > 0$) and contracting ($Q < 0$) version. Four de Sitter like stationary phase states were found $\mathcal{A}_\pm$ and $\mathcal{B}_\pm$, two within the expanding part of the phase space, with the other two being their collapsing versions. Considering the expanding versions of these points, both $\mathcal{A}_+$ and $\mathcal{B}_+$ are *stable* stationary phase states. Two unstable "radiation like" states exist in the expanding sector of the phase space, $\mathcal{G}_+$ and $\mathcal{H}_+$. There are several orbits which connect these "radiation" points to the de Sitter phase states, offering trajectories which resemble the chronological evolution of the scale factor of our universe.

On the surface $y = v$, which renders the model specifying term Γ undefined, a very interesting, non-analytic, *matter-like* point, $\mathcal{K}_+$, was identified which has spiral like instability. There does exist a trajectory which evolves from $\mathcal{K}_+$ toward a de Sitter phase state at $\mathcal{A}_+$. The existence of this trajectory is indicative of the fact that the Hu-Sawicki model provides a modification to gravity consistent with the ΛCDM model.

In order to consider the expansion history generated by the HS model, a finite dynamical systems analysis was performed to confirm that the non-boundary points obtained in the compact analysis were, in fact, finite points. The finite points obtained in this analysis are the analogies of the de Sitter and "radiation like" points, $\mathcal{A}_\pm, \mathcal{B}_\pm, \mathcal{G}_\pm$ and $\mathcal{H}_\pm$.

It was found that the expansion history generated from the initial values and parameter constraints specified in [32] for the *present epoch* resulted in a universe which is dominated until very low redshifts by an equation of state parameter equal to $\frac{1}{3}$, implying that fixing the initial conditions to be exactly those of the ΛCDM conditions produced results inconsistent with ΛCDM. The dimensionless Hubble parameter produced by the theory, in this case, showed a disappointing agreement between the HS model and the ΛCDM predictions. This is due to the fact that for $n = 1$, the slope of the correction $g(R)$ defined by the HS model does not allow for the initial value of $g(R)$ to sit on the constant valued plateau of the function. It is this plateau which facilitates the late time cosmological constant behaviour of the model. We showed that shifting the initial value of the correction so that it is already equal to its "plateau" value, improves the way the HS model matches the ΛCDM model. It produces a dimensionless Hubble parameter that is nearly indistinguishable from ΛCDM. Most importantly, it gives an equation of state parameter which behaves as that of dust for most of the expansion history, and begins to tend toward -1 to indicate the domination of a cosmological constant term, at low redshifts.

It is proposed that large values of n in the HS model will correct the behaviour of the model, even using the exact ΛCDM values today as initial conditions. Unfortunately, large values of n can not be considered in a dynamical systems analysis in terms of the dynamical variables defined in Section 4.3 and 4.4. Finding a set of variables which *can* facilitate the dynamical systems analysis of the general HS model in order to perform a complete analysis of the general phase space poses an interesting problem.

We also considered the Cardone fitting function approximation to the specific HS model studied here ($n = 1$, $c_1 = 1$), and showed that it does excellently in the case that the correction is initialised on the plateau of the function $g(R)$.

The dynamical systems analysis enabled the extraction of qualitative information of the Hu-Sawicki model

$(n = 1, c_1 = 1)$, regarding the existence of stable de Sitter equilibria, as well as an unstable spiral matter point. We were able to ascertain that for this specific model, the correction function $g(R)$ does not assume its artificial cosmological constant value at the present epoch and therefore does not mimic ΛCDM at high redshifts. Improving the match to ΛCDM comes at the cost of adjustments to the values of h_0 and q_0 as initial conditions.

5.3 Future work

Future interests related to dynamical systems investigations of this model involve constructing a phase space for the general HS model, as well as possibly considering its response in a universe where flatness is not assumed initially. The parameters n, c_1, c_2 and C need still to be constrained by data, and such an investigation (to optimise the parameter values toward a fit of ΛCDM) is of great interest and importance in deciding the viability of the model.

More generally, in addressing the greater interests of the field of $f(R)$ gravity, it is important to establish a method of testing generic forms of $f(R)$ models in order to make comparisons with observational data. The response of the Cosmic Microwave Background power spectrum, the growth of structure and the Newtonian limit, to the general modification of GR must be investigated and examined against current observations such as the latest CMB data from Planck [51], BAO and gravitational lensing data to obtain new constraints on the form of $f(R)$. Another issue of paramount concern is the development of a set of exact and approximate analytical tools to facilitate the study of most forms for $f(R)$, making it possible to manoeuvre the complexities of higher order gravity more smoothly.

5.4 End note

In its development, modern cosmology has had its face changed several times, each time more dramatically than the last, due to advancements in technological and observational capabilities. Most recently, the discovery of the accelerated expansion of the universe threatens to change almost all of modern physics with explanations, neither of which are satisfactory nor verifiable, reducing to one of two things :

- there exists a new, mysterious form of unclustered energy in universe, which is only now becoming prevalent and detectable (via the accelerated expansion)
- or, the underlying assumptions and/or gravitational physics are incomplete.

With this discovery, Modified Gravity has finally found a strong enough motivation to leave the realm of speculation and enter the ring as a contender of Dark Energy worth the investment and exploration.

The field of modified gravity is relatively fresh, and much of the progress made within it, with particular reference to $f(R)$ theories, appears to be a complicated manner of "feeling in the Dark". It is important to note that the major motivation behind such generalisations is to realise the fact that modifications to the Einstein-Hilbert action *can* result in a universe which exhibits the observed phenomena *without the need for exotic forms of energy*. This is definitely not to say (at least not at this stage) that any particular proposed model is the theory to replace GR. In fact, the degeneracy of models which satisfy the requirements and constraints set by observations, is inevitable, and breaking this degeneracy remains a tall order due to the inability to actively experiment with the gravitational field.

Gravitational physics remains a foggy domain, with discrepancies not confined to cosmology, but also from a quantum physics perspective. It is, therefore, absolutely imperative to continuously probe our understanding of the gravitational interaction, if not to prove a modification is required, then, to deepen our appreciation for and understanding of General Relativity.

Appendices

Appendix A

Stability of equilibrium point $\mathcal{A}_{\pm}$

As indicated in Table 4.4, the eigenvalues of the Jacobian of the system evaluated at $\mathcal{A}_{+/-}$ have two negative/positive values and one value precisely equal to zero. This implies that this equilibrium state is non-hyperbolic. The Center Manifold theorem, which states that the flow on the center manifold of a non-hyperbolic fixed point is indicative of the stability of the fixed point, is used to assess the stability of $\mathcal{A}_{+}$, while the behaviour of perturbations is used to determine the stability near $\mathcal{A}_{-}$. The details are presented below.

Stability of $\mathcal{A}_{+}$

To benefit from simplicity, taking advantage of the fact that this point does not lie on the boundary of the compact phase space, an analysis of the center manifold of $\mathcal{A}_{+}$ is performed using the non-compact dynamical system, defined by the non-compact variables (4.50). $\mathcal{A}_{+}$ has non-compact coordinates $(\tilde{x}, \tilde{y}, \tilde{v}, \tilde{\Omega}) = (0, 1, 2, 0)$. Making use of the reduced system, and shifting the coordinate system such that the fixed point lies at the origin, we obtain the following dynamical system for *dust:* $w = 0$:

$$\frac{d\tilde{x}}{dt} = -2\tilde{x} + \tilde{v} - 3\tilde{y} - \tilde{x}^2 - \tilde{x}\tilde{v} \ , \tag{A.1}$$

$$\begin{aligned}\frac{d\tilde{y}}{dt} = &-\tilde{x}\tilde{y} - \tilde{x} - 2\tilde{y}\tilde{v} - 2\tilde{v} + \frac{1}{2}\frac{\tilde{x}\tilde{v}^2\tilde{y}}{(-\tilde{v}-1+\tilde{y})^2} + \frac{1}{2}\frac{\tilde{x}\tilde{v}^2}{(-\tilde{v}-1+\tilde{y})^2} \\ &+ 2\frac{\tilde{x}\tilde{y}\tilde{v}}{(-\tilde{v}-1+\tilde{y})^2} + 2\frac{\tilde{x}\tilde{v}}{(-\tilde{v}-1+\tilde{y})^2} + 2\frac{\tilde{x}\tilde{y}}{(-\tilde{v}-1+\tilde{y})^2} + 2\frac{\tilde{x}}{(-\tilde{v}-1+\tilde{y})^2} \ ,\end{aligned} \tag{A.2}$$

$$\begin{aligned}\frac{d\tilde{v}}{dt} = &-4\tilde{v} - 2\,\tilde{v}^2 + \frac{1}{2}\frac{\tilde{x}\tilde{v}^2\tilde{y}}{(-\tilde{v}-1+\tilde{y})^2} + \frac{1}{2}\frac{\tilde{x}\tilde{v}^2}{(-\tilde{v}-1+\tilde{y})^2} + 2\frac{\tilde{x}\tilde{y}\tilde{v}}{(-\tilde{v}-1+\tilde{y})^2} \\ &+ 2\frac{\tilde{x}\tilde{v}}{(-\tilde{v}-1+\tilde{y})^2} + 2\frac{\tilde{x}\tilde{y}}{(-\tilde{v}-1+\tilde{y})^2} + 2\frac{\tilde{x}}{(-\tilde{v}-1+\tilde{y})^2} \ .\end{aligned} \tag{A.3}$$

Clearly, in the above system, the center manifold corresponds to the coordinate $\tilde{y}$, where as the $\tilde{x}$ and $\tilde{v}$ coordinates each represent stable manifolds. As per the prescription in Section 3.3.3, we have the following

functions

$$F_{s,\tilde{x}}(\tilde{x},\tilde{y},\tilde{v}) = \tilde{v} - 3\tilde{y} - \tilde{x}^2 - \tilde{x}\tilde{v} \ , \tag{A.4}$$

$$F_{s,\tilde{v}}(\tilde{x},\tilde{y},\tilde{v}) = -2\,\tilde{v}^2 + \frac{1}{2}\,\frac{\tilde{x}\tilde{v}^2\tilde{y}}{(-\tilde{v}-1+\tilde{y})^2} + \frac{1}{2}\,\frac{\tilde{x}\tilde{v}^2}{(-\tilde{v}-1+\tilde{y})^2} + 2\,\frac{\tilde{x}\tilde{y}\tilde{v}}{(-\tilde{v}-1+\tilde{y})^2} + 2\,\frac{\tilde{x}\tilde{v}}{(-\tilde{v}-1+\tilde{y})^2} + 2\,\frac{\tilde{x}\tilde{y}}{(-\tilde{v}-1+\tilde{y})^2} + 2\,\frac{\tilde{x}}{(-\tilde{v}-1+\tilde{y})^2} \ , \tag{A.5}$$

$$F_{c,\tilde{y}}(\tilde{x},\tilde{y},\tilde{v}) = -\tilde{x}\tilde{y} - \tilde{x} - 2\tilde{y}\tilde{v} - 2\tilde{v} + \frac{1}{2}\,\frac{\tilde{x}\tilde{v}^2\tilde{y}}{(-\tilde{v}-1+\tilde{y})^2} + \frac{1}{2}\,\frac{\tilde{x}\tilde{v}^2}{(-\tilde{v}-1+\tilde{y})^2} + 2\,\frac{\tilde{x}\tilde{y}\tilde{v}}{(-\tilde{v}-1+\tilde{y})^2} + 2\,\frac{\tilde{x}\tilde{v}}{(-\tilde{v}-1+\tilde{y})^2} + 2\,\frac{\tilde{x}\tilde{y}}{(-\tilde{v}-1+\tilde{y})^2} + 2\,\frac{\tilde{x}}{(-\tilde{v}-1+\tilde{y})^2} \ , \tag{A.6}$$

which define the nonlinear terms of the differential equations for $\tilde{x}, \tilde{y}$ and $\tilde{v}$. The subscript s or c denotes whether the function corresponds to the stable or center manifolds respectively, and the subscript $\tilde{x}, \tilde{y}$ or $\tilde{v}$ denotes which differential equation it corresponds to.

Recall that the the functions $h1(\tilde{y})$ and $h2(\tilde{y})$, which define the local center manifold, satisfy the following equations:

$$Dh1(\tilde{y})[C_{\tilde{y}}\tilde{y} + F_{c,\tilde{y}}(h1(\tilde{y}),\tilde{y},h2(\tilde{y}))] = S_{\tilde{x}}h1(\tilde{y}) + F_{s,\tilde{x}}(h1(\tilde{y}),\tilde{y},h2(\tilde{y})) \ , \tag{A.7}$$

$$Dh2(\tilde{y})[C_{\tilde{y}}\tilde{y} + F_{c,\tilde{y}}(h1(\tilde{y}),\tilde{y},h2(\tilde{y}))] = S_{\tilde{v}}h2(\tilde{y}) + F_{s,\tilde{v}}(h1(\tilde{y}),\tilde{y},h2(\tilde{y})) \ , \tag{A.8}$$

where $C_{\tilde{y}}$ represents the coefficient of the term linear in $\tilde{y}$ of $\frac{d\tilde{y}}{dt}$ - which is equal to zero, given that it corresponds to center. $S_{\tilde{x}}$ represents the coefficients of the terms linear in $\tilde{x}$ in the expression for $\frac{d\tilde{x}}{dt}$ (A.1) and $S_{\tilde{v}}$ represents the coefficients of the terms linear in $\tilde{v}$ in the expression for $\frac{d\tilde{v}}{dt}$ (A.3). The functions $h1(\tilde{y})$ and $h2(\tilde{y})$ are chosen to be the following expansions:

$$h1(\tilde{y}) = a\tilde{y} + b\tilde{y}^2 + O(\tilde{y}^3) \ , \tag{A.9}$$

$$h2(\tilde{y}) = c\tilde{y} + d\tilde{y}^2 + O(\tilde{y}^3) \ , \tag{A.10}$$

with $Dh1(\tilde{y})$ and $Dh1(\tilde{y})$ equal to their derivatives with respect to $\tilde{y}$.

Substituting (A.9) and (A.10), along with $S_{\tilde{x}} = -2, S_{\tilde{v}} = -4, C_{\tilde{y}} = 0$ into equations (A.7) and (A.8) allows one to infer the values of the constants a, b, c and d, which specify the functions $h1$ and $h2$:

$$h1(\tilde{y}) = \frac{9}{4}\tilde{y}^2 + O(\tilde{y}^3) \ , \tag{A.11}$$

$$h2(\tilde{y}) = 3\tilde{y} - \frac{45}{2}\tilde{y}^2 + O(\tilde{y}^3) \ . \tag{A.12}$$

Thereafter, these functions are substituted back into the differential equation for $\tilde{y}$ (A.2) in order to find the flow on the center manifold. We obtain the following polynomial:

$$\frac{d\tilde{y}}{dt} = -6\tilde{y} + O(\tilde{y}^2) \ . \tag{A.13}$$

The lowest order in the above polynomial differential equation is odd. In this case, as stated in Section 3.3.3, the sign of $\tilde{x}$ and $\tilde{v}$ near the equilibrium point must be considered. Substituting (A.11) and (A.12) into (A.1) and (A.3), the following expressions for $\frac{d\tilde{x}}{dt}$ and $\frac{d\tilde{v}}{dt}$, in terms of $\tilde{y}$, result :

$$\frac{d\tilde{x}}{dt} = -27\tilde{y}^2 + O(\tilde{y}^3) \ , \tag{A.14}$$

$$\frac{d\tilde{v}}{dt} = -12\tilde{y} + O(\tilde{y}^2) \ . \tag{A.15}$$

The coefficients of the lowest order in the equations for $\frac{d\tilde{x}}{dt}$, $\frac{d\tilde{y}}{dt}$ and $\frac{d\tilde{v}}{dt}$, in terms of $\tilde{y}$, are all *negative*. This implies that $\mathcal{A}_+$ is a topological attractor. Similarly, we assess the stability of this equilibrium state in systems for which $w = \frac{1}{3}$ and $w = 0$, to find the same result.

Stability of $\mathcal{A}_-$

The point $\mathcal{A}_-$ does not appear in the non-compact coordinate system, and so we can not use the coordinates above to assess its stability. We, therefore, resort to testing the behaviour of small second order perturbations about this equilibrium state using the *compact* coordinates defined by (4.28). If we label the differential equations in terms of the compact variables (x, Q, v) as

$$\begin{aligned} \frac{dx}{dt} &= \mathbf{F}_1 \ , \\ \frac{dQ}{dt} &= \mathbf{F}_2 \ , \\ \frac{dv}{dt} &= \mathbf{F}_3 \ , \end{aligned} \tag{A.16}$$

the Jacobian matrix and eigenvalues are given by:

$$J_{\mathcal{A}_-} = \begin{pmatrix} \frac{\partial \mathbf{F}_1}{\partial x} & \frac{\partial \mathbf{F}_1}{\partial Q} & \frac{\partial \mathbf{F}_1}{\partial v} \\ \frac{\partial \mathbf{F}_2}{\partial x} & \frac{\partial \mathbf{F}_2}{\partial Q} & \frac{\partial \mathbf{F}_2}{\partial v} \\ \frac{\partial \mathbf{F}_3}{\partial x} & \frac{\partial \mathbf{F}_3}{\partial Q} & \frac{\partial \mathbf{F}_3}{\partial v} \end{pmatrix} = \begin{pmatrix} -\frac{\sqrt{2}}{6} & -\frac{2\sqrt{2}}{3} & \frac{1}{6} \\ \frac{\sqrt{2}}{6} & \frac{2\sqrt{2}}{3} & \frac{1}{12} \\ 0 & 0 & \frac{\sqrt{2}}{2} \end{pmatrix}, \qquad \begin{pmatrix} 0 \\ \frac{1}{\sqrt{2}} \\ \frac{1}{\sqrt{2}} \end{pmatrix} .$$

However, $J_{\mathcal{A}_-}$ is a singular matrix, therefore, it is not invertible. This implies that the matrix constructed from its eigenvectors is not invertible, so it is not possible to diagonalise $J_{\mathcal{A}_-}$. The Center Manifold Theorem can not be used to ascertain the stability of $\mathcal{A}_-$, because the coordinate corresponding to the center is not clear. So, we resort to assessing the behaviour of the perturbed system (to second order), using perturbations around the fixed point in compact coordinates; where these coordinates are $\mathbf{x_0} = (x_0, Q_0, v_0) = (0, -\frac{1}{\sqrt{2}}, 1)$:

$$\begin{aligned} x &= x_0 + \Delta x \ , \\ Q &= Q_0 + \Delta Q \ , \\ v &= v_0 + \Delta v \ . \end{aligned} \tag{A.17}$$

The second order equations for the perturbed compact dynamical system are (the prime denotes a time deriva-

tive) :

$$\Delta x' = \frac{1}{6}\Delta v - \frac{1}{6}\Delta x^2 - \frac{2}{3}\sqrt{2}\Delta Q - \frac{1}{6}\sqrt{2}\Delta x + \frac{1}{3}\Delta x\Delta Q + \frac{1}{4}\sqrt{2}\Delta x\Delta v - \frac{1}{12}\frac{\Delta x^2}{\left(-\frac{1}{2} - \Delta v + \sqrt{2}\Delta Q - \Delta Q^2 + \sqrt{2}\Delta x - 2\Delta x\Delta Q - \Delta x^2\right)^2} , \tag{A.18}$$

$$\begin{aligned}\Delta Q' = {} & \frac{1}{12}\Delta v - \frac{5}{12}\,\Delta x^2 + \frac{2}{3}\,\sqrt{2}\Delta Q + \frac{1}{2}\,\Delta v\,\sqrt{2}\Delta Q + \frac{1}{4}\,\Delta x\,\Delta v\,\sqrt{2} - \frac{2}{3}\,\Delta Q^2 - \frac{2}{3}\,\Delta x\,\Delta Q \\ & + \frac{1}{12}\frac{\Delta x\Delta v\,\sqrt{2}}{\left(-\Delta v - \frac{1}{2} + \sqrt{2}\Delta Q - \Delta Q^2 + \Delta x\,\sqrt{2} - 2\,\Delta x\,\Delta Q - \Delta x^2\right)^2} \\ & + \frac{1}{6}\frac{\Delta x^2}{\left(-\Delta v - \frac{1}{2} + \sqrt{2}\Delta Q - \Delta Q^2 + \Delta x\,\sqrt{2} - 2\,\Delta x\,\Delta Q - \Delta x^2\right)^2} \\ & + \frac{1}{24}\frac{\Delta x\,\sqrt{2}}{\left(-\Delta v - \frac{1}{2} + \sqrt{2}\Delta Q - \Delta Q^2 + \Delta x\,\sqrt{2} - 2\,\Delta x\,\Delta Q - \Delta x^2\right)^2} \\ & + \frac{1}{12}\frac{\Delta x\,\Delta Q}{\left(-\Delta v - \frac{1}{2} + \sqrt{2}\Delta Q - \Delta Q^2 + \Delta x\,\sqrt{2} - 2\,\Delta x\,\Delta Q - \Delta x^2\right)^2} ,\end{aligned} \tag{A.19}$$

$$\begin{aligned}\Delta v' = {} & \frac{4}{3}\Delta x\,\sqrt{2}\Delta Q - \Delta x\,\Delta v + \frac{1}{2}\,\Delta v\,\sqrt{2} - \Delta v\,\Delta Q + \frac{1}{2}\,\Delta v^2\sqrt{2} + \frac{5}{6}\,\Delta x^2\sqrt{2} \\ & - \frac{1}{6}\frac{\Delta x\,\Delta v}{\left(-\Delta v - \frac{1}{2} + \sqrt{2}\Delta Q - \Delta Q^2 + \Delta x\,\sqrt{2} - 2\,\Delta x\,\Delta Q - \Delta x^2\right)^2} .\end{aligned} \tag{A.20}$$

The search for exact analytic solutions to the above system is unendurable. The system is, thus, solved numerically and the behaviour of the perturbations are examined from different perspectives of the equilibrium point $\mathcal{A}_-$. The directions are examined by permuting positive and negative signs on each of the coordinates, accounting for each of the eight quadrants about the equilibrium point.

Below we include several plots of the time evolution of the perturbations, with initial conditions close to the equilibrium points.

From Figure A.1, which illustrates the behaviour of the perturbations near $\mathcal{A}_-$, it is simple to conclude that this point corresponds to a de Sitter repellor. From the center manifold analysis above, it can be concluded that $\mathcal{A}_+$ is a *stable* late time de Sitter point and can, therefore,be considered in the context of Dark Energy.

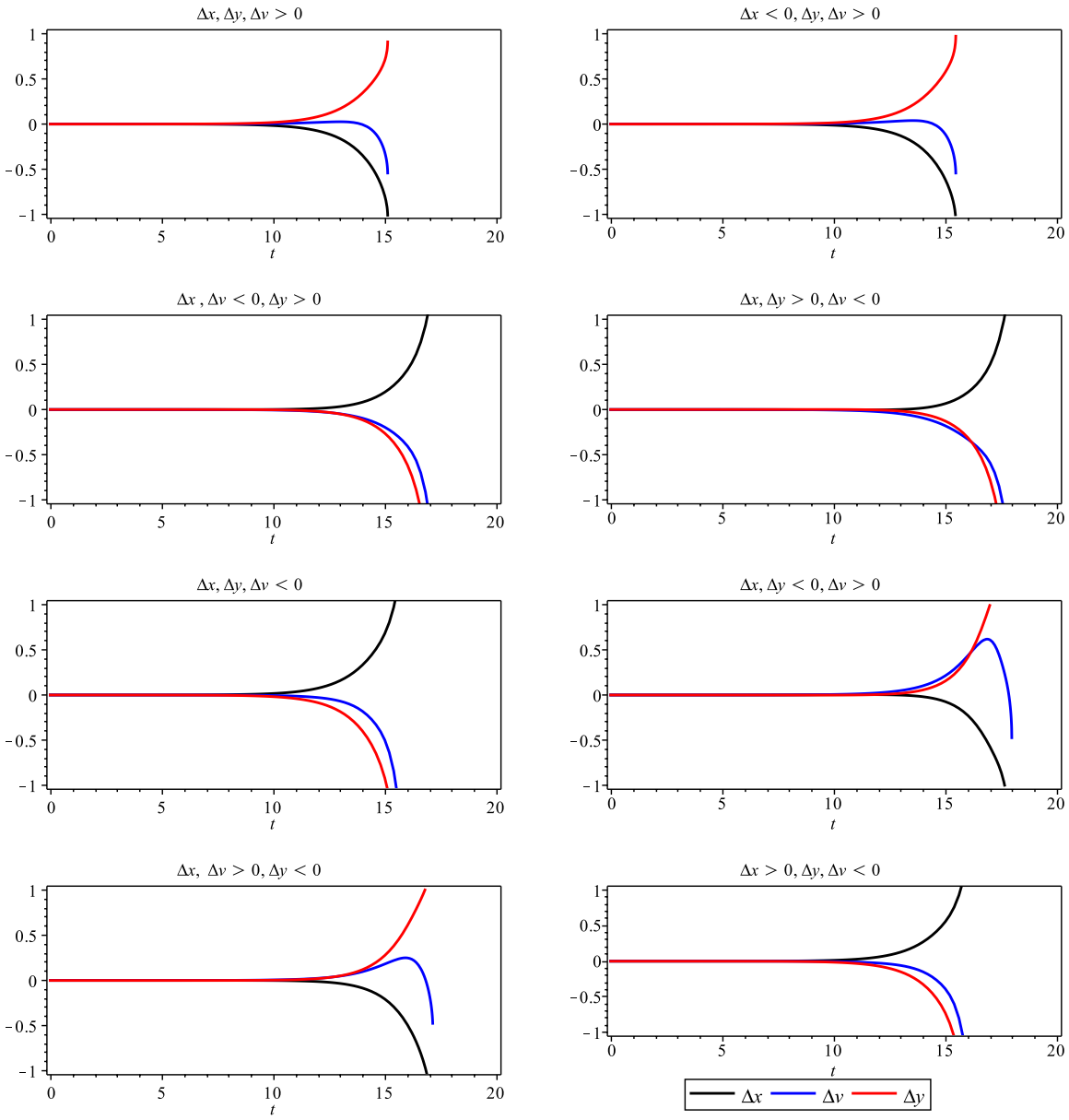

Figure A.1: The above plots show the time evolution of the perturbations $\Delta x, \Delta y, \Delta v$ which are the numeric solutions of the perturbed system given by (A.18) - (A.20), near the equilibrium point $\mathcal{A}_{-}$. The vertical axis runs through the values of the perturbations and the horizontal axis is time, the variable of integration. The solid black, red and blue lines represent the evolution of $\Delta x, \Delta y$ and Δv, respectively, when initial values of each are chosen very to close the equilibrium state $\mathcal{A}_{-}$. It is clear that the perturbations diverge as t increases, and therefore send solution trajectories of the dynamical system (both compact and non-compact) away from $\mathcal{A}_{-}$. This behaviour occurs regardless of the direction of approach, and therefore implies that this equilibrium state is unstable.

Bibliography

[1] Abdelwahab, M *et al. Class. Quantum Grav.* **25** 135002 (2008) arXiv:0706.1375 [gr-qc]

[2] Abdelwahab, M *et al. Phys. Rev.* D**85** 083511 (2012) arXiv:1111.0171 [gr-qc]

[3] Arrowsmith, D. K. and Place, C. M. *An Introduction to Dynamical Systems.* Cambridge University Press, 1994. Print.

[4] Barrow, J. D. and Ottewill, A. C. (1983) *J. Phys. A: Math. Gen.* **16** 2757

[5] Capozziello, S. (2009) arXiv:0909.4672 [gr-qc]

[6] Capozziello, S. and Faraoni, V. *Beyond Einstein Gravity: A Survey of Gravitational Theories for Cosmology and Astrophysics.* New York: Springer, 2011. Print.

[7] Cardone, V. F. *et al. JCAP02*(2012)030 arXiv:1201.3272 [astro-ph]

[8] Calcagni, G. *et al. Nucl. Phys.* B**752** (2006) 404-438

[9] Carloni, S. *et al. Class. Quantum Grav.* **25** 035008 (2008) arXiv:0701009 [gr-qc]

[10] Carloni, S. *et al. Gen.Rel.Grav.* **41** (2009) 1757-1776 arXiv:0706.0452 [gr-qc]

[11] Carloni, S. *et al.*(2008) arXiv:0812.2211 [astro-ph]

[12] Carloni, S. *et al. J. Phys. A: Math. Theor.* **40** 6919 (2007) arXiv:0611122 [gr-qc]

[13] Carroll, B.W. and Ostlie, D.A. *An Introduction to Modern Astrophysics,* 2^{nd} *Ed.* Pearson Education, 2006. Print.

[14] Carroll, S. M. *et al. Phys.Rev.* D**71** (2005) 063513

[15] Chevallier, M. and Polarski, D. *Int.J.Mod.Phys.* D**10** (2001) 213 arXiv:0009008 [gr-qc]

[16] Chiba, T. (2003) *Phys.Lett.* B **575**, 1-3 arXiv:0307338 [astro-ph]

[17] Clifton, T. *et al. Phys.Rept.* **513** (2012) 1-189 arXiv:1106.2476 [astro-ph.CO] (and all references therein)

[18] de Block, W. J. G. *Adv.Astron.* **2010** 789293 arXiv:0910.3538 [astro-ph.CO]

[19] de Souza, J. C. C and Faraoni, V. *Class. Quantum Grav.* **24** 3637-3648 (2007) arXiv:0701009 [gr-qc]

[20] DeWitt, B. S *Dynamical Theory of Groups and Fields.* New York: Gordon and Breach, 1965. Print.

[21] Dodelson, S. *Modern Cosmology.* Academic Press, 2003. Print

[22] de la Cruz-Dombriz, A. *et al.* (2013) arXiv: 1312.2022 [gr-qc]

[23] Dunsby, P. K. S. *et al.* (2010) arXiv:1005.2205 [gr-qc]

[24] Faraoni, V. (2008) arXiv:0810.2602 [gr-qc]

[25] Fleury, P. *et al. Phys.Rev.* D**87** (2013) 123526 arXiv:1302.5308 [astro-ph.CO]

[26] Gannon, T. *Nucl.Phys.* B**670** (2003) 335-358 arXiv:0305070 [hep-th]

[27] Goheer, N. *et al. Class. Quantum Grav.* **25** 035013 (2008) arXiv:0909.4672 [gr-qc]

[28] Goheer, N. *et al. Class. Quantum Grav.* **24** 5689 (2007) arXiv:0710.0814 [gr-qc]

[29] Goliath, M. and Ellis, G. F. R. *Phys.Rev.* D**60** (1999) 023502 arXiv:9811068 [gr-qc]

[30] Hobson, M. P. , Efstathiou, G. P., Lasenby, A. N. *General Relativity : An Introduction for Physicists.* Cambridge University Press, 2006. Print.

[31] Hu, W. *Annals Phys.* **303** (2003) 203-225 arXiv:0210696 [astro-ph]

[32] Hu, W. *et al. Phys.Rev.* D**76** (2007) 064004 arXiv:0705.1158 [astro-ph]

[33] Igari, K. *Publ. RIMS, Kyoto Univ* **9** (1974) 613-629.

[34] Kehagias, A. (2013) arXiv:1312.1155 [hep-th]

[35] Khoury, J. and Weltman, A. (2004) *Phys.Rev.Lett.* **93**, 171104 arXiv:0309300 [astro-ph]

[36] Kofman, L. (1996) arXiv:9605155 [astro-ph]

[37] Langlois, D. *Lect.Notes Phys.* **800** (2010) 1-57 arXiv:1001.5259 [astro-ph.CO]

[38] Liddle, A. *An Introduction to Modern Cosmology,* 2^{nd} *Ed.* John Wiley & Sons, 2003. Print.

[39] Linder, E. V. *Phys.Rev.Lett* **90** (2003) 091301 arXiv:0208512 [astro-ph]

[40] Martinelli, M. *et al. Phys.Rev.* D**79** (2009) 123516 arXiv:0906.2350 [astro-ph]

[41] Mizohata, S. *et al. Lectures on Cauchy Problem* Bombay, 1965.

[42] Mota, D. F. *et al.* (2004) *Mon.Not.Roy.Astron.Soc.* **349**, 291 arXiv:0309273 [astro-ph]

[43] Peebles, P. J. E *Principles of Physical Cosmology.* New Jersey: Princeton University Press, 1993. Print.

[44] Peebles, P. J. E. and Ratra, B. *Rev. Mod. Phys.* **75** (2003) 559-606

[45] Percival, I. and Richards, D. *Introduction to Dynamics.* Cambridge: Cambridge University Press, 1994. Print.

[46] Perko, L. *Texts in Applied Mathematics 7: Differential Equations and Dynamical Systems* New York: Springer, 2001. Print.

[47] Perlmutter, S. *et al Nature* **391** (1998) 51-54

[48] Planck collaboration (Ade, P.A.R. *et al.*) arXiv:1303.5076 [astro-ph.CO]

[49] Planck collaboration (Ade, P.A.R. *et al.*) arXiv:1303.5062 [astro-ph.CO]

[50] Planck collaboration (Ade, P.A.R. *et al.*) arXiv:1303.5082 [astro-ph.CO]

[51] Planck collaboration (Ade, P.A.R. *et al.*) arXiv:1303.5075 [astro-ph.CO]

[52] Rajagopal, S. and Kumar, A. (2013) arXiv:1303.6026 [gr-qc]

[53] Saito, K. and Ishibashi, A. *PTEP* (2013) 013E04 arXiv:1209.5159 [gr-qc]

[54] Santos, B. *et al. A&A* **548** A31 (2012) arXiv:1207.2478 [astro-ph]

[55] Scarpa, R. *AIP Conf.Proc.* **822** (2006) 253-265 arXiv:0601478 [astro-ph]

[56] Schmidt, F. *et al. Phys.Rev.* D**80** (2009) 083505 arXiv:0908.2457 [astro-ph.CO]

[57] Schneider, P. *Extragalactic Astronomy and Cosmology: An Introduction.* Berlin: Springer, 2006. Print

[58] Shafieloo, A. *et al. Phys. Rev.* D**84** (2011) 063519 arXiv:1107.1033 [astro-ph.CO]

[59] Sotiriou, T. P. and V. Faraoni (2010) *Rev.Mod.Phys.* **82**, 451-497 arXiv:0805.1726 [gr-qc]

[60] Sotiriou, T. P. (2010) *Phys.Lett.* B **664**, 225-228 arXiv:0805.1160 [gr-qc]

[61] Sotiriou, T. P. (2007) arXiv:0710.4438 [gr-qc] (and all references therein)

[62] Starobinsky, A. A. *JETP Lett.* **86** (2007) 157-163 arXiv:0706.2041 [astro-ph]

[63] Starobinsky, A. A. astro-ph/9605155 UH-IFA-96-28

[64] Wainwright, J. and Ellis, G. *Dynamical Systems in Cosmology*. Cambridge: Cambridge University Press, 1997. Print.

[65] Weinberg, S. *Gravitation and Cosmology: Principles and Applications of the General Theory of Relativity* John Wiley & Sons, 1972. Print.